

Journal of Science & Technology in the Tropics

Volume 8 Number 2 December 2012

STEERING COMMITTEE

Academician Tan Sri Datuk Seri Dr Salleh B. Mohd. Nor
(Co-Chairman)
Dato' Dr Ong Eng Long (Co-Chairman)
Professor Ir Ruslan Hassan
Academician Professor Emeritus Dr Yong Hoi Sen
Ir Yong Kee Chiang
Dr Loo Koi Sang
Mr Kanesan Solomalai
Ms Nooni Ezdiani Yasin

EDITORIAL BOARD

Academician Professor Emeritus Dr Yong Hoi Sen
Chief Editor
Genetics, Systematics, Biodiversity
Academy of Sciences Malaysia; University of Malaya,
Malaysia

Ir Professor Dato' Dr Chuah Hean Teik
Electrical Engineering, ICT
University Tunku Abdul Rahman, Malaysia

Ir Professor Dato' Dr Goh Sing Yau
Biomedical Engineering, Mechanical Engineering
University Tunku Abdul Rahman, Malaysia

Dr Goh Swee Hock
Organic Chemistry, Natural Product Chemistry
Academy of Sciences Malaysia, Malaysia

Professor Dr Ah-Ng Tony Kong
Biomedical Sciences, Genomics, Phytochemicals
Rutgers, The State University of New Jersey, USA

Professor Dr Lee Soo Ying
Theoretical Chemistry, Ultrafast Spectroscopy
Nanyang Technological University, Singapore

Dr Lim Phaik Eem
Molecular Biology, Phycology
University of Malaya, Malaysia

Professor Emeritus Dato Dr C. P. Ramachandran
Medical Sciences, Infectious and Tropical Diseases
COSTAM, Universiti Sains Malaysia

Professor Dr Kurunathan Ratnavelu
Theoretical Physics, Atomic and Molecular Physics
University of Malaya, Malaysia

Professor Dr Abu Bakar Salleh
Agricultural Sciences
University Putra Malaysia, Malaysia

Dr Paul William Smith
Pulsed Power Technology
University of Oxford, UK

Professor Dr Hideaki Takabe
Laser Plasma, Plasma Astrophysics
Osaka University, Japan

Dr Tan Swee Lian
Genetics, Plant Breeding
MARDI, Malaysia

Professor Dr Wang Xin Xin
Electrical Engineering, Plasma Technology
Tsinghua University, China

Professor Dr Wong Chiow San
Experimental Physics, Plasma Technology
University of Malaya, Malaysia



JOSTT

DEDICATED TO THE ADVANCEMENT OF SCIENCE AND
TECHNOLOGY RELATED TO THE TROPICS

Journal of Science & Technology in the Tropics

Journal of Science & Technology in the Tropics

Volume 8 Number 2 December 2012

Volume 8 Number 2
December 2012

ISSN 1823-5034



9 771823 503009



Journal of Science & Technology in the Tropics

Volume 8 Number 2 December 2012

CONTENTS

Editorial <i>Salleh Mohd. Nor and Ong Eng Long</i>	83
<i>In situ</i> measurement of photosynthetic capacity in scleractinian corals (<i>Acropora formosa</i> and <i>Pocillopora damicornis</i>) during the 2010 massive coral reef bleaching event in Pulau Tioman, Malaysia <i>Kee Alfian Abdul Adzis, Affendi Yang Amri, Julian Hyde, Nasrulkhikim Maidin, Izarenah Md. Repin, Aw Soo Ling and Che Abd. Rahim Mohamed</i>	85
Three new phytotelma mosquitoes of the genus <i>Topomyia</i> (Diptera: Culicidae) from Katibas, Lanjak-Entimau, Sarawak, Malaysia <i>Ichiro Miyagi, Takako Toma, Takao Okazawa, Siew Fui Wong, Moi Ung Leh and Hoi Sen Yong</i>	97
Nucleolar organizer regions of the Indomalayan Pencil-tailed Tree Mouse <i>Chiropodomys gliroides</i> (Rodentia: Muridae) <i>Hoi Sen Yong, Phaik Eem Lim and Praphathip Eamsobhana</i>	119
Distribution mapping of Koak kaok (<i>Philemon buceroides</i>) in the edge forest of Gunung Rinjani National Park, Lombok, Indonesia <i>I Wayan Suana, Kurniasih Sukenti and Sri Puji Astuti</i>	125
Reinforcement of multiwalled carbon nanotubes/natural rubber nanocomposite prepared by latex technology <i>Azira Abd. Aziz, Dayang Habibah Abang Ismawi Hassim, A. B. Suriani and Mohamad Rusop Mahmood</i>	131
Treatment of waste water by ozone produced in a dielectric barrier discharge <i>A. Khadgi, D. P. Subedi, R. B. Tyata and C. S. Wong</i>	141
Low speed bearing monitoring using acoustic emission technique <i>Tonphong Kaewkongka and Jirapong Lim</i>	154

INSTRUCTIONS TO CONTRIBUTORS

JOSTT is a multi-disciplinary journal. It publishes original research articles and reviews on all aspects of science and technology relating to the tropics. All manuscripts are reviewed by at least two referees, and the editorial decision is based on their evaluations.

Manuscripts are considered on the understanding that their contents have not been previously published, and they are not being considered for publication elsewhere. The authors are presumed to have obtained approval from the responsible authorities, and agreement from all parties involved, for the work to be published.

Submission of a manuscript to JOSTT carries with it the assignment of rights to publish the work. Upon publication, the Publishers (COSTAM and ASM) retain the copyright of the paper.

Manuscript preparation

Manuscripts must be in English, normally not exceeding 3500 words. Type double spaced, using MS Word, on one side only of A4 size with at least 2.5 cm margins all round. Number the pages consecutively and arrange the items in the following order: title page, abstract, key words, text, acknowledgements, references, tables, figure legends.

Title page

Include (i) title, (ii) names, affiliations and addresses of all authors, (iii) running title not exceeding five words, and (iv) email of corresponding author.

Abstract and key words

The abstract, not more than 250 words, should be concise and informative of the contents and conclusions of the work. A list of not more than five key words must immediately follow the abstract.

Text

Original research articles should be organized as follows: Introduction, Materials and Methods, Results, Discussion, Acknowledgement, References. The International System of Units (SI) should be used. Scientific names and mathematical parameters should be in italics.

References

References should be cited in the text as numbers enclosed with square [] brackets. The

use of names in the text is discouraged. In the reference section, the following examples should be followed:

1. Yong H.S., Dhaliwal S.S. and Teh K.L. (1989) A female Norway rat, *Rattus norvegicus*, with XO sex chromosome constitution. *Naturwissenschaften* **76**: 387-388.
2. Beveridge W.I.B. (1961) *The Art of Scientific Investigation*. Mercury Book, London.
3. Berryman A.A. (1987) The theory and classification of outbreaks. In Barbosa P. and Schultz J.C. (eds.) *Insect outbreaks* pp. 3-30. Academic Press, San Diego.

Tables

Tables should be typed on separate sheets with short, informative captions, double spacing, numbered consecutively with Arabic numerals, and do not contain any vertical lines. A table should be set up to fit into the text area of at most the entire page of the Journal.

Illustrations

Black-and-white figures (line drawings, graphs and photographs) must be suitable for high-quality reproduction. They must be no bigger than the printed page, kept to a minimum, and numbered consecutively with Arabic numerals. Legends to figures must be typed on a separate sheet. Colour illustrations can only be included at the author's expense.

Proofs and reprints

Authors will receive proofs of their papers before publication. Order for reprints must be made when returning the proofs.

Submission

Manuscripts (including all figures but not original artwork), together with a CD version of the text, should be submitted to:

The Editorial Office
Journal of Science and Technology
in the Tropics
Academy of Sciences Malaysia
902-4 Jalan Tun Ismail
50480 Kuala Lumpur, Malaysia

E-mail: jostt@akademisains.gov.my

JOSTT is listed in Scopus

EDITORIAL

Science and Technology for National Transformation

National Transformation has been set as a national agenda by the Malaysian Government. The Economic Transformation Program is an initiative by the Malaysian government to turn Malaysia into a high income economy by the year 2020. It is managed by the Performance and Delivery Unit (PEMANDU), an agency under the Prime Minister Department of Malaysia.

Launched on 21st September, 2010, it is a comprehensive economic transformation plan to propel Malaysia's economy into high income economy. The program will lift Malaysia's Gross National Income (GNI) to US\$523 billion by 2020, and raise per capita income from US\$6700 to at least US\$15,000, meeting the World Banks' threshold for high income nation. It is projected that Malaysia will be able to achieve the targets set if GNI grows by 6% per annum.

Set to revitalize Malaysia's private sector, 60% of the blueprint's investment would be derived from the private sector, 32% from government linked companies and the remaining 8% from the government. Various sectors for development have been identified and are called National Key Economic Activities (NKEA).

The issue that concerns the scientific community is whether Science and Technology has been or will be given its rightful recognition for its contribution to the Transformation Program. It cannot be denied that investment into Research and Development (R&D) and Science and Technology (S&T) are fundamental prerequisites for any economic development. The role of the private sector in R&D in Malaysia is still minimal and a concerted effort must be made to encourage venture capital injection to encourage innovation in R&D. It is our hope that Government will give serious consideration to increasing the allocation for R&D, and provide greater and more attractive incentives for the private sector to invest in R&D. We have only eight more years before the year 2020 and time is running out. WE need to act now.

Dr Salleh Mohd. Nor and Dr Ong Eng Long

Co-Chairman JOSTT

***In situ* measurement of photosynthetic capacity in scleractinian corals (*Acropora formosa* and *Pocillopora damicornis*) during the 2010 massive coral reef bleaching event in Pulau Tioman, Malaysia**

Kee Alfian Abdul Adzis^{1,2,*}, Affendi Yang Amri³, Julian Hyde⁴, Nasrulkhakim Maidin⁵, Izarenah Md. Repin⁶, Aw Soo Ling⁷ and Che Abd. Rahim Mohamed⁸

¹ Marine Science Programme, School of Environmental & Natural Resource Sciences, Faculty of Science & Technology, National University of Malaysia, Bangi, Selangor, Malaysia

² Marine Ecosystem Research Centre (EKOMAR), Faculty of Science & Technology, National University of Malaysia, Bangi, Selangor Malaysia

³ Institute of Biological Sciences, Faculty of Science, Universiti Malaya, 50603 Kuala Lumpur, Malaysia

⁴ Reef Check Malaysia, Suite 5.19-5.22, Box 606, Wisma Central, Jalan Ampang, 50450 Kuala Lumpur, Malaysia

⁵ Tun Sakaran Marine Park-Sipadan Island Complex, P.O.Box 163, 91307, Semporna, Sabah, Malaysia

⁶ Marine Park Department of Malaysia, Ministry of Natural Resources & Environment, Aras 11, Wisma Sumber Asli, No.25, Persiaran Perdana, Presinct 4, 62574 Putrajaya, Malaysia

⁷ Borneo Marine Research Institute, Universiti Malaysia Sabah, Kota Kinabalu, Malaysia

⁸ Marine Ecosystem Research Centre (EKOMAR), Faculty of Science & Technology, National University of Malaysia, Bangi, Selangor, Malaysia

(*E-mail: alfian@ukm.my / keealf@hotmail.com)

Received 28-03-2012; accepted 01-04-2012

Abstract *In situ* measurement of *Acropora formosa* and *Pocillopora damicornis* photosynthetic capacity was conducted to evaluate the severity of the massive coral reef bleaching event in Pulau Tioman, Peninsular Malaysia in 2010. Diving-PAM was used to measure the effective quantum yield ($\Delta F/F_m'$) which represents the photosynthetic capacity of the corals. The $\Delta F/F_m'$ for *A. formosa* and *P. damicornis* during bleaching were reduced to 88.06% and 38.89% of its pre-bleaching value, respectively. Both species showed significant differences for the two conditions (ANOVA, $P < 0.05$). The suppression of its photosynthetic capacity was further supported by its initial (F_o) and maximum (F_m) fluorescence. During bleaching, F_o for *A. formosa* and *P. damicornis* was reduced to 94.08% and 63.98% of its pre-bleaching value, respectively. For F_m , *A. formosa* and *P. damicornis* recorded 97.88% and 79.30% reduction from its pre-bleaching value, respectively. Both species recorded significant differences for F_o and F_m between pre-bleaching and bleaching conditions (ANOVA, $P < 0.05$). There was massive coral reef bleaching for 16 sites with water temperature of 32°C. This study demonstrated the severity of the massive coral reef bleaching event to *A. formosa* and *P. damicornis* photosynthetic capacity in Pulau Tioman and that it was a not a localized event.

Keywords photosynthetic capacity – *Acropora formosa* – *Pocillopora damicornis* – coral bleaching 2010 – Diving-PAM

INTRODUCTION

Coral bleaching is a sign of stress when the corals are subdued to various stressors, such as temperature [1-3], salinity [4, 5], solar irradiance [4, 6-8] and pollution [9-11]. Globally, however, climate change has been closely tied to massive coral reef bleaching phenomena which is increasing in frequency [12, 13]. In Malaysia, a massive coral reef bleaching event was observed in June-July 2010. The coral reef colour changing to white made many people curious of the phenomenon and many called it as 'Underwater Snow' and 'Snow Blanket' due to the similarity to winter conditions (Scuba divers, pers. comm.). Ironically, these massive coral reef bleaching events are a sign of stress and a sign of environment changes.

During coral bleaching, the symbiotic dinoflagellate (zooxanthellae) is expelled from its coral host [14, 15]. Coral tissues are thin and almost transparent with its calcareous skeleton, the zooxanthellae within them gives them a vibrant colour look, and when they are expelled, the coral will look pale and bleach like, hence the term 'coral bleaching' [4, 8, 16]. Zooxanthellae lives within the coral tissue which provides the coral with energy and nutrition through photosynthesis. A prolong period of zooxanthellae expulsion will starve the corals and eventually will lead to coral mortality [17].

When a coral undergoes bleaching, their photosynthetic capacity is heavily affected. Their ability to process light energy is suppressed by the breakdown of their photosystem and the overproduction of reactive oxygen species (ROS) that will damage cellular components such as nucleic acids, proteins and lipids [18, 19]. The decrease photosynthetic capacity or also known as photoinhibition [20-23] will paralyze photosynthesis processes for the growth and energy supply of the corals [17, 24, 25].

To date in Malaysia, coral reef bleaching event was only documented in four publications [26-29], and some observations of localized bleaching in Pulau Payar in 2002 (pers. observ.), 2008 (pers. observ.) and 2009 (Y. A. Affendi, unpublished data) in Pulau Tioman. There are no known publications on the changes of photosynthetic capacity during a bleaching event. The aim of this paper is to document the photosynthetic capacity changes and also the extent of the massive coral reef bleaching in Malaysia.

MATERIALS AND METHODS

Sites and coral species

The study was conducted in Pulau Tioman which is approximately 40 km from the nearest mainland. It has been gazetted as a Marine Park in 1994 under the jurisdiction of the Department of Marine Park Malaysia. The area of the marine park covers only the water area of two nautical miles from shore.

Two scleractinian coral species were used in this study, viz. *Acropora formosa* (Dana) and *Pocillopora damicornis* (Linnaeus). The effective quantum yield ($\Delta F/F_m$) for *A. formosa* and *P. damicornis* pre-bleaching condition was conducted during monitoring of the photosynthetic capacity of corals before the massive coral reef bleaching event. The pre-bleaching photosynthetic capacity for *A. formosa* was recorded in April 2010 at Pulau Renggis and *P. damicornis* in June 2008 off the beach of Pulau Tioman Marine Park Centre in Tg. Mesoh. During the coral reef bleaching event, measurement of photosynthetic capacity for both species was recorded in June 2010. Both are dominant species in Malaysian waters, especially in Pulau Tioman [30-32].

Coral photosynthetic capacity measurement

Photosynthetic capacity of a coral, reflected through its effective quantum yield ($\Delta F/F_m$) [33], was measured through its chlorophyll fluorescence *in situ* by using a submersible pulse amplitude modulator (PAM) or Diving-PAM (Walz, Germany) (Fig. 1). To obtain effective quantum yield readings, the maximum fluorescence (F_m) was measured using a saturating light pulse (0.8 s, $>2000 \mu\text{mol quanta m}^{-2}\text{s}^{-1}$), and the changes in fluorescence ($\Delta F = F_m - F_o$) was then used to calculate the effective quantum yield ($\Delta F/F_m$) for corals under natural sunlight [34]. For *A. formosa*, readings were taken from a wide colony patch. A total of 8 for pre-bleaching and 33 for during-bleaching readings was taken from upper and lower branches of the interior and exterior of *A. formosa*. *P. damicornis* readings were taken from 3 colonies, with a total of 8 readings taken from upper and lower branches of the interior and exterior of *P. damicornis* for pre-bleaching and during-bleaching.



Figure 1. Photosynthetic capacity *in situ* data collection of scleractinian corals by using Diving-PAM during the massive coral reef bleaching event 2010 in Pulau Tioman.

Statistical analysis

The statistical analysis was conducted by using SigmaPlot 11.0. Mean value and standard deviation (S.D.) was calculated. Significant differences were tested by using ANOVA test between pre- and during-bleaching event for both species.

RESULTS

Effective quantum yield ($\Delta F/F_m$)

The $\Delta F/F_m$ for *A. formosa* and *P. damicornis* during bleaching event was reduced to 88.06% and 38.89% of its pre-bleaching value respectively, indicating that during the massive coral reef bleaching event, the photosynthetic capacity for *A. formosa* and *P. damicornis* was significantly reduced (Fig. 2; $P < 0.05$).

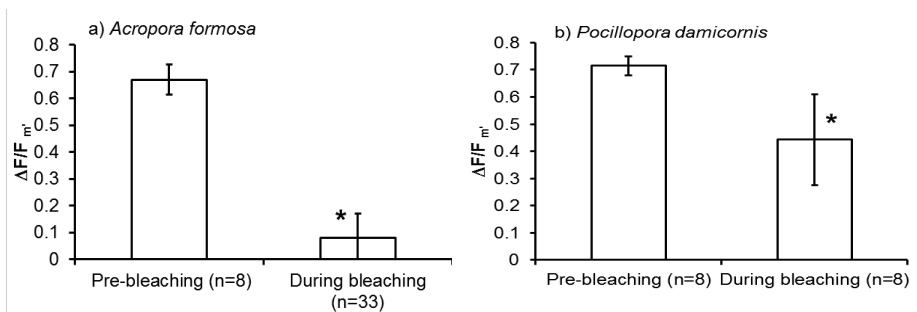


Figure 2. The photosynthetic capacity of (a) *Acropora formosa*, and (b) *Pocillopora damicornis* in Pulau Tioman before and during the massive coral reef bleaching. N represents the number of readings taken on upper and lower branches in the interior and exterior of each colony (*A. formosa* = wide patch; *P. damicornis* = 3 colonies). *represents $P < 0.05$ from the pre-bleaching colonies.

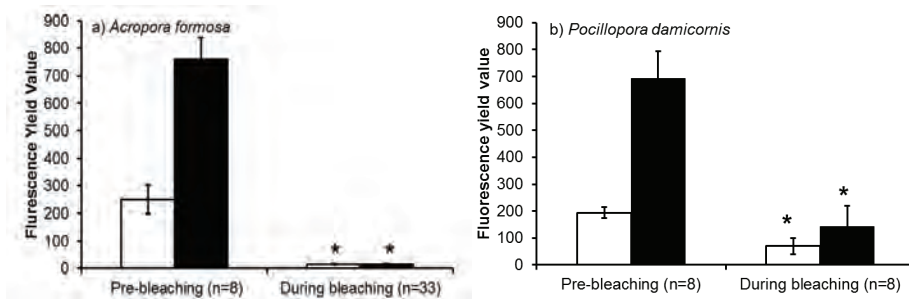


Figure 3. Initial (F_0) and maximum (F_m) fluorescence of (a) *Acropora Formosa*, and (b) *Pocillopora damicornis* in Pulau Tioman before and during the massive coral reef bleaching. N represents the number of readings taken on upper and lower branches in the interior and exterior of each colony (*A. formosa* = wide patch; *P. damicornis* = 3 colony). *represent $P < 0.05$ from the pre-bleaching colonies. □, F_0 ; ■, F_m .

Initial (F_o) and maximum (F_m) fluorescence

During the bleaching event, F_o for *A. formosa* and *P. damicornis* was reduced to 94.08% and 63.98% of its pre-bleaching value, respectively. For F_m , *A. formosa* and *P. damicornis* recorded 97.88% and 79.30% reduction from its pre-bleaching value, respectively. Both species recorded significantly lower F_o and F_m between pre-bleaching and bleaching conditions (Fig. 3; $P < 0.05$).

DISCUSSION

During the 2010 massive coral reef bleaching event in Malaysia, the photosynthetic capacity of *A. formosa* and *P. damicornis* was significantly reduced. Changes in $\Delta F/F_m$ showed a decrease of the photosystem capacity to capture and process photons from incoming lights, or known as 'photoinhibition' [20]. Photoinhibition is part of the daily challenges faced by any photosynthetic organism, such as scleractinian corals [20, 33], to changing illumination of light throughout the daily cycle. The ability of its photosystem to recover or repair damages is essential to its survival [33]. With the suppression of the $\Delta F/F_m$ for both species, the corals zooxanthellae has a lowered capability to conduct photosynthesis. This will eventually weaken the coral and could lead to mortality.

Damage to the zooxanthellae photosynthetic capability was further illustrated by its significantly lower initial fluorescence (F_o) and maximum fluorescence (F_m) between pre-bleaching and during-bleaching for both species. F_o is the measure of the initial energy distribution and efficiency of energy trapping within the photosystem II (PSII), which is also known as the baseline fluorescence [20]. A rise or decrease in F_o indicates damage to the D1 protein and an increase of energy dissipation within the light harvesting antennae of photosystem II [20, 35]. D1 protein in the reaction centre is essential for the repair of damaged PSII [36, 37]. Reduction in F_m can cause interconversion of pigments within the xanthophyll cycle which causes a non-radiative energy dissipation, thus decrease in its fluorescence emissions [35]. Xanthophyll cycle is important because it stimulates energy dissipation within the light harvesting antenna proteins by reducing the amount of energy that reaches the photosynthetic reaction centre [33, 38, 39], thus preventing increase inhibition of D1 protein synthesis for repair of the photosystem reaction centre [20, 35, 38].

Temperature has been known to be one of the factors for coral photosynthetic capacity suppression [1, 4, 37, 41-46] and a major factor causing corals to bleach during a massive bleaching event [47-51]. The elevated seawater temperature regime was recorded by *in situ* temperature loggers in Tekek Reef, Pulau Tioman for 2010 with the highest temperature at 32°C. The temperature of above 31-32°C was recorded for 48 days in Pulau Tioman (Fig 4; Y. A. Affendi, unpublished data). The temperature threshold for corals is at 31-32°C [12, 50-53] and the long

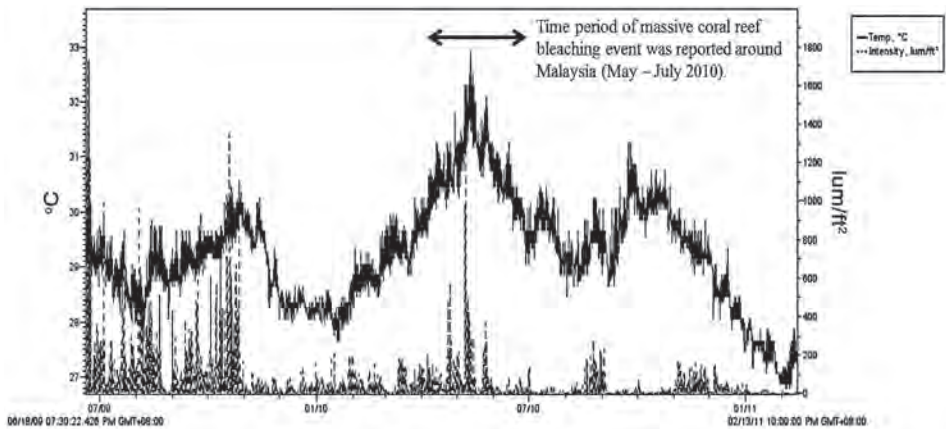


Figure 4. The temperature ($^{\circ}\text{C}$) and light intensity (lum/ft^2) logged in Pulau Tioman for 2009-2011 by Hobo[®] Pendant temperature/light data logger with resolution of 30 minutes. Arrow marked the time period of reports of massive coral reef bleaching around Malaysia. Source: Y.A. Affendi. (unpublished data).

exposure to elevated seawater temperature has been shown to cause corals to bleach [1, 4, 12].

The extent of the mass coral reef bleaching was assessed through email communications with various researchers, scientists, park managers and dive operators within Malaysia and also neighbouring countries between May-June 2010. From the collated information, a total of 16 sites in Malaysia were reported to have mass coral reef bleaching (Fig. 5) with the highest temperature of 32°C , and depth of more than 15 m (Table 1). The bleaching event also affected neighbouring countries with reports of bleaching in Thailand, Singapore and Indonesia (Fig. 5).

The high seawater temperature was confirmed by NOAA's satellite observations that the sea surface temperature (SST) in Malaysia during the bleaching event had increased $1\text{-}2^{\circ}\text{C}$ from its normal temperature (<http://coralreefwatch.noaa.gov/satellite/baa/index.html>). Documentation and monitoring of a coral bleaching event by use of internet was first used during the massive bleaching event in 1998 [48], to disseminate and gather information of the bleaching sites. In Japan, the coral researchers and scientists used the internet to disseminate current coral reef bleaching event and issues [54]. In this age of technology, the use of online networking has become an important tool for many researchers and ecosystem managers.

This paper demonstrates the use of *in situ* measurement to evaluate the severity of damage to *A. formosa* and *P. damicornis* photosynthetic capacity in Pulau Tioman, and generally for Malaysia, during the massive coral reef bleaching of 2010. Coupled with the use of online networking, it can play a major role in getting a more rapid insight and confirmation on the extent of a massive coral

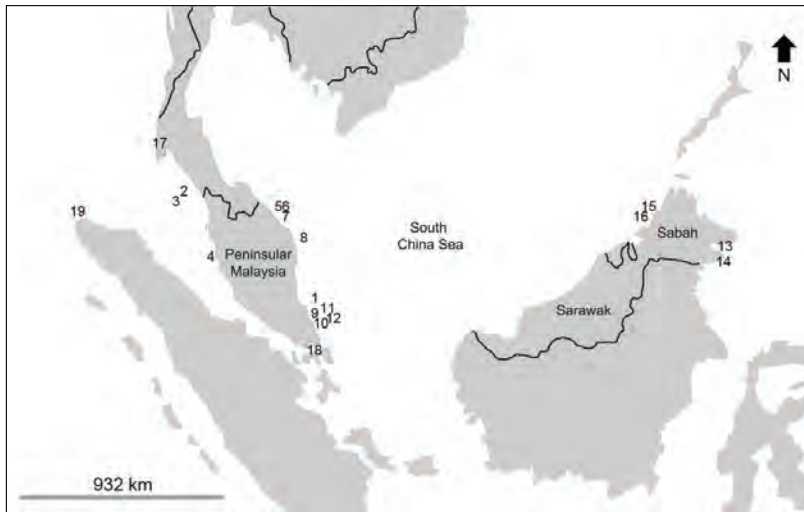


Figure 5. Areas in Malaysia with massive coral reef bleaching in 2010. Sites were represented by numbers. 1. Pulau Tioman, Pahang; 2. Pulau Langkawi, Kedah; 3. Pulau Payar, Kedah; 4. Pulau Pangkor, Perak; 5. Pulau Perhentian, Terengganu; 6. Pulau Redang, Terengganu; 7. Pulau Bidong, Terengganu; 8. Pulau Tenggol, Terengganu; 9. Pulau Tinggi, Johor; 10. Pulau Sibu, Johor; 11. Pulau Aur, Johor; 12. Pulau Dayang, Johor; 13. Taman Marin Tun Sakaran, Sabah; 14. Pulau Sipadan, Sabah; 15. Taman Tunku Abdul Rahman, Sabah; 16. Pulau Tiga, Sabah; 17. Phuket, Thailand; 18. Singapore; 19. Pulau Weh, Indonesia.

Table 1. Information on coral bleaching from various agencies and NGOs through internet networking.

Site	Extents of Bleaching (Wide? Patchy? Certain area)	Temperature (°C)	Depth range (m)	Percentage of bleaching (%)	Source
Pulau Tioman, Pahang	Wide area	31-32	3-22	60-70	- Katie Yewdall, Blueventures Malaysia - Izarenah Md. Repin, Marine Park Malaysia
Pulau Perhentian, Terengganu	Wide area	26-32	<14	Not available	- Badrul Huzaimi Tajuddin, ISB-UM
Taman Marin Tun Sakaran, Semporna, Sabah	Wide area	30	5-25	5-30	- Nasrullahakim Maidin, Sabah Park
Pulau Sipadan, Sabah	Wide area	30	5-26	10-15	- Nasrullahakim Maidin, Sabah Park
Taman Tunku Abdul Rahman, Kota Kinabalu, Sabah	Wide area	28-31	3-14	15-80	- Nasrullahakim Maidin, Sabah Park
Taman Pulau Tiga, Kota Kinabalu, Sabah	Wide area	30.5-31.8	5-12	9-35	- Nasrullahakim Maidin, Sabah Park

reef bleaching. This information is important for relevant government agencies to conduct further action plans to decrease the potential stress towards the coral reef ecosystem during a massive coral reef bleaching event.

Acknowledgements – This study was funded by Science Fund Grant: 04-01-02-8F0117 to Che Abd. Rahim Mohamed, and partially funded by FRGS Fund Grant: UKM-ST-06-FRGS0246-2010 to Kee Alfian Abdul Adzis. The authors would like to acknowledge the Marine Park Department, Malaysia for logistics support. Our appreciation also goes to School of Environmental & Natural Resource Sciences, Faculty of Science & Technology, National University of Malaysia for equipment support. We acknowledge the volunteer and diving assistance provided by 'SEABUDS'.

REFERENCES

1. Jones R.J., Hoegh-Guldberg O., Larkum A.W.D. and Schreiber U (1998) Temperature-induced bleaching of corals begins with impairment of the CO₂ fixation mechanism in zooxanthellae. *Plant, Cell & Environment* **21**: 1219-1230.
 2. Glynn P.W. (1991) Coral-reef bleaching in the 1980s and possible connections with global warming. *Trends in Ecology & Evolution* **6**: 175-179.
 3. Fitt W., Brown B., Warner M. and Dunne R. (2001) Coral bleaching: interpretation of thermal tolerance limits and thermal thresholds in tropical corals. *Coral Reefs* **20**: 51-65.
 4. Brown B.E. (1997) Coral bleaching: causes and consequences. *Coral Reefs* **16**: S129-S138.
 5. Kerswell A.P. and Jones R.J. (2003) Effects of hypo-osmosis on the coral *Stylophora pistillata*: nature and cause of 'low-salinity bleaching'. *Marine Ecology-Progress Series* **253**: 145-154.
 6. Brown B.E., Dunne R.P., Goodson M.S. and Douglas A.E. (2000) Bleaching patterns in reef corals. *Nature* **404**: 142-143.
 7. Brown B.E., Dunne R.P., Warner M.E., Ambarsari I., Fitt W.K., Gibb S.W. and Cummings D.G. (2000) Damage and recovery of Photosystem II during a manipulative field experiment on solar bleaching in the coral *Goniastrea aspera*. *Marine Ecology Progress Series* **195**: 117-124.
 8. Lesser M.P. (2004) Experimental biology of coral reef ecosystems. *Journal of Experimental Marine Biology and Ecology* **300**: 217-252.
 9. Mercurio P., Negri A.P., Burns K.A. and Heyward A.J (2004) The ecotoxicology of vegetable versus mineral based lubricating oils: 3. Coral fertilization and adult corals. *Environmental Pollution* **129**: 183-194.
 10. Jones R. (2005) The ecotoxicological effects of Photosystem II herbicides on corals. *Marine Pollution Bulletin* **51**: 495-506.
 11. Fabricius K.E. (2005) Effects of terrestrial runoff on the ecology of corals and coral reefs: review and synthesis. *Marine Pollution Bulletin* **50**: 125-146.
 12. Hoegh-Guldberg O. (1999) Climate change, coral bleaching and the future of the world's coral reefs. *Marine and Freshwater Research* **50**: 839-866.
 13. Baker A., Glynn P. and Riegl B. (2008) Climate change and coral reef bleaching:
-

- An ecological assessment of long-term impacts, recovery trends and future outlook. *Estuarine, Coastal and Shelf Science* **80**: 435-471.
14. Anya S. Hoegh-Guldberg O. and Coz G. (1998). Bleaching responses of symbiotic dinoflagellates in coral: the effects of light and elevated temperature on their morphology and physiology. *Proceeding of the Australian Coral Reef Society 75th Anniversary Conference, Heron Island*. pp. 199-216.
 15. Douglas A.E. (2003) Coral bleaching—how and why? *Marine Pollution Bulletin* **46**: 385-392.
 16. Apprill A.M., Bidigare R.R. and Gates R.D. (2007) Visibly healthy corals exhibit variable pigment concentrations and symbiont phenotypes. *Coral Reefs* **26**: 387-397.
 17. Jones R.J. (2008) Coral bleaching, bleaching-induced mortality, and the adaptive significance of the bleaching response. *Marine Biology* **154**: 65-80.
 18. Baird A.H., Bhagooli R., Ralph P.J. and Takahashi S. (2009) Coral bleaching: the role of the host. *Trends in Ecology & Evolution* **24**: 16-20.
 19. Nishiyama Y., Yamamoto H., Allakhverdiev S.I., Inaba M., Yokota A. and Murata N. (2001) Oxidative stress inhibits the repair of photodamage to the photosynthetic machinery. *Embo Journal* **20**: 5587-5594.
 20. Hoegh-Guldberg O. and Jones R.J. (1999) Photoinhibition and photoprotection in symbiotic dinoflagellates from reef-building corals. *Marine Ecology Progress Series* **183**: 73-86.
 21. Winters G., Loya Y., Rottgers R. and Beer S. (2003) Photoinhibition in shallow-water colonies of the coral *Stylophora pistillata* as measured *in situ*. *Limnology and Oceanography* **48**: 1388-1393.
 22. Bhagooli R. and Hidaka M. (2004) Photoinhibition, bleaching susceptibility and mortality in two scleractinian corals, *Platygyra ryukyuensis* and *Stylophora pistillata*, in response to thermal and light stresses. *Comparative Biochemistry and Physiology a-Molecular & Integrative Physiology* **137**: 547-555.
 23. Nakamura T., van Woesik R. and Yamasaki H. (2005) Photoinhibition of photosynthesis is reduced by water flow in the reef-building coral *Acropora digitifera*. *Marine Ecology-Progress Series* **301**: 109-118.
 24. Gattuso J-P., Allemand D. and Frankignoulle M. (1999) Photosynthesis and calcification at cellular, organismal and community levels in coral reefs: A review on interactions and control by carbonate chemistry. *American Zoologist* **39**: 160-183.
 25. Schneider K. and Erez J. (2006) The effect of carbonate chemistry on calcification and photosynthesis in the hermatypic coral *Acropora eurystroma*. *Limnology and Oceanography* **51**: 1284-1293.
 26. Kushairi M.R.M. The 1998 bleaching catastrophe of corals in the South China Sea. *Proceedings of the JSPS Seminar on Marine and Fisheries Sciences, Bali, Indonesia*. pp. 2-7.
 27. Kushairi M.R.M. Some observations on the impacts of the Indo-Pacific region 1998 SST anomalies on local coral communities. *Proceedings of the International Conference on the International Oceanographic Data & Information Exchange in the Western Pacific (IODE-WESTPAC), Langkawi, Malaysia*. pp. 1-4.
-

28. Pilcher N., Cabanban A. (2000) *The status of coral reefs in eastern Malaysia*. Townsville: Australia Institute of Marine Science.
 29. Guest J.R., Baird A.H., Maynard J.A., Muttaqin E., Edwards A.J., et al. (2012) Contrasting patterns of coral bleaching susceptibility in 2010 suggest an adaptive response to thermal stress. *Plos One* **7**(3): e33353. doi:10.1371/journal.pone.0033353.
 30. Affendi Y.A., Badrul H.T., Lee Y.L. et al. (2005) Scleractinian coral diversity of Kg. Tekek, Pulau Tioman Marine Park. *Proceedings of Second Regional Symposium on Environment and Natural Resources: 'Natural Resource Utilisation and Environmental Preservation: Issues and Challenges'*. 22-23 March 2005. Pan Pacific Hotel, Kuala Lumpur, Malaysia. Universiti Kebangsaan Malaysia. pp. 20-31.
 31. Toda T., Okashita T., Maekawa T., Kee Alfian B.A.A., Rajuddin M.K., Nakajima R., Chen W., Takahashi K., Othman B.H.R. and Terazaki M. (2007) Community structures of coral reefs around Peninsular Malaysia. *Journal of Oceanography* **63**: 113-123.
 32. Kee Alfian A.A., Affendi Y.A., Oliver J. and Mohamed C.A.R. (2009) Effective and maximum quantum yield of the lace coral *Pocillopora damicornis* (Anthozoa: Scleractinia: Pocilloporidae) in Pulau Tioman, Malaysia. *Journal of Science and Technology in the Tropics* **5**: 13-17.
 33. Warner M.E., Lesser M.P. and Ralph P.J. (2010) Chlorophyll fluorescence in reef building corals. In: Suggett D.J., Prášil O. and Borowitzka M.A. (eds.). *Chlorophyll a Fluorescence in Aquatic Sciences: Methods and Applications* pp. 209-222. Springer Netherlands.
 34. Jones R.J., Kildea T. and Hoegh-guldberg O. (1999) PAM chlorophyll fluorometry: a new *in situ* technique for stress assessment in scleractinian corals, used to examine the effects of cyanide from cyanide fishing. *Marine Pollution Bulletin* **38**: 864-874.
 35. Dias D. and Marengo R. (2006) Photoinhibition of photosynthesis in *Minuartia guianensis* and *Swietenia macrophylla* inferred by monitoring the initial fluorescence. *Photosynthetica* **44**: 235-240.
 36. Mohanty P., Allakhverdiev S.I. and Murata N. (2007) Application of low temperatures during photoinhibition allows characterization of individual steps in photodamage and the repair of photosystem II. *Photosynthesis research* **94**: 217-224.
 37. Takahashi S., Nakamura T., Sakamizu M., Woesik Rv. and Yamasaki H. (2004) Repair machinery of symbiotic photosynthesis as the primary target of heat stress for reef-building corals. *Plant and Cell Physiology* **45**: 251-255.
 38. Ralph P.J., Wilhelm C., Lavaud J., Jakob T., Petrou K. and Kranz, S.A. (2010) Fluorescence as a tool to understand changes in photosynthetic electron flow regulation. In: Suggett D.J., Prášil O. and Borowitzka M.A. (eds.). *Chlorophyll a Fluorescence in Aquatic Sciences: Methods and Applications*. pp. 75-89. Springer Netherlands
 39. Cosgrove J. and Borowitzka M.A. (2010) Chlorophyll fluorescence terminology: An introduction. In: Suggett D.J., Prášil O. and Borowitzka M.A. (eds.) *Chlorophyll*
-

- a Fluorescence in Aquatic Sciences: Methods and Applications*. pp. 1-17. Springer Netherlands.
40. Warner M.E, Fitt W.K. and Schmidt G.W. (1999) Damage to photosystem II in symbiotic dinoflagellates: A determinant of coral bleaching. *Proceedings of the National Academy of Sciences* **96**: 8007-8012.
 41. Jones R.J., Selina W., Affendi Y.A. and Ove H-G. (2000) Changes in quantum efficiency of Photosystem II of symbiotic dinoflagellates of corals after heat stress, and of bleached corals sampled after the 1998 Great Barrier Reef mass bleaching event. *Marine & Freshwater Research* **51**: 63-71.
 42. Jones R.J. and Hoegh-Guldberg O. (2001) Diurnal changes in the photochemical efficiency of the symbiotic dinoflagellates (Dinophyceae) of corals: photoprotection, photoinactivation and the relationship to coral bleaching. *Plant, Cell & Environment* **24**: 89-99.
 43. Hill R., Frankart C. and Ralph P. (2005) Impact of bleaching conditions on the components of non-photochemical quenching in the zooxanthellae of a coral. *Journal of Experimental Marine Biology and Ecology* **322**: 83-92.
 44. Rodriguez-Roman A., Hernandez-Pech X., Thome P.E., Enriquez S. and Iglesias-Prieto R. (2006) Photosynthesis and light utilization in the Caribbean coral *Montastraea faveolata* recovering from a bleaching event. *Limnology and Oceanography* **51**: 2702-2710.
 45. Hill R. and Ralph P.J. (2008) Impact of bleaching stress on the function of the oxygen evolving complex of zooxanthellae from scleractinian corals. *Journal of Phycology* **44**: 299-310.
 46. Lesser M.P. (2011) Coral bleaching: causes and mechanisms. In: Dubinsky Z. and Stambler N. (eds.) *Coral Reefs: An Ecosystem in Transition* . pp. 405-419. Springer Netherlands
 47. Glynn P.W. (1993) Coral-reef bleaching - ecological perspectives. *Coral Reefs* **12**: 1-17.
 48. Wilkinson C. (1998) The 1997-1998 mass bleaching event around the world. In: Wilkinson C.R. (eds.). *Status of coral reefs of the world*. pp. 15-38. Townsville: Australia Institute of Marine Science.
 49. Aronson R.B., Precht W.F., Toscano M.A. and Koltjes KH (2002) The 1998 bleaching event and its aftermath on a coral reef in Belize. *Marine Biology* **141**: 435-447.
 50. Berkelmans R., De'ath G., Kininmonth S. and Skirving W.J. (2004) A comparison of the 1998 and 2002 coral bleaching events on the Great Barrier Reef: spatial correlation, patterns, and predictions. *Coral Reefs* **23**: 74-83.
 51. Baker A.C., Glynn P.W. and Riegl B. (2008) Climate change and coral reef bleaching: An ecological assessment of long-term impacts, recovery trends and future outlook. *Estuarine Coastal and Shelf Science* **80**: 435-471.
 52. McClanahan T.R. (2003) The near future of coral reefs. *Environmental Conservation* **29**(4): 460-483.
 53. Middlebrook R., Anthony K.R.N., Hoegh-Guldberg O. and Dove S. (2010) Heating rate and symbiont productivity are key factors determining thermal stress in the
-

reef-building coral *Acropora formosa*. *Journal of Experimental Biology* **213**: 1026-1034.

54. Nakano Y. (2004) Global environmental change and coral bleaching. In: *Coral Reefs of Japan*. pp. 42-48. Ministry of the Environment, Japan.

Three new phytotelma mosquitoes of the genus *Topomyia* (Diptera: Culicidae) from Katibas, Lanjak-Entimau, Sarawak, Malaysia

Ichiro Miyagi^{1,2*}, Takako Toma¹, Takao Okazawa³, Siew Fui Wong⁴,
Moi Ung Leh⁴ and Hoi Sen Yong⁵

¹ Laboratory of Environmental Health, School of Health Sciences, Faculty of Medicine,
University of the Ryukyus, Nishihara, Okinawa, 903-0215 Japan

² Laboratory of Mosquito Systematics of Southeast Asia and Pacific,
c/o Ocean Health Corporation, 4-21-11, Iso, Urasoe, Okinawa, 901-2132 Japan

³ Faculty Medicine, Kanazawa University, Kakuma, Kanazawa, Ishikawa, 920-1192 Japan

⁴ Sarawak Museum Department, 93566, Kuching, Sarawak, Malaysia

⁵ Institute of Biological Sciences, University of Malaya, 50603 Kuala Lumpur, Malaysia

(*Corresponding author email: topmiyagii@ybb.ne.jp)

Received 23-08-2012, accepted 15-09-2012

Abstract Three new species belonging to the subgenus *Topomyia* of the genus *Topomyia* are described under the name of *Topomyia (Topomyia) katibasensis*, *To. (Top.) chaili* and *To. (Top.) nicksoni*. The adults and pupae are described in detail and illustrations of the male genitalia and pupae are provided. Partial descriptions and illustrations of their fourth-instar larvae are also provided based on associated larval exuviae of the species. These species occur in the secondary rain forest along Katibas River in the Lanjak-Entimau Wildlife Sanctuary at elevation of approximately 200 m. The larvae of these species breed in the leaf axils of phytotelma plants, *Pandanus* sp., *Phrynium* sp. and arrowroot (Marantaceae). The new species described in the present paper are attributed to Miyagi and Toma.

Keywords genus *Topomyia* – subgenus *Topomyia* – new species – phytotelmata – Lanjak-Entimau – Sarawak

INTRODUCTOIN

The genus *Topomyia* is a relatively small group, with 60 species in two subgenera, *Topomyia* (38 species) and *Suaymyia* (22 species). They occur mainly in the Oriental Region, with extensions into the Southern Palaearctic (South Japan and China) and the Australasian (Sulawesi and New Guinea) Regions [1]. After the pioneer works by Leicester [2] and Edwards [3], extensive surveys for *Topomyia* mosquitoes throughout Peninsular Malaysia, Sarawak and Sabah were carried out by Ramalingam and Banu [4–8] and Miyagi and Toma [9–20], and 14 species of the genus have been recorded in these regions. The immature stages of the *Topomyia* mosquitoes are found exclusively in phytotelmata, small water bodies held by living or dead terrestrial plants. Phytotelmata are usually overlooked because

they are small and inconspicuous [21]. Adult *Topomyia* mosquitoes are non-blood sucking and hence not significant from the point of disease transmission. The taxonomic work of the genus still remains to be done.

Since 2005, in connection with the project “Study on taxonomy and bionomics of two winged flies, Diptera in Sarawak”, conducted with the coordination and cooperation of the Sarawak Museum in Kuching, extensive larval collections of *Topomyia* have been made in the leaf axils of many kinds of phytotelma plants in the secondary riparian forests of Matang National Park, Borneo High, Bario and Ba Kelalan Kerabit highlands, and the Lanjak-Entemau Wildlife Sanctuary (LEWS). In the LEWS, collections were made in dipterocarp forest in March and September, 2011 for a total of about 30 days. The immature stages collected in the phytotelmata of different plants by slender glass pipettes with 2–5 mm diameter tip were transported to the Sarawak Museum, Kuching, and reared individually to adults in small tubes with habitat water. Larval and pupal exuviae were preserved in 80% alcohol. The newly emerged adult was reared for about 24 h and then mounted on a minute pin. The associated exuviae and male genitalia were mounted in euparal medium on two slides labeled with the corresponding individual and genital numbers.

Preliminary studies of the materials indicated three new species of *Topomyia* occurring near the headquarter of Katibas, LEWS (N 01°38.777' and E 112°167.709'). They belong to the subgenus *Topomyia* according to Thurman's treatment [22]. We describe the adult males and pupae of the species in this paper. Although several larval exuviae associated with the males of the species are available, they are in poor condition. Some important characters of head and siphon of the larvae are described and illustrated. The siphon and trumpet indices of larva and pupa used here follow Belkin's “Ratio of dorsal length to median width” [23]. Measurements and drawings of pupa and larva are made from pupal and larval skins. Terminology follows mostly Harbach and Knight [24], and Harbach and Peyton [25]. Holotype and some of the paratypes are deposited in the Smithsonian Institution, Washington D.C., USA, and some of the paratypes are in the Sarawak Museum, Kuching, Malaysia.

DESCRIPTIONS AND DISCUSSION

Topomyia (Topomyia) katibasensis Miyagi and Toma new species (Figs. 1, 2, 7E; Table 1)

Description

Male (Figs. 1A, 7E) — Wing, 2.26–2.60 mm (mean 2.43 mm). Proboscis, 1.50 mm. Forefemur, 1.43–1.76 mm (mean 1.59 mm). Small to medium in size; dark brown

Table 1. Numbers of branches for pupae of *Topomyia (Topomyia) katibasensis* n. sp.

Seta no.	Cephalo- thorax	Abdominal segments							
		I	II	III	IV	V	VI	VII	VIII
0	-	-	1	1	1	1	1	1	1
1	2	M	2-8	2-5	2-5	1-3	2-5	1, 2	-
2	2	1(1, 2)	1(1, 2)	1	1	1	1	1	-
3	2-4	1	1, 2	1	2-5	2-4	1-3	1, 2	-
4	1-5	1-4	1-6	2-5	2-5	2-5	1-3	1-3	1
5	4-6	4-8	1-5	2-4	1	1	1	1	-
6	1-3	1, 2	1	1, 2	1, 2	1, 2	1, 2	1-3	-
7	1-3	2-4	1-3	1-5	1-4	1-5	1	1	-
8	1, 2	-	-	1-4	1-4	1-3	1-4	2-6	-
9	2-5	1-3	1	1	1	1	1	19-27*	20-25*
10	2, 3	-	-	1-3	1-4	1, 2	1-3	1, 2	-
11	1	-	-	1, 2	1-3	1, 2	1-3	1, 2	-
12	3-6	-	-	-	-	-	-	-	-
14	-	-	-	-	-	-	-	-	1

M: dendritic with many branches. *aciculated.

Obsolete and missing setae are shown with a hyphen (-).

Specimens examined; 4 pupal exuviae from LEWS, Sarawak, Malaysia

with silver markings on antepronotum, head, scutum and scutellum. *Head:* Occiput and side of head with broad, flat dark brown decumbent scales with green sheen at certain angles. A large patch of flat silvery scales on vertex, just above eyes. Interocular and ocular setae present; erect scales absent. Clypeus oval in shape and elongate, integument brown without scales. Maxillary palpus light brown, about 0.14 of proboscis. Proboscis entirely dark, slender, elongate and slightly swollen at tip; a distinct ventral white line absent but several white scales at basal ventral part. Pedicel of antenna dark brown in colour and bare of scales; flagellum pillose, as long as or little shorter than proboscis. *Thorax:* Integument of scutum and scutellum brown covered with dark scales; a silver central line starting at anterior promontory and extending caudally to approximately the wing roots; the line broad uniformly in anterior part and towards the end. Scutal-fossal, dorsocentral, prescutellar and supraalar setae well developed. Median scutellar lobe with a patch of silver scales, lateral lobes with small patches of brown scales, without silver scales; conspicuous setae present on all three lobes posteromarginally. Mesopostnotum bare. Antepronotal lobe with conspicuous silver patch on dorsum, dark brown scales present on lower side; a row of prominent setae on anterior side. Postpronotum covered with flat brown scales on upper 2/3 and a few silver scales on lower margin; single prominent seta present at middle of the posterior border. Three fine prespiracular setae present. Postspiracular setae absent. Pleuron covered with patches of silver scales.

Paratergite bare. Silver scales forming large patch to cover most of the pleuron, including post- and subspiracular areas, most of the mesokatepisternum and the mesepimeron. Metepisternum bare. Several setae present on upper mesepimeron and prealar areas. *Legs*: All coxae and trochanters covered with silver scales. Dorsal part of all legs covered with small dark brown scales, and ventral part with a white line extending from base of femora to tips of tarsi, the line not so clear in foreleg. Junction between apical part of tibia and basal part of first tarsus with a line of fine setae (ciliation). Foretarsus Ta-I₂ shorter than Ta-I₃, apical tarsomeres

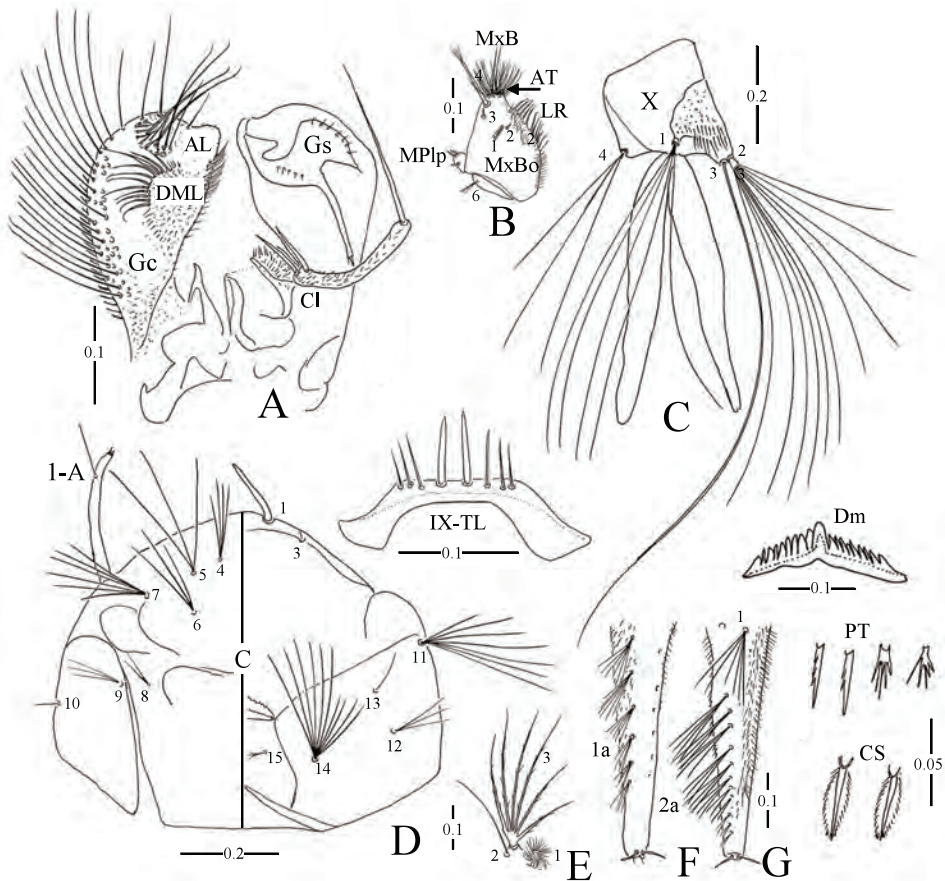


Figure 1. *Topomyia (Topomyia) katibasensis*, new species. Male (A) and 4th instar larva (B-G). A, male genitalia (paratype G-1); B, maxilla; C, abdominal segment X; D, head; E, prothoracic setae 1-3; F, siphon; G, siphon in different view. AL, apical lobe; Cl, claspette; DML, dorsomesal lobe; Gc, gonocoxite; Gs, gonostylus; IX-TL, terugam IX; AT, apical teeth; LR, laciniarastrium; MPlp, maxillary palpus; MxB, maxillary brush; MxBo, maxillary body; Dm, dorsomentum; 1-A, antennal seta 1; CS, comb scale; PT, pecten. Scales in mm.

elbowed, directed posteriorly. Ungues on all legs small, simple and equal. *Wing*: Brown-scaled. Cell R_2 about 4 times length of its stem. Alula with a row of fine, hair-like scales; upper calypter bare. *Halter*: Pedicel and capitellum covered with dark brown scales. *Abdomen*: Terga I–VIII densely covered with small, dark brown scales, except upper border of pale strip appearing as a straight line in lateral view. Sterna II–VII entirely covered with flat pale scales. *Genitalia* (Figs. 1A, 7E): Tergum of IX segment arched and broad throughout, two large (one pair) flattened spines tapering towards a point, situated centrally, close to each other on either side of midline; usually 3 fine setae on the outer side of the spine (Fig. 1, IX-TL). Gonocoxite (Gc) length about 2.5 times width at middle, narrow at base and fairly broad at apical end; on the dorsal aspect, outer 2/3 of gonocoxite is highly sclerotized and bears many long incurved setae; apical lobe (AL) with a bunch of 5–7 stout setae; dorsomesal lobe (DML) situated at slightly above the center, outer margin of the lobe bearing about 12 flattened setae and fine setae scatteringly. Dorsal lobe of claspette (Cl) is composed of broad rod-like stem which bears 2 or 3 spines basally and many fine setae uniformly from base to tip and with a narrow long elongated apical spine tapering to a point. The spine longer than the rod-like stem. Gonostylus (Gs) broad, expanded into two lobes, the outer lobe broad with several fine marginal setae and inner one slender with a gonostylar claw and with minute setae apex. Paraproct long with sclerotized arms.

Female — Unknown.

Pupa (Fig. 2, Table 1) — Abdomen (I–VIII), 2.10–2.25 mm (mean 2.17mm). Trumpet, 0.24–0.26 mm (mean 0.25 mm). Paddle, 0.46–0.48 mm (mean 0.47 mm). Integument of cephalothorax and abdomen pale yellow, with yellow brown stripes on anterodorsal aspect of abdominal segments II–VII. Chaetotaxy as figured. *Cephalothorax* (Fig. 2B): Trumpet (T), dark yellow, with distinct sculpturing; index, 3.7–4.7 (mean 4.2). *Abdomen* (Fig. 2A, C), microtrichia present on all abdominal segments. Paddle with marginal spicules. Male genital lobe large, extending to 0.59–0.63 of paddle.

Fourth-instar larva (Fig. 1B–G) — Head, 0.65 mm. Siphon, 0.51–0.55 mm (mean 0.53). Chaetotaxy of head and terminal abdominal segments as in Fig. 1C, D. Setae lightly pigmented. Abdominal and thoracic setae conspicuous and many branched. Setae 1–III–VII well developed, stellate with many branches. *Head*: Integument smooth, pale yellow in colour. Maxillar as in Fig. 1B, maxillary horn absent. Dorsomentum with a prominent middle tooth with 9 to 10 small regular teeth on either side. Seta 1-C single, prominent, thick and slightly curved inwardly, with blunt end; seta 4 with 4 branches; seta 5-C long with 3 branches, placed well behind 4-C; seta 6 long with 3 branches; seta 7 with 6 branches; setae

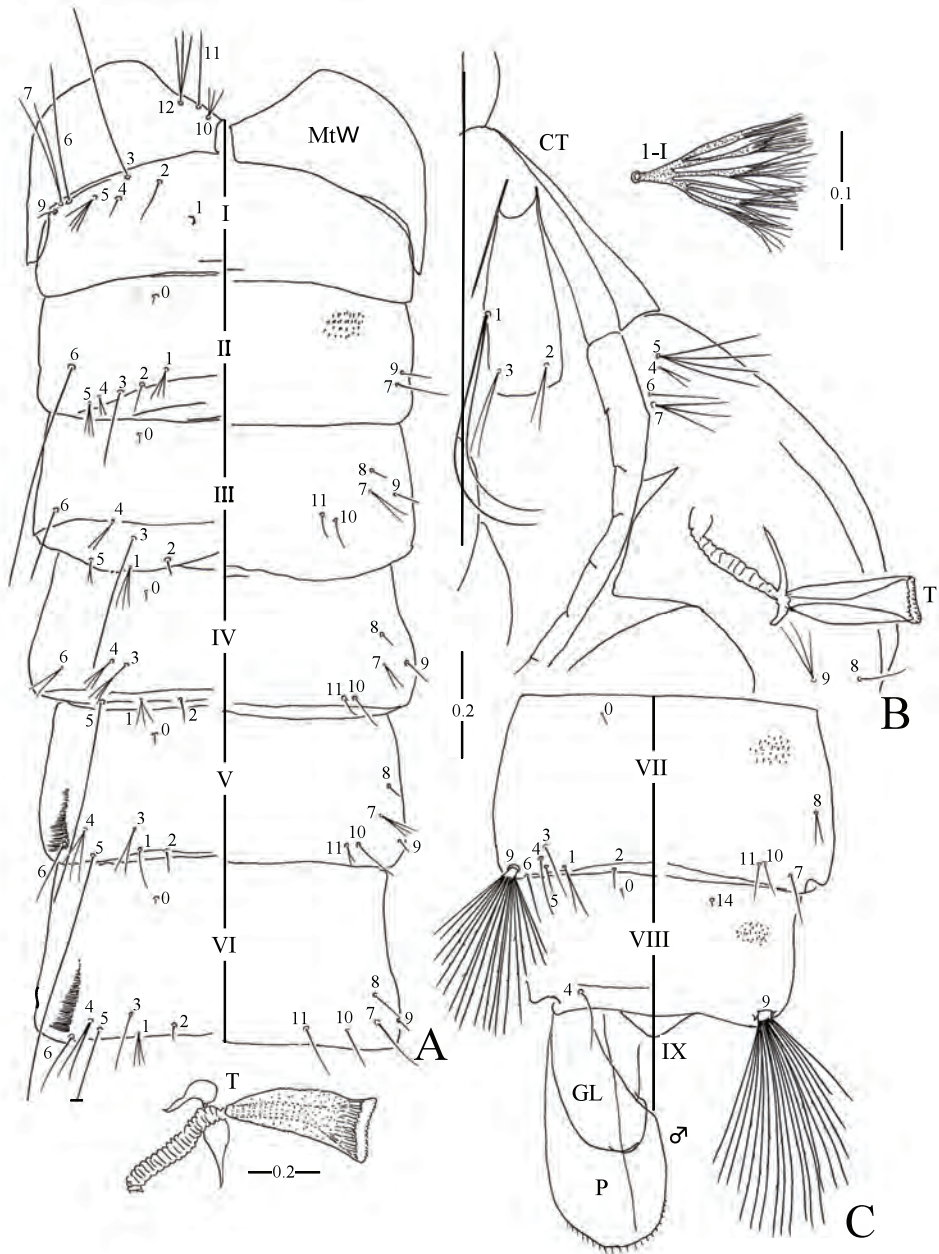


Figure 2. Pupal exuviae (A – C) of *Topomyia (Topomyia) katibasensis*, new species. A, metathoracic wing (MtW) and abdominal segments I – VI; B, cephalothorax (CT); C, abdominal segments VII – IX with genital lobe (GL) and paddle (P). T, trumpet; 1-I, seta 1 of abdominal segment I. Scales in mm.

11- and 12-C prominent with more than 7 branches. Prothoracic seta 1–3 as in Fig. 1E. *Antenna*: Length about 0.25 mm; shaft with slight narrowing of width from base to tip. Integument smooth, without spicules; seta 1-A long and single, placed on 0.75 from base. *Abdomen*: Segment VIII: Comb scales approximately 20, in irregular row or patch; very finely fringed marginally and pointed at tip (Fig. 1 CS). Segment X (Fig. 1C): Saddle incomplete, spicules present on caudolateral border; anal papilla about 2.5 times the length of the anal segment, with rounded ends. Seta 1-X long, with 5 branches, 2-X with 10, 11 branches, 3-X single, longer than the others, 4-X with 3 branches. All these setae without pectination. Siphon (Fig. 1F, G): Pale yellow pigmentation, smooth integument. Index, 5.7–6.5 (mean 6.1). Pecten with approximately 100 teeth, extending from base to apical 0.1 of siphon. Seta 1-S long with usually 6 branches; usually 6 subventral setae (1a-S), each with 2–6 branches; usually 11 or 12 subdorsal setae (2a-S) with 2–4 branches as figured (Fig. 1F, G). Comb scales (CS) as in Fig. 1, and pectens (PT) have two types as in Fig. 1.

Type specimens

Holotype ♂ (20110227-10) on pin with L (fourth-instar larva) and P (pupa) exuviae mounted on slide (159) and genitalia on other slide (G-59) with following collection data; Headquarters (N 01°38.777' and E 112°167.709') of LEWS on 27 February, 2011. Paratypes. 3♂ (20110301-3) with P (146, 287, 178) and G (G-55, -124, -69); 1♂ (20110304-5) with G (G-1); 1♂ (20110910-6) with P, L (356) with G (G-173) same place as the holotype.

Etymology

The species name *katibasensis* refers to the name of the river, Sg. Katibas that flows through the LEWS, where this new species was found.

Taxonomic Discussion

Topomyia katibasensis, new species, is separated from all other known species of the subgenus *Topomyia* by the following distinctive structures of the male genitalia: (1) A bunch of about 5–7 stout setae is present on the apical lobe of the gonocoxite; (2) Dorsomesal lobe bears about 12 flattened setae with whip-like tips; (3) Gonostylus expanded basally and bifurcated, the outer lobe is broad with several fine marginal setae and inner one is slender with a claw and minute setae apex; and (4) Tergum of IX segment arched and broad throughout, with two (one pair) large, flattened spines tapering towards a point. The spines situated centrally, close to each other on either side of midline; three fine setae are situated on outer side of the spine; they are apparently shorter than the central spines.

As the detailed descriptions of the immature stages of most species of the subgenus are not available, it is not feasible to point out the distinctive characters

of these stages of *To. katibasensis*, but a lateral patch of distinct spicules or ciliations in abdominal segments V and VI in the pupa is characteristic of *To. katibasensis*. In the larva, on the presence of many conspicuous stiff stellate setae on the thorax and abdomen and many scattered pecten on lateral and ventral sides of the siphon, this species may be closely related to *Topomyia hardini* Miyagi and Toma [10] from Sarawak but it is easily separated from the latter by the head setae 4-, 5-, 6- and 7-C which are usually 4, 3, 3 and 6 branched respectively, while in *To. hardini*, these setae are usually all single.

Biological notes

Larvae of *To. katibasensis* were collected in association with *Topomyia gracilis*, *Malaya* sp. *Aedes* sp. (*kochi* group) and *Toxorhynchites* sp. in the leaf axils of screw pines (*Pandanus*).

Distribution

Katibas, Lanjak-Entemau Wildlife Sanctuary, Sarawak, Malaysia.

***Topomyia (Topomyia) chaii* Miyagi and Toma new species** (Figs. 3, 4, 7C; Table 2)

Description

This species resembles the preceding species, *To. katibasensis*, in general appearance. It is differentiated by the following:

Male (Fig. 3A, 7C) — Wing, 2.60–2.66 mm (mean 2.63 mm). Proboscis, 1.50–1.80 mm (mean 1.65 mm). Forefemur, 1.50–1.80 mm (mean 1.65 mm). Medium in size. **Head:** Maxillary palpus brown, small, about 0.1 of proboscis. Proboscis entirely dark dorsally, elongate and swollen at tip; white scale patch at base and a narrow ventral line of white scales extending forward to the tip of proboscis. Flagellum pillose, as long as proboscis. **Thorax:** Usual silver line on scutum broad gradually toward end. All three lobes of scutellum with a patch of silver scales, often obsolete on laterals. Anteprenotal lobe with conspicuous silver scale patch uniformly and with a row of several setae on anterior side. Postpronotum covered with flat silver scales and with single prominent seta at middle. Four fine prespiracular setae present. Pleuron covered with patches of silver scales. **Legs:** All coxae and trochanters covered with silver scales. Dorsal part of all legs covered with small dark brown scales and ventral part with a white line extending from base of femora to tips of tarsi, but the line not so clear in foreleg. Joint between apical part of tibia and basal part of first tarsal segment of the hindleg with a line of fine setae (ciliation). Foretarsomere Ta-I₂ equal or shorter than Ta-I₃, apical tarsomeres usually not elbowed. Ungues of all legs small, simple and

equal. *Wing*: Brown-scaled. Cell R_2 about 3.9 times length of stem. *Abdomen*: Terga I-VIII densely covered with small, dark brown scales, except upper border of this pale strip appearing as a straight line in lateral view. Sterna II-VII entirely covered with flat pale scales. *Genitalia* (Figs. 3A, 7C): Tergum of IX segment arched and broad throughout, slightly concave on posterocentral surface, with two median flattened spines tapering towards a point, situated close to each other on either side of midline, the outer side of the spine with usually 2 flattened setae which are apparently longer than the median spines (Fig. 3, IX-TL). Gonocoxite (Gc) length about 2.4 times width at middle, narrow at base and at apical end with a row of many fine setae of inner apical margin. On the dorsal aspect, outer 2/3 of gonocoxite is sclerotized and bears many long setae; dorsomesal lobe (DML) bearing many fine and well developed hair-like setae. Dorsal lobe of claspette (Cl) bear 5-8 basal spines and composed of broader rod-like stem which bears a narrow elongated spine tapering to a point. The spine is shorter than the rod-like stem. Gonostylus (Gs) simple and slender with hook-like apex. Paraproct long with sclerotized arms.

Female — Wing, 2.30 mm. Proboscis, 1.40 mm. Forefemur, 1.50 mm. Resembles male except for following characters. Whitish scale patch on ventral aspect of proboscis absent. All coxae and trochanters covered with silvery scales. Remaining parts of legs uniformly covered with small dark brown scales dorsally, except for

Table 2. Numbers of branches for pupae of *Topomyia (Topomyia) chaii* n. sp.

Seta no.	Cephalo-thorax	Abdominal segments								
		I	II	III	IV	V	VI	VII	VIII	
0	-	-	1	1	1	1	1	1	1	1
1	2	M	1-6	1-3	2-4	1-4	1-3	1, 2	-	-
2	1-4	1	1	1	1	1	1	1	-	-
3	2-5	1	1	1-3	1-4	1-4	1-3	1-3	-	-
4	2-4	1, 2	2-4	1-5	1-4	1-6	1-4	1-4	1, 2	-
5	2-5	3-7	1, 2	1, 2	1	1	1	1	-	-
6	1	1-3	1	1-4	1-3	1-3	1, 2	1, 2	-	-
7	1-5	1-4	1-3	1-5	1-4	1-4	1, 2	1, 2	-	-
8	1, 2	-	-	1-4	1-5	1-4	1-4	1-4	-	-
9	1-3	1, 2	1	1	1	1	1	7-14*	11-15*	-
10	1-3	-	-	1-3	1, 2	1, 2	1, 2	1, 2	-	-
11	1	-	1-3	1-3	1-3	1, 2	1-3	2-4	-	-
12	2, 3	-	-	-	-	-	-	-	-	-
14	-	-	-	-	-	-	-	-	-	1

M: dendritic with many branches. *aciculated.

Obsolete and missing setae are shown with a hyphen (-).

Specimens examined; 5 pupal exuviae from LEWS, Sarawak, Malaysia

a ventral line of pale scales extending from base to apical part of femur; antenna about same length as forefemur. *Abdomen*: Terga 1–VIII densely covered with flat, dark brown scales. Lateral margin of all terga without strip of pale scales. Sterna I–VII covered by flat silver colored scales.

Pupa (Fig. 4; Table 2) — Abdomen (I–VII), 2.62–2.80 mm (mean 2.71 mm). Trumpet, 0.28–0.32 mm (mean 0.30 mm). Paddle, 0.45–0.49 mm (mean 0.47

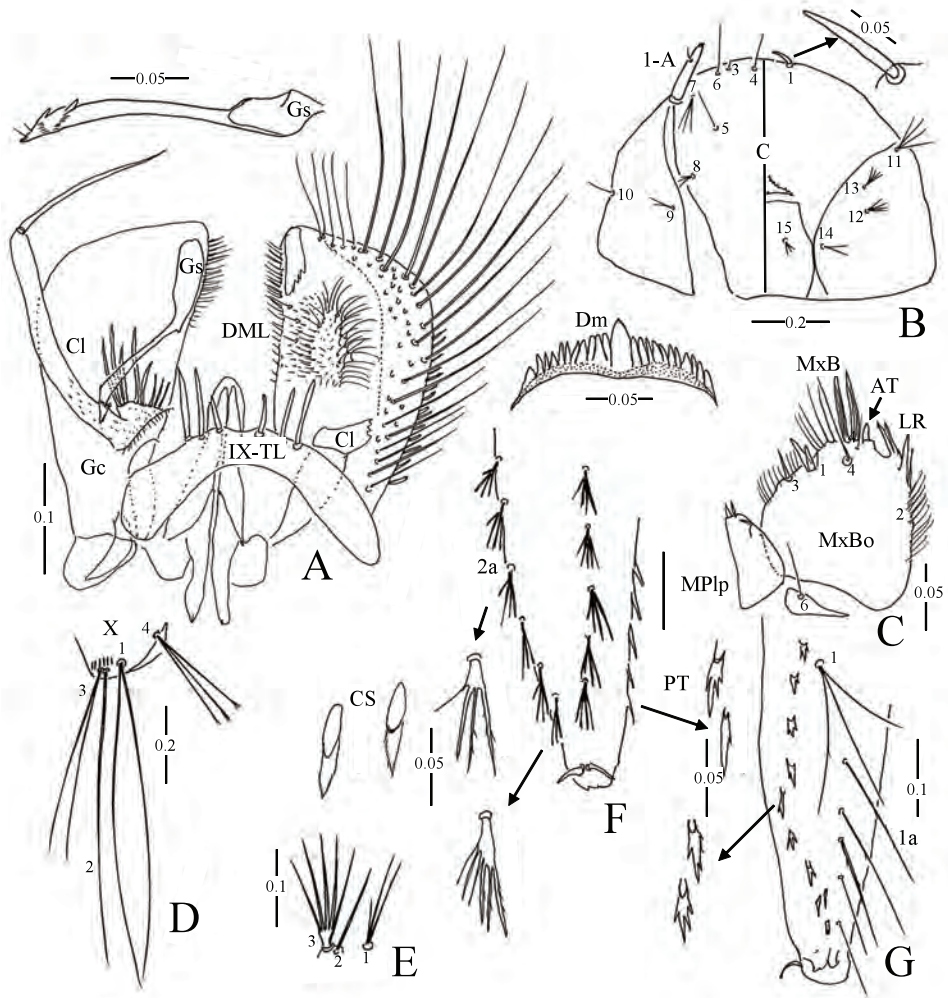


Figure 3. *Topomyia (Topomyia) chaih*, new species. Male (A) and 4th instar larva (B–G). A, male genitalia (paratype G-21); B, head; C, maxilla; D, abdominal segment X; E, prothoracic setae 1–3; F, siphon; G, siphon in different view. Cl, claspette; DML, dorsomesal lobe; Gc, gonocoxite; Gs, gonostylus; IX-TL, terugam IX; AT, apical teeth; LR, laciniarastrum; MP1p, maxillary palpus; MxB, maxillary brush; MxBo, maxillary body; Dm, dorsomentum; 1-A, antennal seta 1; CS, comb scale; PT, pecten. Scales in mm.

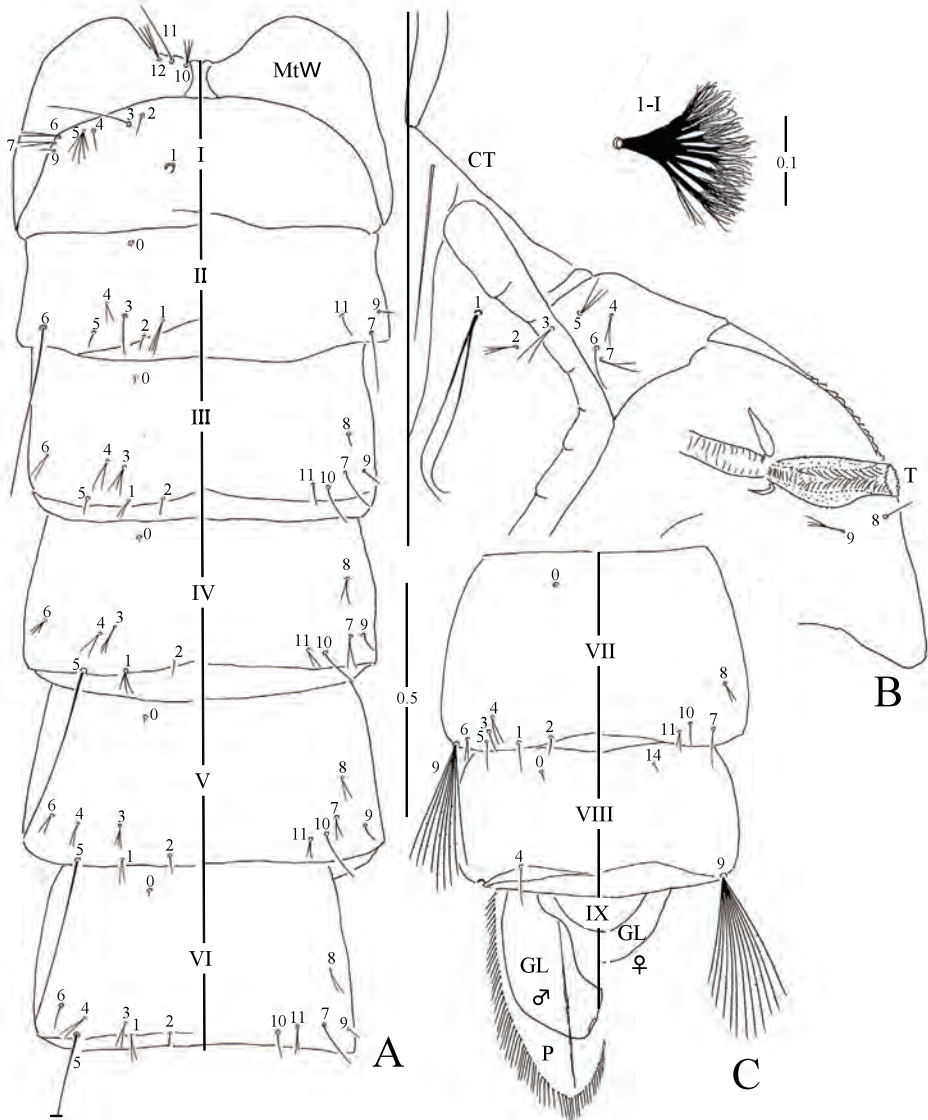


Figure 4. Pupal exuviae (A-C) of *Topomyia (Topomyia) chaii*, new species. A, metathoracic wing (MtW) and abdominal segments I-VI; B, cephalothorax (CT); C, abdominal segments VII-IX with genital lobe (GL) and paddle (P). T, trumpet; 1-I, seta 1 of abdominal segment I. Scales in mm.

mm). Integument of cephalothorax and abdomen pale yellow, with darker yellow brown stripes on anterodorsal aspect of abdominal segments II–VII. Chaetotaxy as figured. *Cephalothorax*: Trumpet: Dark yellow, with sculpturing, slightly expanded medially, index, 2.80–3.25 (mean 3.0). *Abdomen*: Microtrichia scanty on all abdominal segments. Seta 1-I long, conspicuous (Fig. 4, 1-I). Paddle with conspicuous marginal fringe. Male genital lobe (GL) large, extending to 0.73 of paddle.

Fourth-instar larva (Fig. 3 B–G) — Head, 0.65–0.79 mm (mean 0.72 mm). Siphon, 0.52–0.55 mm (mean 0.53 mm). Chaetotaxy of head and terminal segments as figured. Stellate setae present. *Head* (Fig. 3B): Width about 1.33 of length. Integument smooth, pale yellow in colour. Mouth brushes well-developed. Maxillar (Fig. 3C), horn absent. Dorsomenta (Dm) with a prominent middle tooth with 11 or 12; head seta 1-C prominent, thick, with blunt end; seta 3 single minute, 4–6-C usually single, 7-C 3 branched, 11-C developed 4 branched, 14-C bifid shorter than seta 11-C. *Antenna*: Length about 0.33 of head. Shaft with very slight narrowing of width from base to tip. Integument smooth, without spicules; pale yellow in colour. Seta 1-A short, single, situated about 0.87 from base. Prothoracic seta 1–3 as in Fig. 3E. *Abdomen*: Comb scales (CS) approximately 17 in a row; lightly pigmented; free portion finely fringed and pointed at tip. *Siphon* (Fig. 3F, G): Index, 2.61–3.14 (mean 2.87). Pecten (PT) with about 20 teeth extending from base to apical 0.85, each with a large denticle and 2, 3 small lateral denticles; seta 1-S large with 3 branches; ventral setae (1a-S) as figured, 5 setae, all these setae well developed, single; subdorsal setae (2a-S) 4–6 in number, each stellate, pointed tip, fringed laterally (Fig. 3 F). Segment X (Fig. 5D): Seta 1 long, bifid; 2 bifid; 3 long, single; 4 short triple. All setae without pectination.

Type specimens

Holotype ♂ (20110909-5) on pin with L (larva) and P (pupa) exuviae mounted on slide (247) and G (genitalia) on same slide (G-114) with following collection data: Headquarter (N 01°38.777' and E 112°167.709') of LEWS, Sarawak on 9 September, 2011. Paratypes 6 ♂♂ (20110909-5), L, P (121, 70, 93, 85, 226), G (G-24, -16, -37, -50, -104, -23), collection data same as the holotype; 1 ♂ (20110227-6), P, L (57), G (G-21) on 27 February 2011; 1 ♀ (20110909-5), P, L (119) on 9 September 2011; 1 ♀ (20110911-5), P, L (117), on 11 September, 2011, at the same place as the holotype.

Etymology

The species name *chaii* is in honour of Dr Paul Chai for his many contributions to the biodiversity conservation in the Lanjak-Entimau Wildlife Sanctuary, Sarawak.

Taxonomic discussion

Topomyia chaii has similarities in the general appearance of male genitalia with *Topomyia yongi* from Gombak, Malaysia [11]. However, *To. chaii* can be separated from the latter by following characters. The gonocoxite has a dense tuft of many curved short hair-like setae on dorsomesal lobe and apical part of gonocoxite without dense patch of setae. The rod-like dorsal lobe of claspette is not setaceous and longer than the apical spine. Two median spines of IX tergum are apparently shorter than the outer spines. As the larva of *To. chaii* is described partially and most larvae of the genus are as yet unknown, it is difficult to discuss the characteristic feature of *To. chaii*. However, the followings may be characteristic of *To. chaii*: Head seta 14-C is small with 2 branches, siphonal seta 1-S is long triple; 1a-S 5–7 in number, each seta is single branched; seta 2a-S is stellate with 5–6 branches.

Biological notes

Larvae of *To. chaii* were collected in association with *To. katibasensis*, *To. gracilis*, *Malaya* sp. and *Aedes* sp. (*kochi* group) in leaf axils of screw pines. They are not predacious.

Distribution

Katibas, Lanjak-Entemau Wildlife Sanctuary, Sarawak, Malaysia.

***Topomyia (Topomyia) nicksoni* Miyagi and Toma new species** (Figs. 5, 6, 7A, 7B; Table 3)

Description

This species resembles *To. katibasensis* in general appearance. It is differentiated as follows.

Male (Fig. 5A, 7B) — Wing, 2.16–2.60 mm (mean 2.38 mm). Proboscis, 1.60–1.66 mm (mean 1.63 mm). Forefemur, 1.66–2.00 mm (mean 1.83 mm). Medium in size, dark brown with silver markings on antepnotum, head, scutum and scutellum. *Head*: Maxillary palpus light brown, small, about 0.12 of proboscis. Proboscis slender and slightly swollen at tip; entirely dark dorsally, without distinct ventral white line but several white scales at base and apex ventrally. Vertex with several erect scales. Flagellum less pillose, about same length as proboscis. *Thorax*: Integument of scutum and scutellum brown. A median silver line on scutum straight from anterior promontory to the wing root. Scutal-fossal, dorsocentral, prescutellar and supraalar setae present. All three lobes of scutellum with dark scales, without patch of silver scales; setae present on all lobes. Antepnotal lobe with conspicuous silver patch on dorsum, dark brown scales

present on lower side; several prominent setae on anterior margin. Postpronotum covered with flat brown scales, without silver scales. Three fine prespiracular setae present. Paratergite bare. Silver scales forming large patch to cover most of the pleuron, including post- and subspiracular areas, most of the mesokatepisternum and the mesanepimeron. Metepisternum bare. Upper mesepimeron and prealar areas without setae. *Legs*: All coxae and trochanters covered with silver scales. Dorsal part of all legs covered with small dark brown scales, and ventral part with a white line extending from base of femora to tips of tarsi, but the line not so clear in foreleg. Junction between apical part of tibia and basal part of first tarsus of hindleg with a line of fine setae (ciliation). Foretarsomere Ta-I₂ apparently longer than Ta-I₃, apical tarsomeres elbowed, directed posteriorly. Ungues on all legs small, simple and equal. *Wing*: Brown-scaled. Cell R₂ about 4 times length of the stem. Alula with a row of fine, hair-like scales; upper calypter bare. *Abdomen*: terga with dark scales; sterna I–VII pale, mingled with dark scales; sternum VIII with dark scales. Genitalia (Figs. 5A, 7D). Tergum of IX segment arched and broad throughout, slightly concave on postercental surface, with two large and flattened spines tapering towards a point, situated close to each other on either side of midline, the outer side of the spine without lateral setae (IX-TL). Sternum IX broad, lateral borders sclerotized, with scattered scales and setae. Gonocoxite (Gc) length about 3.5 times width at middle, narrow at apical end. On the dorsal aspect, outer 2/3 of gonocoxite is highly sclerotized with a row of many long incurved setae; dorsomesal lobe (DML) bearing hair-tufts, composed of bundle long setae situated inner corner and many long matted and twisted setae. Dorsal lobe of claspette (Cl) composed of broader rod-like stem which bears 2 spines at base and a narrow long elongated spine at apex. The spine shorter than the rod-like stem. Gonostylus (Gs) slender, curved at apical half, with a gonostylar claw and two fine setae at apex. Paraproct long with sclerotized arm.

Female (Fig. 7A) — Wing, 2.83 mm. Proboscis, 1.93 mm. Forefemur, 1.93 mm. Resembles male except for following characters. *Head*: Whitish scale patch on ventral aspect of proboscis absent. Antenna pilose, about same length as forefemur. *Legs*: All coxae and trochanters covered with silvery scales; remaining parts of legs uniformly covered with small dark brown scales dorsally, except for a line of pale scales extending from base to apical part of ventral aspect of femur. *Abdomen*: Terga 1–VIII covered with flat, dark brown scales with metallic green sheen at certain angles. Lateral margin of all terga without strip of pale scales. Sterna I–VIII covered by flat silver colored scales.

Pupa (Fig. 6, Table 3) — Abdomen (I–VII), 2.32–2.62 mm (mean 2.47 mm). Trumpet, 0.23–0.29 mm (mean 0.26 mm). Paddle, 0.48 mm. Integument of cephalothorax and abdomen pale yellow, with yellow brown stripes on anterodorsal

Table 3. Numbers of branches for pupae of *Topomyia (Topomyia) nicksoni* n. sp.

Seta no.	Cephalo- thorax	Abdominal segments							
		I	II	III	IV	V	VI	VII	VIII
0	-	-	1	1	1	1	1	1	1
1	2	M	2-6	1-5	2-5	2-4	2-4	1-3	-
2	1-3	1	1	1	1	1	1	1	-
3	1-3	1	1	1	2, 3	2, 3	1, 2	1	-
4	2-4	1	1-6	2-4	1-5	2-4	1, 2	1	1
5	2-9	3-5	2, 3	1-3	1	1	1	1	-
6	1-4	1, 2	1	1, 2	1-3	1-3	1	1-3	-
7	1, 2	1	1, 2	1-3	1-4	2-4	1	1	-
8	1, 2	-	-	1-3	2, 3	1-4	1-3	2-4	-
9	1, 2	1, 2	1	1	1	1	1	11-26*	15-20*
10	1-4	-	-	1, 2	1-3	1, 2	1-3	1, 2	-
11	1, 2	-	1-3	1-3	1-3	1-3	1, 2	1	-
12	2-4	-	-	-	-	-	-	-	-
14	-	-	-	-	-	-	-	-	1

M: dendritic with many branches. *aciculated.

Obsolete and missing setae are shown with a hyphen (-).

Specimens examined; 4 pupal exuviae from LEWS, Sarawak, Malaysia

aspect of abdominal segments II–VII. Chaetotaxy as figured. Abdominal seta 1-I conspicuous 7 or 8 basal branched, each branch with many apical branches (Fig. 6, 1-I). *Cephalothorax*: Trumpet (T), dark yellow, with distinct sculpturing. Index, 3.2–4.0 (mean 3.6). Seta 1 long, conspicuous, bifid. *Abdomen*: Microtrichia absent on all segments. Paddle with conspicuous marginal fringe. Male genital lobe (GL) large, extending to 0.84 of paddle.

Fourth-instar larva (Fig. 5 B–F) — Head, 0.71–0.75 mm (mean 0.72 mm). Siphon, 0.57–0.59 mm (mean 0.58 mm). Chaetotaxy of head and terminal segments as figured. Setae lightly pigmented. Stellate setae present on all abdominal segments. A strongly sclerotized stellate seta with 11–13 brush-like tip branches is found in the mesothracic setae (Fig. 5, MT). *Head* (Fig. 5B): Width about 1.28 of length. Integument smooth, pale yellow in colour. Mouth brushes well-developed, brown in colour. Maxillary (Fig. 5D), horn absent. Dormontal plate with a prominent middle tooth with 8 to 10 small regular teeth on either side. Seta 1-C single, prominent, thick and slightly curved, with blunt end; setae 4–7-C rather long, single; 9-C with 4 branches; 11 and 14-C conspicuous with 5, 6 branches. *Antenna*: 0.26 mm length, about 0.38 of head; shaft with slight narrowing of width from base to tip. Integument smooth, without spicules; pale yellow in colour; seta 1-A single, situated at about 0.78 from base. *Abdomen*: Comb scales (CS) approximately 20, in 2 or 3 rows; each pointed at tip with fine

fringes at base. Siphon (Fig. 5F, G) yellow pigmentation, integument smooth; index 3.83–4.55 (mean 4.0). Pecten (PT) extending from base to apex of siphon; individual pecten pointed towards tip and finely fringed. Seta 1 of siphon large with 4 branches; accessory ventral setae (1a-S) about 7 setae in a row, each with 1–4 branches; accessory subdorsal setae (2a-S) 4 with 3–5 branches. Segment X (Fig. 5C), seta 1 with 6 branches, 2 with 7 branches, 3 single, 4 with 6 branches. All setae with fine pectination.

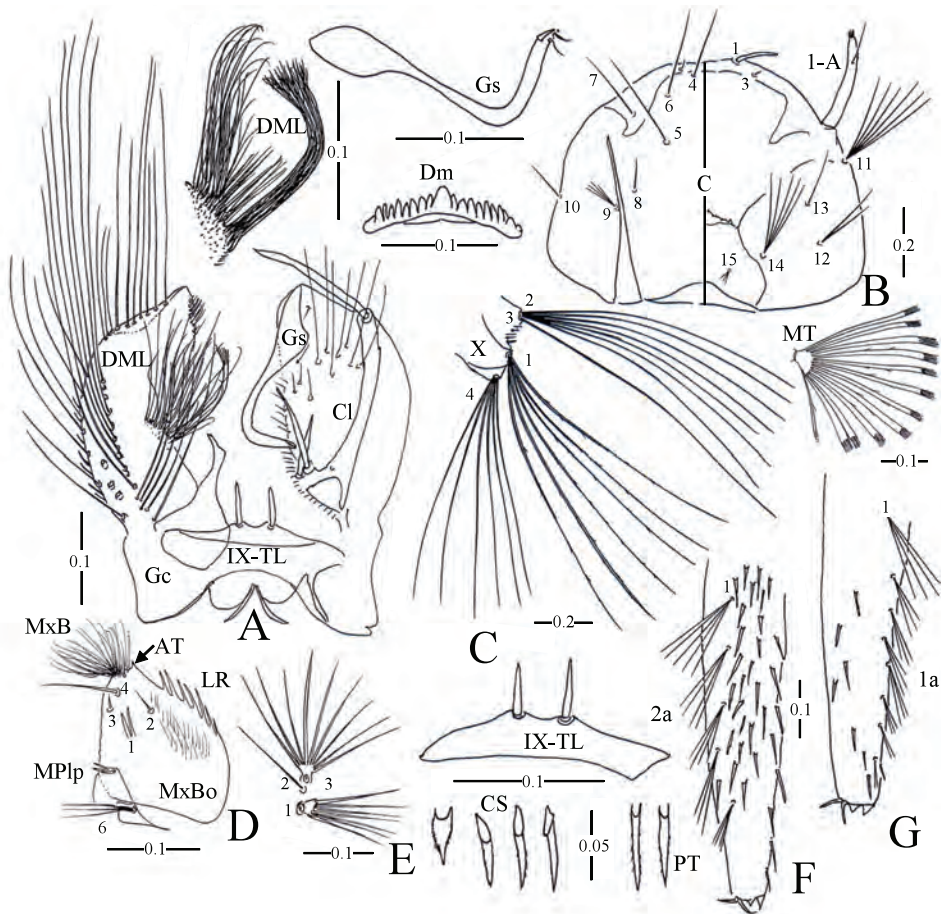


Figure 5. *Topomyia (Topomyia) nicksoni*, new species. Male (A) and 4th instar larva (B–G). A, male genitalia (paratype G-87); B, head; C, abdominal segment X; D, maxilla; E, prothoracic setae 1–3; F, Siphon; G, Siphon in different view. Cl, claspette; DML, dorsomesal lobe; Gc, gonocoxite; Gs, gonostylus; IX-TL, terugam IX; AT, apical teeth; LR, laciniarastrium; MPip, maxillary palpus; MxB, maxillary brush; MxBo, maxillary body; Dm, dorsomentum; 1-A, antennal seta 1; MT, mesothracic seta; CS, comb scale; PT, pecten. Scales in mm.

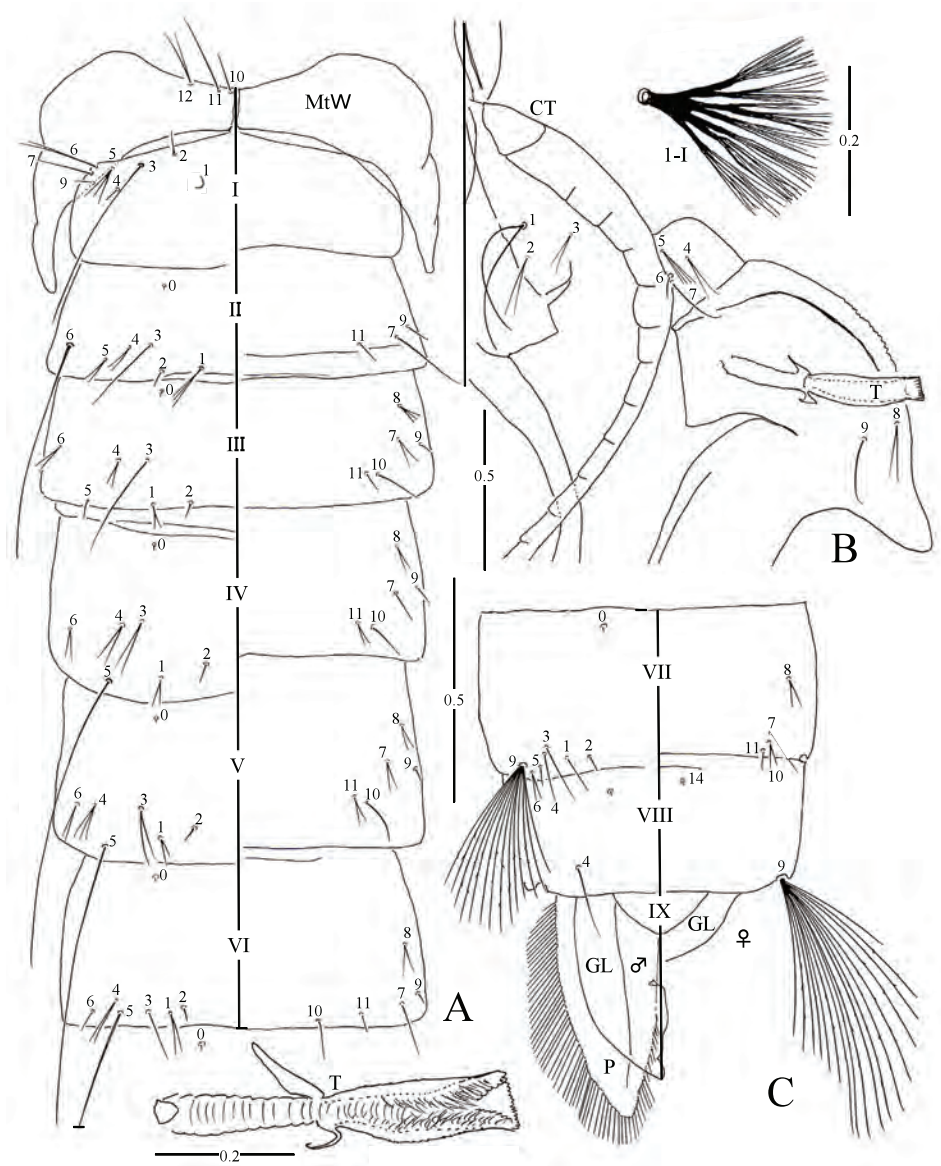


Figure 6. Pupal exuviae (A-C) of *Topomyia (Topomyia) nicksoni*, new species. A, metathoracic wing (MtW) and abdominal segments I-VI; B, cephalothorax (CT); C, abdominal segments VII-IX with genital lobe (GL) and paddle (P). T, trumpet; 1-I, seta 1 of abdominal segment I. Scales in mm.

Type specimens

Holotype ♂ (20110305-10) on pin with L (fourth-instar larva) and P (pupa) exuviae mounted on slide (239) and G (genitalia) on another slide (G-126) with following collection data: Headquarter (N 01°38.777' and E 112°167.709') of LEWS, Sarawak on 5 March, 2011. Paratypes 1♂ (20110303-2) with P, L (213), G (G-87), 3 March, 2011; 2♂♂ (20110909-5), with P, L (158,16), G (G-119, -8) on 9 Sept. 2011; 1♂ (20110911-5) with P, L (157), G (G-47) on 11 September, 2011; 2♀♀ (20110909-5) with P, L (282, 316) on 9 September, 2011.

Etymology

The species name *nicksoni* is in honour of Mr Nickson Joseph Robi, Warden, LEWS, Sarawak, for his many contributions to the biodiversity conservation and for his support and encouragement during our filed research in the Lanjak-Entimau Wildlife Sanctuary, Sarawak.

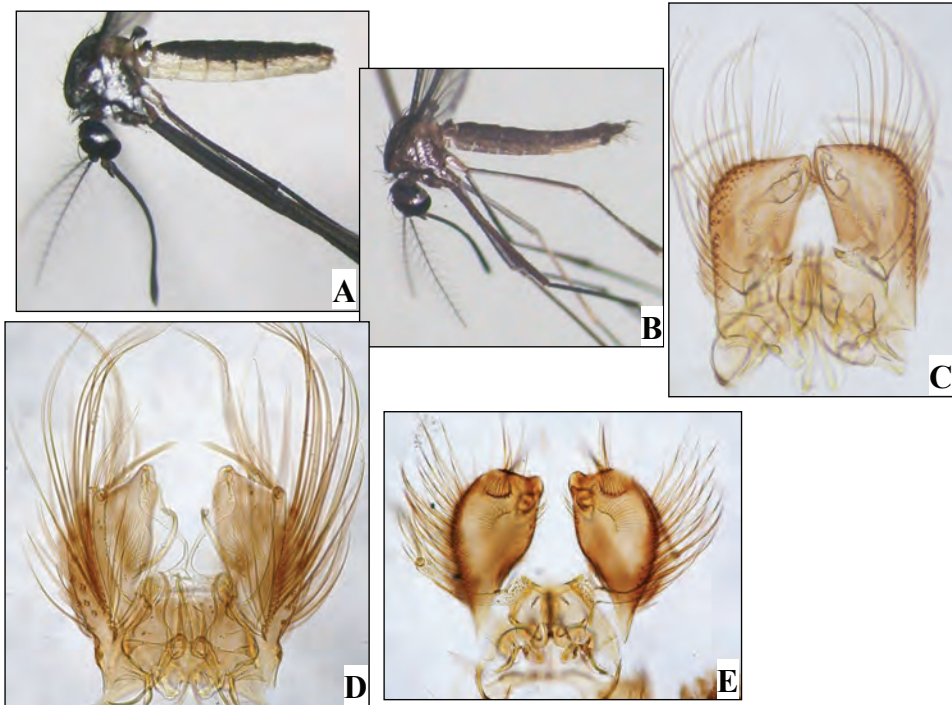


Figure 7.

- A. Female *Topomyia (Topomyia) nicksoni*, new species (lateral view)
- B. Male *Topomyia (Topomyia) nicksoni*, new species (lateral view)
- C. Male genitalia, *Topomyia (Topomyia) chaiti*, new species (ventral view)
- D. Male genitalia, *Topomyia (Topomyia) nicksoni*, species (ventral view)
- E. Male genitalia, *Topomyia (Topomyia) katibasensis*, new species (ventral view)

Taxonomic discussion

Topomyia nicksoni has the following distinctive structures of the male genitalia. Dorsomesal lobe in the gonocoxite bears conspicuous hair-tuft, composed of bundle of long setae situated at inner corner and with many long matted and twisted setae. Gonostylus is slender and curved, apical half with a gonostylar claw and 2 minute setae at apex. The IX tergum is convex at postercentral margin and bearing only one (one pair) conspicuous spine at center, without additional lateral setae. The pupa of this species is very similar to *To. chaiti* but easily separated by short trumpet, with index 3.3 (2.9 in *To. chaiti*) and the large male genital lobe, extending to 0.84 of paddle (in *To. chaiti* extending to 0.73). The larva of *To. nicksoni* has characteristic conspicuous stellate seta with 11–13 brush-tipped setae in mesothorax. This species is also related to *To. katibasensis* but differs in having head setae 4–7-C which are all single, while in the latter species, seta 4-C is 3 or 4 branched, setae 5- and 6-C are usually 3 branched, 7-C is usually 6 branched.

Biological notes

Larvae of this species were collected in the leaf axils of *Phrynium* sp. and arrowroot (Marantaceae) in association with *Topomyia* sp. near *Topomyia sabahensis* in riparian forest. They are not predacious.

Distribution

Katibas, Lanjak-Entemau Wildlife Sanctuary, Sarawak, Malaysia.

Acknowledgements – We wish to express our gratitude to the Forest Department of Sarawak for granting permission for sampling of the two-winged flies (Diptera) in the LEWS. Special thanks are also due to Dr Paul P.K. Chai, Project Manager, Transboundary Biodiversity Conservation, The Pulong Tau National Park, Sarawak for his kind help. We would like to thank Mr Joseph Nickson (Park Warden at Katibas), Ms Sir Lily (Conservation Executive) for their kind assistance in the field survey of Katibas, LEWS.

REFERENCES

1. Walter Reed Biosystematics Unit (2011) *Systematic Catalog of Culicidae*. Walter Reed Biosystematics Unit [accessed July 1, 2011]. <http://www.mosquitocatalog.org>.
2. Leicester G.F. (1908) The Culicidae of Malaya. *Studies of Medical Research Federated Malay States* 3: 18-261.
3. Edwards F.W. (1922) A synopsis of adult Oriental Culicidae (including Megarhinine and Sabethine) mosquitoes. Part II. *Indian Journal Medical Research* 10: 430-475.
4. Ramalingam S. (1975) A new species of *Topomyia* from Peninsular Malaysia (Diptera: Culicidae). *Mosquito Systematics* 7: 185-192.

5. Ramalingam S. (1983) *Topomyia haughtoni* Feng, a new record in Malaysia and a redescription of the adult and immature stages. *Mosquito Systematics* **15**: 33-40.
 6. Ramalingam S. (1987) Description of a new species of *Topomyia* from peninsular Malaysia (Diptera: Culicidae). *Mosquito Systematics* **19**: 245-250.
 7. Ramalingam S. and Banu Q. (1987) Studies on the genus *Topomyia*: 2. Description of a new species from Sabah, Malaysia (Diptera: Culicidae). *Tropical Biomedicine* **4**: 119-124.
 8. Ramalingam S. and Ramakrishna K. (1988) Studies of the genus *Topomyia* 1. A new species from Sabah, Malaysia. *Mosquito Systematics* **20**: 33-40.
 9. Miyagi I., Toma T., Ramakrishna K. and Ramalingam S. (1989) Studies on the genus *Topomyia*: 3. Redescription of *spathulirostris* and transfer to the subgenus *Suaymyia*. *Mosquito Systematics* **21**: 40-49.
 10. Miyagi I., Toma T. and Ramalingam S. (1989) *Topomyia (Topomyia) hardini*, a new species from Sarawak Malaysia (Diptera: Culicidae). *Tropical Biomedicine* **6**: 91-98.
 11. Miyagi I., Toma T. and Ramalingam S. (1990) *Topomyia (Topomyia) yongi*, a new species of mosquito from Peninsular Malaysia (Diptera: Culicidae). *Mosquito Systematics* **22**: 185-191.
 12. Miyagi I. and Toma T. (2005) *Topomyia roslihashimi*, a new species of the subgenus *Suaymyia* (Diptera: Culicidae) from Gombak, Peninsular Malaysia. *Medical Entomology and Zoology* **56**: 275-282.
 13. Miyagi I., Toma T. and Okazawa T. (2006) Redescription of *Topomyia argenteoventralis* Leicester, 1908 (Diptera, Culicidae) from Malaysia. *Medical Entomology and Zoology* **57**: 347-354.
 14. Miyagi I. and Toma T. (2007) A redescription of *Topomyia decorabilis* Leicester, 1908 (Diptera, Culicidae) from Malaysia and Indonesia. *Medical Entomology and Zoology* **58**: 251-259.
 15. Miyagi I. and Toma T. (2007) A new mosquito of the genus *Topomyia* (Diptera: Culicidae) from *Nepenthes* pitcher plants in a Bario highland of Sarawak, Malaysia. *Medical Entomology and Zoology* **58**: 164-174.
 16. Miyagi I. and Toma T. (2008) Description of a new species *Topomyia (Suaymyia) lehcharlesi* (Diptera: Culicidae) from Sarawak, Malaysia. *Medical Entomology and Zoology* **59**: 163-170.
 17. Miyagi I., Okazawa T., Toma T., Higa Y. and Leh M.U. (2009) Culicidae and Corethrellidae (Diptera) collected in Sarawak, Malaysia from 2005 to 2008. *Sarawak Museum Journal* **66**: 313-331.
 18. Miyagi I. and Toma T. (2010) Descriptions of *Topomyia auriceps* Brug and *Topomyia pseudoauriceps*, n. sp. from Sarawak, Malaysia (Diptera: Culicidae). *Medical Entomology and Zoology* **61**: 27-38.
 19. Miyagi I. and Toma T. (2010) *Topomyia (Suaymyia) kelabitensis* (Diptera: Culicidae), a new species from Sarawak, Malaysia. *Medical Entomology and Zoology* **61**: 353-361.
 20. Miyagi I., Toma T., Okazawa T. and Leh M.U. (2011) Description of pupa and larva of the Malaysian mosquito *Topomyia (Topomyia) rubithoracis* Leicester (Diptera, Culicidae). *Medical Entomology and Zoology* **62**: 93-99.
-

21. Mogi M. (2000) Phytotelmata: cryptic mosquito habitats. In Ng F.S.P. and Yong H.S. (eds) *Mosquitoes and mosquito-borne diseases* pp. 255-272. Academy of Sciences Malaysia, Kuala Lumpur.
 22. Thurman E.B. (1959) *A contribution to a revision of the Culicidae of Northern Thailand. Bull. A-100*. University of Maryland Agriculture Experiment Station, Maryland.
 23. Belkin J.N. (1962) *The mosquitoes of the South Pacific (Diptera)*. Vols. I & II. University of California Press, Berkeley and Los Angeles.
 24. Harbach R.E. and Knight K.L. (1980) *Taxonomists' glossary of mosquito anatomy*. Plexus Publishing Inc., Marlton.
 25. Harbach R.E. and Peyton E.L. (1993) Morphology and evolution of the larval maxilla and its importance in the classification of the Sabethini (Diptera: Culicidae). *Mosquito Systematics* **25**: 1-16.
-

Nucleolar organizer regions of the Indomalayan Pencil-tailed Tree Mouse *Chiropodomys gliroides* (Rodentia: Muridae)

Hoi Sen Yong^{1,*}, Phaik Eem Lim^{1,2} and Praphathip Eamsobhana³

¹Institute of Biological Sciences, University of Malaya, 50603 Kuala Lumpur, Malaysia

²Institute of Ocean and Earth Sciences, University of Malaya, 50603 Kuala Lumpur, Malaysia

³Department of Parasitology, Faculty of Medicine Siriraj Hospital, Mahidol University, Bangkok 10700, Thailand

(*E-mail: yong@um.edu.my)

Received 15-09-2012; accepted 29-09-2012

Abstract The chromosome complement of *Chiropodomys gliroides* from Peninsular Malaysia consists of two pairs of nucleolar organizer regions (NORs) – the longest acrocentric pair and the small metacentric. The NORs in both pairs are located at the terminal end; in the long acrocentric at the end of the long arm. In the metaphases, at least one element in both pairs exhibited the presence of Ag-NOR activity. The karyotype differences between the Peninsular Malaysia and Thailand taxa of *C. gliroides* and the possible existence of cryptic species are highlighted.

Keywords chromosomes – NORs – mammal – systematics – karyotype – cryptic species – *Micromys* division – Peninsular Malaysia

INTRODUCTION

Murid rodents of the genus *Chiropodomys* are characterized by the tail only sparsely covered with hair, and with the end resembling a pencil, whence the common name ‘pencil-tailed tree mice’. The genus is currently classified under the *Micromys* division of the subfamily Murinae, together with the genera *Haeromys*, *Hapalomys*, *Micromys*, *Vandeleuria*, and *Vernaya* [1]. It is represented by some six extant species – Palawan Pencil-tailed Tree Mouse *C. calamianensis*, Indomalayan Pencil-tailed Tree Mouse *C. gliroides*, Koopman’s Pencil-tailed Tree Mouse *C. karlkoopmani*, Large Pencil-tailed Tree Mouse *C. major*, Gray-bellied Pencil-tailed Tree Mouse *C. muroides*, and Small Pencil-tailed Tree Mouse *C. pusillus* [1, 2].

Of the pencil-tailed tree mice, the conventional karyotypes of *C. gliroides* have been documented for the taxa from Peninsular Malaysia [3] and Thailand [4-6]. In addition, the G- and C-banded karyotypes have been reported for the taxon from Peninsular Malaysia [7]. We report here the nucleolar organizer regions (NORs) for the taxon from Peninsular Malaysia.

MATERIALS AND METHODS

Two female *C. gliroides* were used in the present study. Metaphase chromosomes were prepared by the conventional air-drying technique [3, 8-10]. The metaphase chromosomes were treated with 7 parts 50% AgNO_3 and 3 parts of 0.02% formic acid for 2 hour at 60 °C, then stained with 4% Giemsa for 1 hour [11]. At least 20 well-spread metaphases of each specimen were photographed under oil immersion for Ag-NOR analysis.

RESULTS

The chromosome complement of the Peninsular Malaysia *C. gliroides* possessed two pairs of NORs – the longest acrocentric and the autosomal metacentric (Figs 1, 2). The NORs in both pairs were located at the terminal end; in the long acrocentric at the end of the long arm. In the metaphases, at least one element in both pairs exhibited the presence of Ag-NOR activity.

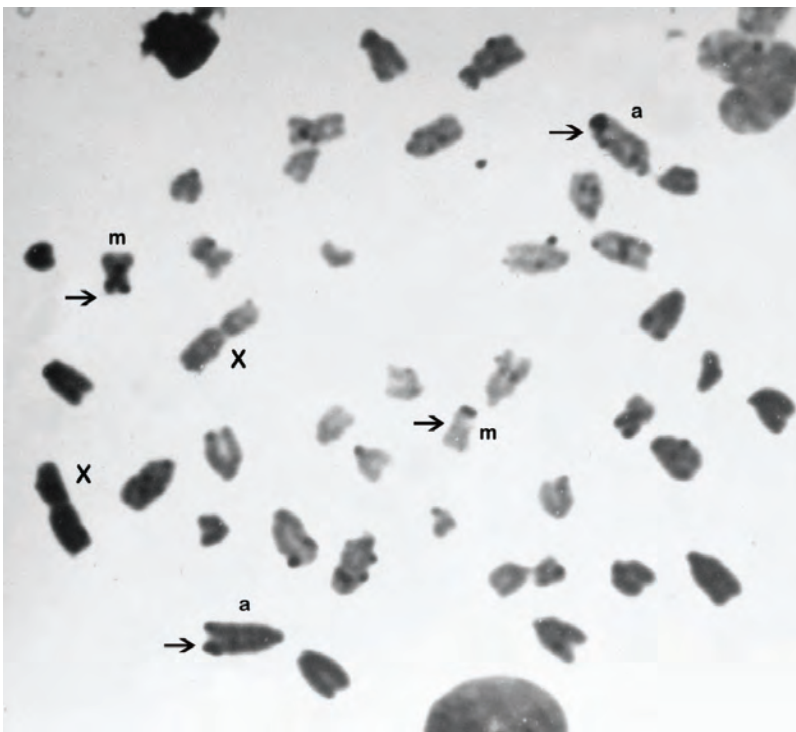


Figure 1. Metaphase chromosomes of a female *Chiropodomys gliroides* with two pairs of Ag-NORs (arrowed).



Figure 2. Metaphase chromosomes of a female *Chiropodomys gliroides* with both elements of the longest acrocentric and a single metacentric element showing Ag-NOR activity (arrowed).

DISCUSSION

Chiropodomys gliroides is a widespread species distributed in northeastern India, south China (including Hainan island), Myanmar, Thailand, Lao PDR, eastern Cambodia, Vietnam, Peninsular Malaysia and Indonesia (Java, southern Sumatra, the Mentawai Islands and other islands) [1]. Its synonyms include: *ana* Thomas and Wroughton, 1909; *jingdongensis* Wu and Deng, 1984; *niadis* Miller, 1903; *peguensis* (Blyth, 1859); and *penicillatus* Peters, 1868 [1]. The Peninsular Malaysia taxon is referred to *C. gliroides peguensis* [12], while some authors recognize *jingdongensis* as a distinct species.

This common species has been extensively studied. Various aspects of the biology of the Peninsular Malaysia *C. gliroides* have been well documented – life history [12, 13]; cytogenetics [3, 7]; and sperm morphology [14]. In the Thailand *C. gliroides*, 10/30 PCR primers of mouse satellite loci gave specific products, and 9 PCR primers of rodent (1 mouse, 8 rat) satellite loci gave positive products [15].

The chromosome complement of *C. gliroides* consists of $2N=42$ [3-7].

However there are differences in the morphology of the autosome complement as well as the sex chromosomes. The autosomes and sex chromosomes in the Thailand taxon are entirely telocentric (or acrocentric). On the other hand, the Peninsular Malaysia taxon consists of 18 pairs of acrocentric/telocentric chromosomes, one pair of small metacentrics, one pair of small submetacentrics, a large metacentric X chromosome, and a medium-size submetacentric Y [3, 7]. These karyotype differences are highly indicative of the occurrence of cryptic/sibling species in *C. gliroides*.

Similar karyotypic differences have also been found in a related genus *Hapalomys* of the *Micromys* division. The karyotype of *H. delacouri* from Thailand consists of $2n=48$ chromosomes and $NFa=92$. All the autosomes were bi-armed (metacentric or submetacentric), and the metacentric X is the largest in the karyotype while the acrocentric Y is the smallest element [4]. On the other hand, the diploid karyotype of the Vietnam *H. delacouri* is 38 ($NFa=48$), consisting of six pairs of bi-armed and 12 pairs of acrocentric autosomes decreasing in size; plus a large metacentric X chromosome and Y chromosome, also metacentric, that is equal in size to the largest pair of acrocentric autosomes [16].

The significantly different karyotypes for *H. delacouri* from northern Thailand and Vietnam indicate the two taxa are distinct species, with the Thailand taxon probably referable to the taxon *H. pasquieri* described from north-central Laos [16]. The usefulness of karyotype for species discrimination is also supported by the karyotype of a congeneric species *H. longicaudatus* from Peninsular Malaysia which has $2n=50$, with 23 pairs of uniarmed and 1 pair of small bi-armed autosomes, metacentric X and subacrocentric Y sex chromosomes [17]. The X chromosome is the largest element in the complement, while the Y-chromosome is the only morphological type among the larger sized chromosomes.

As far as known there is no report on NORs for any taxa of *C. gliroides*. It remains to be determined if taxa from other geographical areas possess similar NOR pairs. The information, coupled with the karyotype, will provide insights into the existence of cryptic/sibling species.

Acknowledgements – This work is supported by research grants H-5620009 and H-50001-00-A000025. We thank the University of Malaya and Mahidol University for supporting our collaborative research.

REFERENCES

1. Musser G.G. and Carleton M.D. (2005) Superfamily Muroidea. In: D.E. Wilson and D.M. Reeder (eds). *Mammal Species of the World. A Taxonomic and Geographic Reference*. 3rd ed. pp. 894-1531. Johns Hopkins University Press, Baltimore.
2. Corbet G.B. and Hill J.E. (1992) *The mammals of the Indomalayan Region: a systematic review*. British Museum (Nat. Hist.), London.

3. Yong H.S. (1973) Chromosomes of the pencil-tailed tree mouse, *Chiropodomys gliroides* (Rodentia, Muridae). *Malayan Nature Journal* **26**: 159-162.
 4. Badenhorst D., Herbreteau V., Chaval Y., Pagès M., Robinson T.J., Rerkamnuaychoke W., Morand S., Hugot J.-P. and Dobigny G. (2009) New karyotypic data for Asian rodents (Rodentia, Muridae) with the first report of B-chromosomes in the genus *Mus*. *Journal of Zoology* **279**: 44-56.
 5. Marshall J.T. Jr. (1977) Family Muridae: rats and mice. In: Lekagul B. and McNeely J.A. (Eds) *Mammals of Thailand* pp. 396-487. Association for the Conservation of Wildlife, Sahakarnbhat Co., Bangkok, Thailand.
 6. Tsuchiya K., Yosida T.H., Moriwaki K., Ohtani S., Kulta-Uthai S. and Sudto P. (1979) Karyotypes of twelve species of small mammals from Thailand. *Report Hokkaido Institute of Public Health* **29**: 26-29.
 7. Yong H.S. (1983) Heterochromatin blocks in the karyotype of the pencil-tailed tree-mouse *Chiropodomys gliroides* (Rodentia: Muridae). *Experientia* **39**: 1039-1040.
 8. Yong H.S. (1968) Karyotype of four Malayan rats (Muridae, genus *Rattus* Fischer). *Cytologia (Tokyo)* **33**: 174-180.
 9. Yong H.S. (1969) Karyotypes of Malayan rats (Rodentia-Muridae, genus *Rattus* Fischer). *Chromosoma* **27**: 245-267.
 10. Yong H.S., Eamsobhana P. and Lim P.E. (2012) Sex chromosome constitution and supernumerary chromosomes in the large bandicoot rat, *Bandicota indica* (Rodentia, Muridae) from Peninsular Malaysia. *Journal of Science and Technology in the Tropics* **8**: 21-27.
 11. Yong H.S. (1984) Robertsonian translocation, pericentric inversion and heterochromatin block in the evolution of the Tailless Fruit Bat. *Experientia* **40**: 875-876. [now: Cellular and Molecular Life Sciences Volume 40, Number 8 (1984), 875-876, DOI: 10.1007/BF01952004]
 12. Medway Lord (1978) *The wild mammals of Malaya (Peninsular Malaysia) and Singapore*, second edition. Oxford University Press, Kuala Lumpur.
 13. Medway Lord (1967) Breeding of the pencil-tailed tree-mouse. *Journal of Mammalogy* **48**: 20-26.
 14. Breed W.G. and Yong H.S. (1986) Sperm morphology of murid rodents from Malaysia and its possible phylogenetic significance. *American Museum Novitates* No. 2856: 1-9.
 15. Srikwan S., Field D. and Woodruff D.S. (1996) Genotyping free-ranging rodents with heterologous PCR primer pairs for hypervariable nuclear microsatellite loci. *Journal of Science Society Thailand* **22**: 267-274.
 16. Abramov A.V., Aniskin V.M. and Rozhnov V.V. (2012) Karyotypes of two rare rodents, *Hapalomys delacouri* and *Typhlomys cinereus* (Mammalia, Rodentia) from Vietnam. *Zookeys* **164**: 41-49. doi: 10.3897/zookeys.164.1785.
 17. Yong H.S., Dhaliwal S.S. and Lim B.L. (1982) Karyotypes of *Hapalomys* and *Pithecheir* (Rodentia, Muridae) from Peninsular Malaysia. *Cytologia* **47**: 535-538. doi: 10.1508/cytologia.47.535
-

Distribution mapping of Koak kaok (*Philemon buceroides*) in the edge forest of Gunung Rinjani National Park, Lombok, Indonesia

I Wayan Suana*, Kurniasih Sukenti and Sri Puji Astuti

Department of Biology, Faculty of Mathematic and Natural Sciences, University of Mataram.

Jalan Majapahit 62, Mataram 83125, Lombok, Indonesia

(*Email: iwayansuana.unram@gmail.com)

Received 14-11-2012; accepted 24-11-2012

ABSTRACT *Philemon buceroides* (Lombok: koak kaok) is a Wallacea endemic bird found in Lombok. In 1980s, koak kaok was widely distributed in all areas of Lombok. Because of hunting to keep as pet, koak kaok is rarely found in Lombok nowadays. The aim of this study is to obtain the distribution map of koak kaok in the edge forest of Gunung Rinjani National Park, so that this site could be managed as a conservation area to conserve koak kaok in Lombok. Two methods (interview and observation) were used in this study. Interview was directed to the people living around the forest, and then followed by field observation. Forest areas where koak kaok could be found were marked using Global Positioning System (GPS). Data from the GPS were processed using MapSource, ArcView GIS and AutoCAD in order to obtain the distribution map of koak kaok in Lombok. Based on the interview there were 15 areas that contained koak kaok, whereas from field observation there were only eight areas where koak kaok could be found. As koak kaok rearing is still a problem, it is advocated that the only way to conserve it in Lombok is to gazette the edge forest of Gunung Rinjani National Park into a conservation area.

Keywords *Philemon buceroides* – Gunung Rinjani National Park – mapping – distribution

INTRODUCTION

Philemon buceroides (Lombok: koak kaok) is a Wallacea endemic bird. Lombok Island is one area that contains koak kaok [1]. Koak kaok is a nectarivore but also eats insects and fruits [2]. It usually lives singly or in pairs, rarely found in groups except when plants are in blossom or bearing fruits [3].

Based on Indonesia's Government Policy Number 7 in 1999, koak kaok is a protected species. Nevertheless, hunting of koak kaok cannot be stopped yet because of its high economic value. Lack of strict monitoring and law enforcement and the low awareness of people about nature conservation are factors contributing to the decrease of koak kaok population in Lombok. The threat of extinction becomes more serious because koak kaok ex-situ rearing is still a problem [4, 5]. Therefore the best solution is in-situ conservation.

Up to 1980s, koak kaok was usually found in Lombok. It looked for food and nested in plantation near the human settlement (Nursati, personal communication). Because of increasing hunting, it is difficult to find koak kaok around the village nowadays. Based on the information from people around the village, koak kaok still exists in the limited area in the edge forest of Gunung Rinjani National Park. It is therefore important to conduct a study to determine the occurrence and distribution of koak kaok in that area. The resulting distribution map could be a reference for forest management in Gunung Rinjani National Park to gazette the edge forest as a conservation area to preserve the koak kaok in Lombok.

MATERIALS AND METHODS

Study site

This study was carried out in the edge forest of Gunung Rinjani National Park in July till December 2010.

Sampling

Two methods, interview and field observation, were used in this study. Interview was directed to 90 respondents domiciled around the study area. Interview was also directed to the officials of Gunung Rinjani National Park Office, Natural Resources Office and World Wide Foundation for Nature. Data from the interview served as early guideline for field observation.

Field observation was conducted by visiting the area that presumably contained the koak kaok, based on the interview. Areas that contained koak kaok were then marked using GPS. Point coordinates of the location where koak kaok could be found were plotted on digital maps of Lombok Island and Gunung Rinjani National Park. In addition to marking the location coordinates, data on the abundance of koak kaok and characteristic of the habitat were also collected.

Data analysis

Data collected from observation were processed using MapSource 3.00, ArcView GIS 3.3 and AutoCAD, and then analyzed descriptively.

RESULTS AND DISCUSSION

Based on the interview, koak kaok was presumably present in 15 areas of the forest of Gunung Rinjani National Park. However field observation revealed only eight areas that contained koak kaok (Table 1, Fig. 1).

At Gangga forest, koak kaok twitter was heard during observation at about 1100 hr. The bird was not seen because of the steep area. The forest in Gangga is dominated by *Erythrina subumbrans*. The plantations directly adjacent to the

Table 1. Distribution of koak kaok in the edge forest of Gunung Rinjani National Park based on the interview and observation.

No.	Forest	Interview	Observation
1	Gangga	Present	Present
2	Monggal	Present	None
3	Santong	Present	Present
4	Salut	Present	Present
5	Belanting	Present	Present
6	Obel-Obel	Present	Present
7	Loloan	Present	None
8	Semotoh	Present	Present
9	Joben	Present	Present
10	Jeruk Manis	Present	None
11	Lemor	Present	None
12	Perigi	Present	None
13	Kerandangan	Present	Present
14	Sesaot	Present	None
15	Kumbi	Present	None

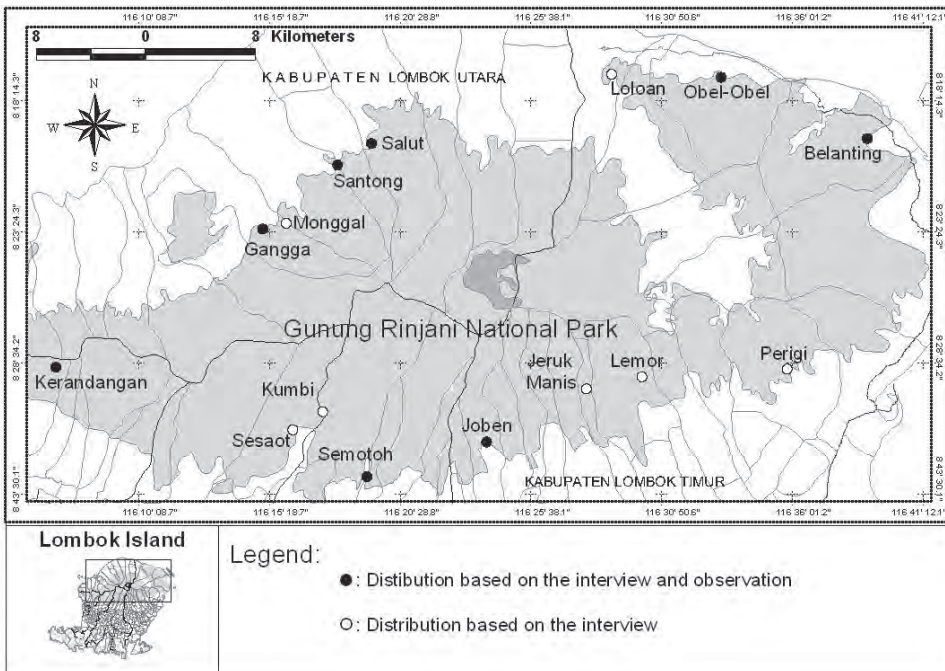


Figure 1. Distribution map of koak kaok in the edge forest of Gunung Rinjani National Park, Lombok, Indonesia.

forest were cultivated with coffee, banana and cacao. In addition to nectar from *E. subumbrans*, the people around the forest said koak kaok frequently entered their plantation looking for food.

Koak kaok was also being caught by some people using birdlime. A bird was kept in the cage in a villager's house. This bird was caught from the villager's plantation area.

At Monggal forest, field observation did not record any koak kaok, although the interview indicated its presence in this area. Its absence might be due to weather and food availability. Cloudy weather can influence the presence of birds, not only koak kaok but also birds in general. Besides, the koak kaok's favourite nectar source (*E. subumbrans*) was not in bloom.

Because of heavy rain, koak kaok was not observed in Santong forest during the observation period, although the interview indicated its existence in this area, and evidenced by a villager keeping a koak kaok baby bird taken from its nest in Santong forest several days before this observation.

Based on the characteristic of the habitat and food availability, Santong forest is a suitable site for koak kaok's existence. Koak kaok prefers tall tree with low density of branches, like *Ceiba pentandra* and *E. subumbrans* which are abundant in this area.

Field observation at Salut forest did not record any koak kaok in this area. However some birds were kept by a villager. The owner revealed that those birds were caught using birdlime, around the plantation. This is indicative of koak kaok's existence in this area.

Based on the interview, koak kaok twitter was still heard frequently from Belanting forest and Tritip forest situated across Belanting. Sometimes, the villagers who looked for firewood near Tritip forest could hear the koak kaok twitter. This bird was heard twitting at 0900 hr during the field observation, indicating its existence in this area.

Obel-Obel forest in the north coastal-area of Lombok consisted of rice cultivation area, human settlements or production forest and primary forest. According to the villagers, koak kaok twitter could be heard frequently very early in the morning or about 0400 hr and in the afternoon at about 1800 hr. During the field observation, koak kaok twitter was heard at about 1500 and 1600 hr around the primary forest beside the production forest.

Loloan forest, adjacent to Bayan area, is dominated by shrubs. Field observation did not record any koak kaok because this was an open area. Koak kaok does not like open area because it needs a place for going back after foraging [2]. Some respondents stated that koak kaok was difficult to find since 1990s.

Semotoh forest, close to Teratak village, is a distribution zone for koak kaok. This forest was not too dense and had many big trees, making it suitable for foraging and roosting. The edge of this forest also contained a lot of *E. subumbrans*. Koak kaok twitter was heard at 0900 hr during the field observation.

Based on the interview with the villagers around the edge of Joben forest, koak kaok frequently twitted back and forth in the morning and at night. Field

observation however did not record any koak kaok in the hill close to the entrance of Joben forest. Nonetheless a bird was kept by a villager who trapped it with birdlime.

At Jeruk Manis forest, the villagers stated that koak kaok twitter was frequently heard around the forest. Because of heavy rain, no bird was evident during the field observation. It also might be because the *E. subumbrans* was not in bloom at that time.

Lemor forest is close to the entrance of Gunung Rinjani National Park. Based on the interview, the villagers carrying out some activities in this forest heard koak kaok twitter frequently. However there were no signs of koak kaok during the field observation.

Perigi forest is close to coconut cultivation. Field observation did not reveal any koak kaok, although some villagers stated that they usually heard koak kaok twitter in this area.

At Kerandangan forest, koak kaok was found at about 1600 hr around Taman Wisata Alam Kerandangan, after hearing their twitter earlier.

The interview indicated some koak kaoks to be present in Sesaot forest. However no bird was observed during the study.

Field observation did not reveal any koak kaok in Kumbi forest, although some respondents stated that the bird still existed here.

The presence of koak kaok in a particular habitat is not determined by dominant plant species, but more influenced by blooming season of the plant and the height of the tree [2]. One of the suitable plant species for koak kaok's habitat is *E. subumbrans*, especially when it is in bloom [3]. Most of the *E. subumbrans* in the study area were not blooming during field observation, hence the absence or slim chance of finding the bird. Besides, koak kaok is a solitary bird rarely found in large number.

The tall trees with branches and twigs which are not too dense are the favourite habitat of koak kaok. Shrubs and open area are not preferred by koak kaok, because they always roost after catching their prey [2]. All these factors make the secondary forest between primary forest and cultivation area in Gunung Rinjani National Park a suitable habitat for koak kaok.

Koak kaok is frequently seen foraging at the villager's cultivation areas adjacent to the forest. This attracts the villagers to hunt them, especially the market demand of this bird is high. The increase of koak kaok hunting for pet or for trading can cause the decrease of its population in the natural environment especially its presence is rare nowadays. If this situation persists for a long time, it will possibly result in the extinction of koak kaok in Lombok. It therefore requires serious thoughts and action to preserve the koak kaok in nature. It is of paramount importance because koak kaok is difficult to rear in captivity [4]. In-situ conservation is the most suitable way for conserving the species.

Illegal logging, as in Belanting, can also cause disturbances in koak kaok habitat. In addition to damaging the koak kaok's habitat, felling of trees using sawing machine can also lead to sound pollution. The sound of sawing machine can be heard within the radius of two kilometers from the logging area. It is without doubt that it can disturb the koak kaok, considering that this bird is very sensitive to noise.

CONCLUSION

Some of the areas at the edge of Gunung Rinjani National Park are the natural habitat for koak kaok in Lombok. The edge forest of Gunung Rinjani National Park should therefore be turned into in-situ conservation area for koak kaok to preserve it in Lombok.

Acknowledgements – Thank you to M. Feizar Rezamudra Sahidu, S. Si.; Iwan Desimal, S. Si.; Lalu Rizani Bain, S.Si.; and Ahmad Ruhardi, S.Si. for the field assistance. To Research Division of the University of Mataram, thank you for the research agreement.

REFERENCES

1. Coates B.J. and Bishop K.D. (2000) *Birds of Wallacea: Celebes, Moluccas and Nusa Tenggara*. BirdLife International-Indonesia Programmed & Dove Publications Pty Ltd., Bogor.
 2. Endang T. (2009) Koakkiau. http://id.wikipedia.org/wiki/Gunung_Rinjani.
 3. Yamin M. (2003) Population and association between *Philemon buceroides* and plant species in its habitat in the Hunting Park of Moyo Island. *Journal of Biologi Tropis* 4: 43-50.
 4. Prana M., Utami E.B. and Widyabrata (1993) Bird rearing programmed in Taman Mini Indonesia Indah. Paper of one day seminar on bird and its conservation. Department of Biology, University of Indonesia, Jakarta.
 5. Setio P. and Takandjandji M. (2006) Ex-situ conservation of endemic rare bird through rearing. The main paper of research gain expose: conservation and rehabilitation of forest resource, Padang, 20 September 2006.
-

Reinforcement of multiwalled carbon nanotubes/natural rubber nanocomposite prepared by latex technology

**Azira Abd. Aziz^{1,a}, Dayang Habibah Abang Ismawi Hassim¹,
A. B. Suriani² and Mohamad Rusop Mahmood³**

¹Advanced Rubber Technology Unit, Technology & Engineering Division, Malaysian Rubber Board, RRIM Research Station Sg. Buloh, 47000 Selangor, Malaysia

²Department of Physics, Faculty of Science and Mathematics, Universiti Pendidikan Sultan Idris, 35900 Tanjung Malim, Malaysia

³NANO-SciTech Centre, Institute of Science, Universiti Teknologi MARA, 40450 Shah Alam, Selangor, Malaysia

(^aEmail: azira@lgm.gov.my)

Received 12-10-2012; accepted 18-10-2010

Abstract Reinforcement of natural rubber was achieved using multiwalled carbon nanotubes (MWCNTs) dispersed with non-ionic, polymeric-based surfactant. MWCNTs were first dispersed in aqueous solution of INUTEC driven by sonication and then mixed with natural rubber latex. From these mixtures MWCNTs with natural rubber were prepared by casting method. The morphology of the reinforced latex films was investigated by FESEM and AFM. When applying adequate preparation conditions, MWCNTs were well dispersed and homogeneously incorporated in the natural rubber matrix. Mechanical and electrical test results showed an increase in the tensile strength and conductivity than to pure natural rubber. The nanocomposites possess the good tensile strength even without extensive purification on the nanomaterials produced and without any pretreatment on the natural rubber used. The approach presented can be adapted to other MWCNTs/polymer latex systems.

Keywords Multi-walled carbon nanotubes – natural rubber composite – tensile strength

INTRODUCTION

Organic-inorganic hybrid materials have been extensively studied lately [1-3]. Incorporation inorganic structures, such as clusters or particles in organic matrix [4], with the formation of hybrids using porous or layered inorganic materials either by interpenetration of the organic polymers into voids [5] or by exfoliations of the inorganic materials, have been carried out. A recent method involves the 'in-situ' generations of inorganic scaffolds within the polymeric matrix by sol-gel/mixing with the latex techniques. The main advantage of this technique is low temperature requirement for the formation of composites.

The incorporation of microscale or larger inorganic fillers into organic polymers has been scientifically well explored. However, decrease in size of

the inorganic component into the nanodimensions and simultaneous increase in surface area result in new extraordinary material properties, including thermal [6], mechanical [7], electrical [8] and magnetic [9], which can be engineered through various means.

From a thermodynamic point of view, one can distinguish between several ways to incorporate inorganic systems in organic polymers through the mixing method, depending on the nature of interactions between the moieties: materials with strong (covalent, ionic and coordination bonds) [10, 11] or weak (van-der-Waals, hydrogen bonds, hydrophilic-hydrophobic balance) [12, 13] interaction or even without any chemical interaction between the two components [14]. Energetically favourable interactions at the organic-inorganic interfaces bring down the interfacial tension and help in attaining homogeneity within the hybrid composite systems. In our earlier communication, we have reported novel organic-inorganic hybrid nanocomposite from natural rubber and MWCNTs by using wet mixing technique [15]. It has been observed that with substantial physical interaction, the mechanical properties can be significantly improved just by MWCNTs dispersion.

Due to very good intrinsic mechanical properties, high aspect ratio, low density, and high surface area, MWCNTs seem to be ideal candidate for the application as fillers in polymer matrices [16]. Most efforts have dealt with glassy matrices, such as polyvinyl alcohol, polymethyl methacrylate, epoxy, etc, where significant level of reinforcement has been achieved [16]. In contrast, there are few reports on using carbon nanotubes as reinforcing fillers in rubber matrices, although the first work by Froglet *et al.* [17] showed that MWCNTs are very promising for this application. In the specific case of natural rubber (NR), Bokobza and Kolodziej [18] have made detailed investigation of the reinforcing effect by MWCNT and also concluded that CNTs are efficient reinforcing elements. They suggest that surface modification can be used to modify the reinforcing ability of CNTs. Atieh *et al.* [19] also achieved significant reinforcement of natural latex with MWCNT.

To incorporate CNTs in polymer matrices, several methods have been proposed, including melt-processing [20, 21] and extrusion [22], mechanical stretching [23], spin coating [24], the use of latex technology [25] or magnetic fields [26], a coagulation method [27], and in situ polymerization [28]. Recent studies have demonstrated that latex technology can be successfully applied to prepare MWCNT/polymer nanocomposites [15]. In the present study, we investigate the dispersion capability of MWCNTs with biodegradable stabilizer (Inutec) and in the natural rubber matrix by using FESEM, AFM and FTIR, respectively. The morphological results obtained are correlated with the conductivity of the nanocomposites.

MATERIALS AND METHODS

The two main materials used in this work were: (1) Natural Rubber latex 'HA latex' in ammonia solution, kindly supplied by the USTL, Malaysian Rubber Board, with the total solid content of 60.5%; and (2) MWCNTs purchased from Shenzhen Nanotech (China). The samples were synthesized by thermal chemical vapour decomposition of hydrocarbon gases, with 10-20 nm diameter, 5-15 μm length, and 95% purity.

For the preparation of nanocomposites containing 0.1, 0.5, 0.7 and 1.0 wt% of MWCNTs, Inutec (stabilizer) was dispersed in 10 mL of water by sonicating the mixture in bath sonicator for 30 min. The dispersion was then added to natural rubber latex and stirred magnetically for 24 h and sonicated for 30 min in a bath sonicator. Finally the mixture was poured into a film casting mould and dried at 60 $^{\circ}\text{C}$ for 24 h to obtain freestanding nanocomposite films.

RESULTS AND DISCUSSION

Figure 1 shows the FESEM micrographs of 0% (blank), 0.3%, 0.5%, 0.7% and 1.0% nanocomposites. All the images except 0% (blank) as control showed the existence of MWCNTs as the white spots (marked with the black arrow), dispersed within the natural rubber matrix. MWCNTs were scattered and their average dimensions were around 20 nm.

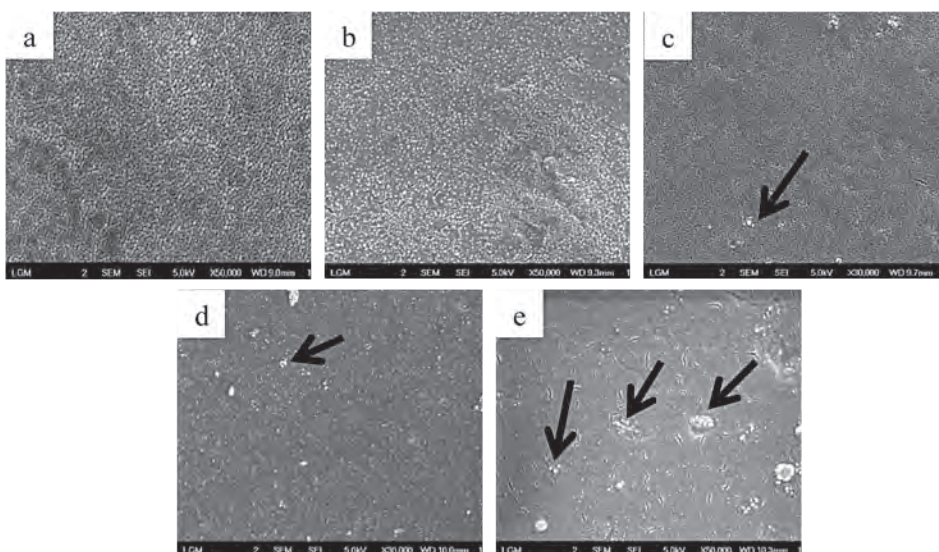


Figure 1. FESEM images on surfaces of the MWCNTs/NR nanocomposites at (a) 0% (b) 0.3%, (c) 0.5%, (d) 0.7% and (e) 1.0%. Arrow indicates MWCNT.

The 0.3% MWCNTs nanocomposites contained the lowest MWCNTs concentration, therefore also the least number of MWCNTs (Fig. 1b). Dispersed MWCNTs, in this case, increased in number along with their average dimensions, within the range of 30-40 nm. The increment in diameter of the MWCNTs was due to the higher MWCNTs formation in the hybrid nanocomposites.

The micrograph does not show clear indications for the formation of MWCNTs networks. The filler-polymer interaction at the organic-inorganic interfaces within the composites probably played the key role in dispersing the MWCNTs over the rubber matrix instead of forming any network structure within the matrix. The 1.0% MWCNTs nanocomposites discretely exhibited a dense MWCNTs structure (Fig. 1e), due probably to very high concentration of MWCNTs in the leading to embedded tubes within the films.

AFM imaging (Fig. 2) did not show any aggregates, confirming that MWCNTs were properly embedded in the films and did not impede latex spheres coagulation.

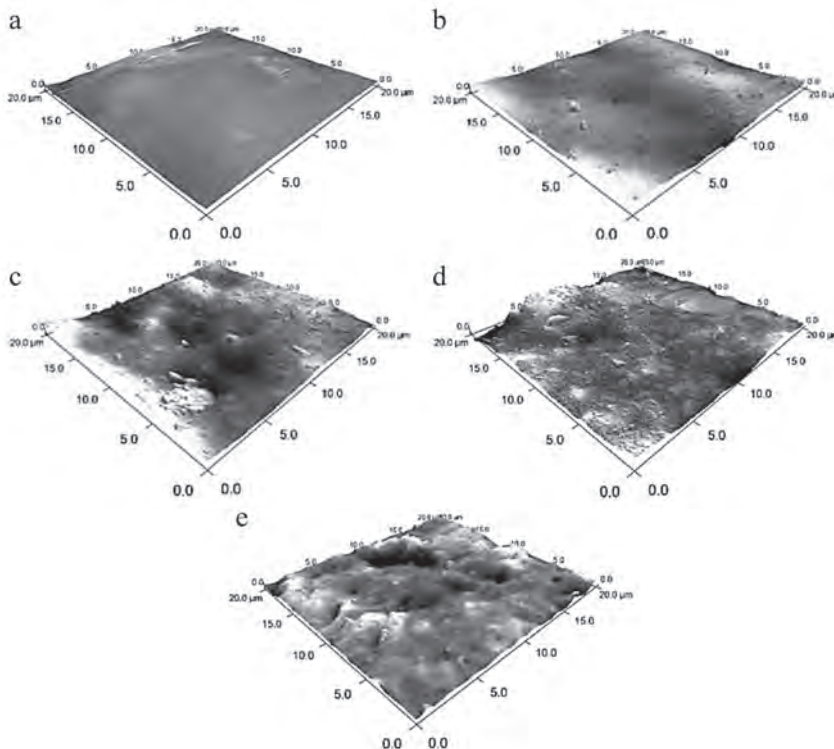


Figure 2. AFM images on the surface of the MWCNTs/NR nanocomposites at (a) 0%, (b) 0.3%, (c) 0.5%, (d) 0.7%, and (e) 1.0%. The derivative of topography signal is shown to highlight the morphology of the film after water evaporation. It was not possible to resolve individual nanotubes at the film surface. No clusters of MWCNTs were observed, either, showing that macroscopic dispersion was good, in agreement with optical microscopy observations. The MWCNTs are represented by the bright lines.

Because of the different capability for charge transport of the conductive MWCNT and the insulating natural rubber matrix, the secondary electron yield was enriched at the location of the MWCNT, which resulted in the contrast between the MWCNT network and the natural rubber matrix.

The MWCNTs were homogeneously distributed in the natural rubber matrix, without visible MWCNT large aggregations. Because local charging of the polymer matrix around the MWCNTs could render the average diameter of the MWCNTs to be larger than expected, it might be an indication for the presence of small MWCNT bundles. The AFM image indicates that most of the MWCNTs were individually dispersed and well incorporated in natural rubber matrix. Inspecting the volume distribution of the MWCNTs within the natural rubber matrix, we are able to state that the MWCNTs were not aggregated; most of them just close to each other without any contact.

The stress-strain curves for MWCNTs with natural rubber nanocomposites prepared by latex mixing process are shown in Figure 3. When 0.3 % of MWCNTs were added to the rubber the stress level for the nanocomposite material increased to 2.03 MPa. Addition of the % MWCNTs to the natural rubber increased the stress level gradually. At 0.5 % of MWCNTs the stress value obtained reached 8.82 MPa which is 22 times that of pure natural rubber. The result indicates that, by increasing the amount of MWCNTs added into the rubber the ductility decreased and the material became stronger and tougher but at the same time more brittle. The clear trend observed here is that as nanotube load increases, the tube breaking strain decreases. It also shows that the highest strain value was obtained for the nanocomposite at 1.0% of the MWCNTs. This nanocomposite at this percentage is more ductile and more elastic compared to other percentages of MWCNTs.

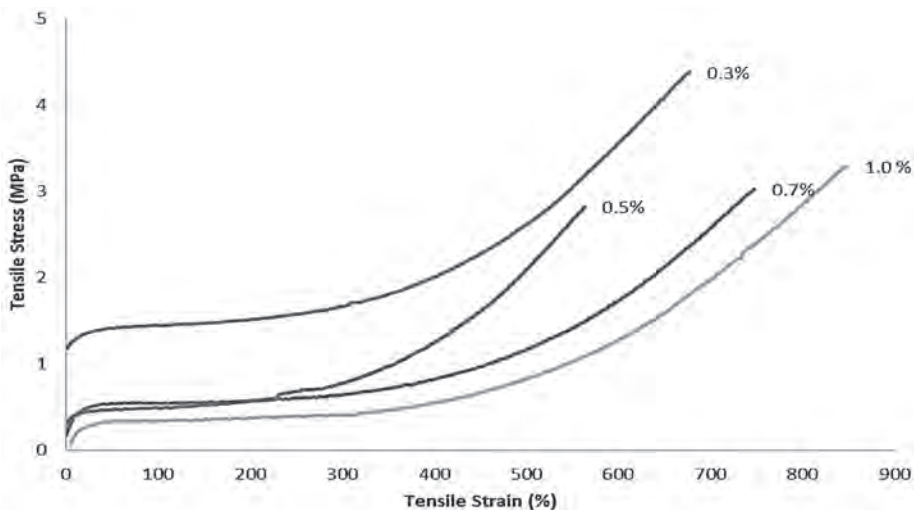


Figure 3. Stress-strain curves of the MWCNTs/NR nanocomposites.

The dispersions of MWCNTs in natural rubber can also be inhomogeneous, but corresponding to the natural rubber matrix, the MWCNTs will gain better compatibility between the polymeric phase and the nanotube phase. Therefore, it can be assumed that the tensile properties of MWNTs/NR nanocomposites depended not only on the dispersion of MWCTs particles but also on the compatibility of the nanotubes phase within the rubber matrix.

Figure 4 shows the effect of MWCNT concentration on the volume conductivity of MWCNTs/NR nanocomposites. A drastic increase in the electrical conductivity was obtained for the composites when the MWCNTs content attained about 0.7%, indicating that the percolation threshold for formation of a conductive MWCNT network in the natural rubber matrix was reached. For higher MWCNTs concentrations no pronounced increase of the conductivity could be observed; however, the maximum conductivity of about 1 S m^{-1} had been obtained for composites with MWCNT concentration of 1.0%.

Raman spectroscopy is a powerful non-destructive tool for structural characterization of carbon materials [29, 30]. The Raman spectra of all carbon materials show several common features in the $800\text{-}2000 \text{ cm}^{-1}$ region, namely the D and the G band lying in the $1300\text{-}1400$ and $1530\text{-}1640 \text{ cm}^{-1}$ regions [31]. Carbon nanotubes, moreover, show enhanced peaks in the $2600\text{-}2800 \text{ cm}^{-1}$ and $3100\text{-}3300 \text{ cm}^{-1}$ regions, due to second order resonant Raman processes [32]. These are usually addressed as the 2D band (also called G'), and the 2G band. The D and the G peaks are due to vibrations of the sp^2 domains.

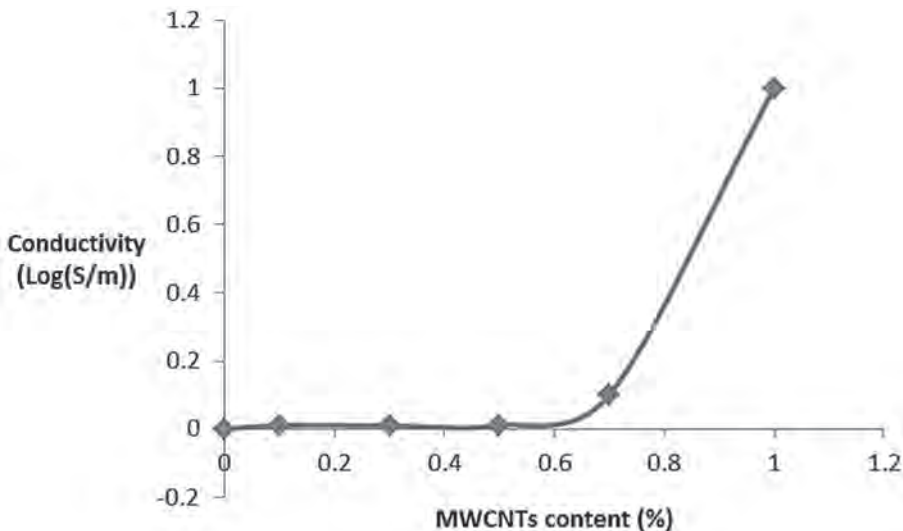


Figure 4. Volume conductivity of the MWCNTs/NR nanocomposites. Values represent an average of 10 measurements; standard variation is below 10%.

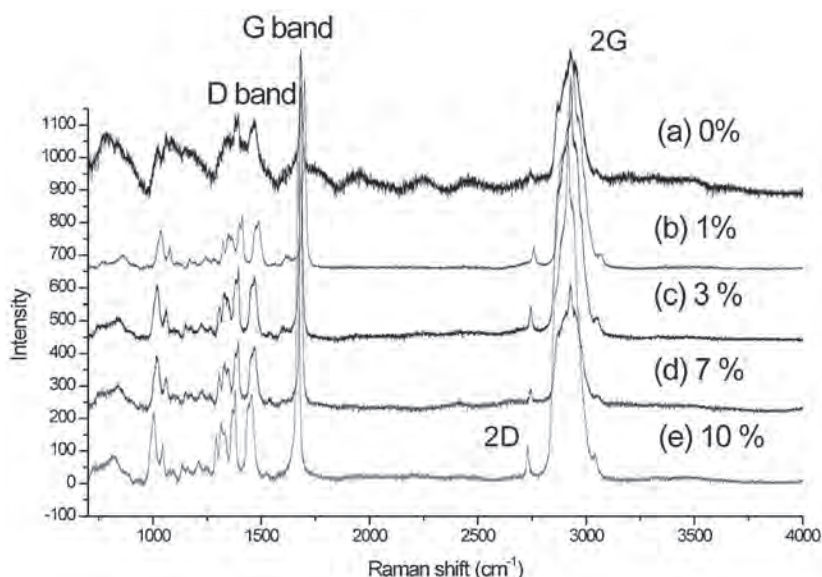


Figure 5. Raman spectrum of the MWCNTs/NR nanocomposites at (a) 0%, (b) 0.3%, (c) 0.5%, (d) 0.7%, and (e) 1.0%.

Figure 5 gives a general view of the Raman spectra from MWCNTs with natural rubber nanocomposites. The lower trace shows the two dominant Raman features, the RBM and the tangential (G band) features. In the upper trace, the background intensity is increased to show the rich Raman spectra over the entire first- and second-order phonon frequency range between the RBM and G features, including the disorder-induced D band and other lower intensity features.

In Figure 5 we clearly see the occurrence of the D and G bands peaked at 1327 and 1639 cm^{-1} , respectively. G band splitting is large for large diameter tubes; this indicated that double-peak G band splitting for large diameter MWNTs is smeared out because of the diameter distribution and therefore the G feature predominantly exhibits a weakly asymmetric characteristic line-shape.

Figure 5 shows also the occurrence of the second order 2D Raman mode around 2640 cm^{-1} , whose intensity is decreased in the MWCNT with respect to the concentration of the tubes but still well visible, assessing the good degree of crystallinity of the tubes present in the composite. It is interesting to note that on some zones of the sample the spectra show the appearance of two intermediate peaks at 1374 and 1403 cm^{-1} due to the Raman emission from the polymer matrixes. The slight shift and broadening of the intermediate peaks observed in the spectrum can be therefore attributed to the presence of local damage or stress in the composite.

The 2G bands (3090 cm^{-1}) could be superimposed with the G-line of residual graphite [33]. Small particles probably from the natural rubber as well as structural

imperfections are known to broaden the peaks of graphite. These results indicate the presence of MWCNTs in the rubber matrix.

CONCLUSION

Nanocomposites of MWCNT/NR were prepared by using latex technology. MWCNTs were first dispersed in Inutec solution driven by sonication. Inutec stabilizes and prevents reaggregation of MWCNTs after disentangling and separation from bundles; however, it also affects the conductivity of the system and reduces charge transport at MWCNT junctions within the conductive network. After sonicating, mixing with HA latex and drying; homogeneously dispersed MWCNTs were found in the NR matrix of the composites. A pronounced percolation threshold has been observed for a quite low value of 1.0% MWCNTs in the NR matrix. A conductive MWCNT network was formed in the NR matrix, allowing the dramatic increase of volume conductivity from $10^{-10} \text{ S m}^{-1}$ for the neat NR to 1 S m^{-1} for the conductive composites. The nanocomposites also showed a very high degree of increase in the tensile strength in the rubbery region at room temperature, probably due to rigid networking effect favoured by segregation effects coming from latex structure and cross-linking via functional groups at the surface of CNT and organic molecules present in the natural latex solution.

REFERENCES

1. Laine R.M., Sanchez C., Brinker C.J. and Giannelis E. (Eds) (2000) 628 *Organic/Inorganic Hybrid Materials*. Materials Research Society, Warrendale, PA.
 2. Sanchez C. and Lebean B. (2001) Design and properties of hybrid organic-inorganic nanocomposites for photonics. *Materials Research Society Bulletin* **26**: 377-387.
 3. Ogoshi T., Itoh H., Kim K.M. and Chujo Y. (2002) Synthesis of organic-inorganic polymer hybrids having interpenetrating polymer network structure by formation of ruthenium-bipyridyl complex. *Macromolecules* **35**: 334-338.
 4. Nagata K., Kodama S., Kawasaki H., Deki S. and Mizuhata M. (1995) Influence of polarity of polymer on inorganic particle dispersion in dielectric particle/polymer composite systems. *Journal of Applied Polymer Science* **56**: 1313-1321.
 5. Schollhorn R. (1996) Intercalation systems as nanostructured functional materials. *Chemistry of Materials* **8**: 1747-1757.
 6. Gilman J.W. (1999) Flammability and thermal stability studies of polymer layered-silicate (Clay) nanocomposites. *Applied Clay Science* **15**: 31-49.
 7. Okada A. and Usuki A. (1995) The chemistry of polymer-clay hybrids. *Materials Science and Engineering* **C3**: 109-115.
 8. Armes S.P. (1995) Electrically conducting polymer colloids. *Polymer News* **20**: 233-237.
-

9. Godovski D.Y. (1995) Electron behavior and magnetic properties of polymer nanocomposites. *Advances in Polymer Science* **119**: 79-122.
 10. Okada A. and Usuki A. (2006) Twenty years of polymer-clay nanocomposites. *Macromolecular Materials and Engineering* **291**: 1449-1476.
 11. Buetrich R., Kahlemberg F., Popall M., Dannberg P., Muler-Fiendler R. and Rosh O. (2001) ORMOCER®s for optical interconnection technology. *Journal of Sol-Gel Science and Technology* **20**: 181-186.
 12. Deng Q., Moore R.B. and Mauritz K.A. (1995) Novel Nafion/ORMOSIL hybrids via in situ sol-gel reactions. 1. Probe of ORMOSIL phase nanostructures by infrared spectroscopy. *Chemistry of Materials* **7**: 2261-2270.
 13. Shao P.L., Mauritz K.A. and Moore R.B. (1996) Perfluorosulfonate ionomer/[SiO₂-TiO₂] nanocomposites via polymer-in situ sol-gel chemistry: Sequential alkoxide procedure. *Journal of Polymer Science, Part B: Polymer Physics* **34**: 873-882.
 14. Judenstein P. and Sanchez C. (1996) Hybrid organic-inorganic materials: a land of multidisciplinary. *Journal of Material Chemistry* **6**: 511-525.
 15. Azira A.A., Dayang H.A.I.H., Suriani A.B. and Rusop M.M. (2012) Characterization of multi-walled carbon nanotubes/natural rubber nanocomposite by wet mixing method. *Nano Hybrids* **1**: 81-97.
 16. Salvetat J.P., Bhattacharyya S. and Pipes R.B. (2006) Progress on mechanics of carbon nanotubes and derived materials. *Journal of Nanoscience and Nanotechnology* **6**: 1857-1882.
 17. Frogley M.D., Ravich D. and Wagner H.D. (2003) Mechanical properties of carbon nanoparticle-reinforced elastomers. *Composite Science and Technology* **63**: 1647-1654.
 18. Bokobza L. and Kolodziej M. (2006) On the use of carbon nanotubes as reinforcing fillers for elastomeric materials. *Polymer International* **55**: 1090-1098.
 19. Atieh M.A., Girun N., Mahdi E.-S., Tahir H., Guan C.T., Alkhatib M.F., *et al.* (2006) Effect of multi-wall carbon nanotubes on the mechanical properties of natural rubber. *Fullerenes Nanotubes Carbon Nanostructures* **14**: 641-649.
 20. Haggemueller R., Gommans H.H., Rinzler A.G., Fischer J.E. and Winey K.I. (2000) Aligned single-wall carbon nanotubes in composites by melt processing methods. *Chemical Physics Letters* **330**: 219-225.
 21. Manchado M.A.L., Valentini L., Biagiotti J. and Kenny J.M. (2005) Thermal and mechanical properties of single-walled carbon nanotubes-polypropylene composites prepared by melt processing. *Carbon* **43**: 1499-1505.
 22. Cooper C.A., Ravich D., Lips D., Mayer J. and Wagner H.D. (2002) Distribution and alignment of carbon nanotubes and nanofibrils in a polymer matrix. *Composite Science and Technology* **62**: 1105-1112.
 23. Jin L., Bower C. and Zhou O. (1998) Alignment of carbon nanotubes in a polymer matrix by mechanical stretching. *Applied Physics Letters* **73**: 1197-1199.
 24. Xu X.J., Thwe M.M., Shearwood C. and Liao K. (2002) Mechanical properties and interfacial characteristics of carbon-nanotube-reinforced epoxy thin films. *Applied Physics Letters* **81**: 2833-2835.
-

25. Grossiord N., Loos J. and Koning C.E. (2005) Strategies for dispersing carbon nanotubes in highly viscous polymers. *Journal of Material Chemistry* **15**: 2349-2352.
 26. Kimura T., Ago H., Tobita M., Ohshima S., Kyotani M. and Yumura M. (2002) Polymer composites of carbon nanotubes aligned by a magnetic field. *Advanced Materials* **14**: 1380-1383.
 27. Du F.M., Fischer J.E. and Winey K.I. (2003) Coagulation method for preparing single-walled carbon nanotube/poly(methyl methacrylate) composites and their modulus, electrical conductivity, and thermal stability. *Journal of Polymer Science Part B: Polymer Physics* **41**: 3333-3338.
 28. Barraza H.J., Pompeo F., O'Rear E.A. and Resasco D.E. (2002) SWNT-filled thermoplastic and elastomeric composites prepared by miniemulsion polymerization. *Nano Letter* **2**: 797-802.
 29. Dresselhaus M.S., Dresselhaus G. and Ecklund P.C. (1996) *Science of Fullerenes and Carbon nanotubes*. Academic Press, New York.
 30. Ferrari A.C. and Robertson J. (2001) Resonant Raman spectroscopy of disordered amorphous, and diamond-like carbon. *Physical Review B* **64**: 0754141-1-13.
 31. Thomsen C. (2000) Second-order Raman spectra of single and multiwalled carbon nanotubes. *Physical Review B* **61**: 4542-4544.
 32. Hiura H., Ebbesen T., Tanigaki K. and Takahashi H. (1993) Raman studies of carbon nanotubes. *Chemical Physics Letters* **202**: 509-512.
-

Treatment of waste water by ozone produced in a dielectric barrier discharge

A. Khadgi¹, D. P. Subedi¹, R. B. Tyata^{1,2} and C. S. Wong³

¹ Department of Natural Science, Kathmandu University, Dhulikhel, Nepal

² Department of Physics, Khwopa College, Dekocha, Bhaktapur, Nepal

³ Plasma Technology Research Centre, Physics Department, University of Malaya, 50603 Kuala Lumpur, Malaysia

(*Email: deepaksubedi2001@yahoo.com)

Received 05-10-2012; accepted 09-10-2012

Abstract This study focuses on the application of dielectric barrier discharge (DBD) at atmospheric pressure to generate ozone for the treatment of waste water. Waste water samples from domestic source, dairy industry and paint industry were collected and various parameters of the samples before and after the treatment were measured. Treatment time of 20 minutes was used for all types of samples. Our results showed that ozone treatment significantly increased dissolved oxygen (DO); reduced chemical oxygen demand (COD), fecal coliform, heavy metals and total solids (TS), but the changes in pH and conductivity were not statistically significant.

Keywords dielectric barrier discharge – ozone treatment – waste water – pH – DO – COD – fecal coliform

INTRODUCTION

Waste water is a complex solution which may contaminate the human environment, i.e. air, water, food, land and shelter. The common sources of water pollution can range from purely natural to several man-made sources of domestic and industrial waste water [1, 2]. Wastes from different industries are more dangerous since they contain xenobiotic compounds which are not bio-degradable, thus persist for longer time and can be transported through rivers to other parts of the country. The waste released from these sources into rivers will ultimately lead to water pollution. Also, polluted rivers act as breeding ground for various disease causing agents and the smell from the polluted river sometimes becomes unbearable. Thus, waste water released from various sources should be treated before it is released into rivers.

There are various methods of treatment, some of which are activated sludge method, chemical coagulations, chlorination etc. One of the emerging technologies is the use of ozone which is an industrially accepted application of electrical discharges for treatment of water and waste water [3]. In a DBD (dielectric barrier discharge) reactor the electrical discharge takes place between electrodes where

at least one of the electrodes is covered with a thin layer of dielectric material [4]. The dielectric material used is a type of insulator and is made of ceramic, glass, PVC etc.

When an AC voltage is applied across the electrode, discharge is generated with the production of UV. Electrical discharges taking place in an air or oxygen environment convert oxygen into ozone. In addition to ozone, electrical discharges in air produce a variety of chemically active species, such as O_3^* , N_2^* , N^* , OH^* , O_2^* , O^* , O^{+2} , N^{+2} , N^+ , O^+ [5]. These species are short lived and decay before ozone enriched air gets into the water where it oxidizes various organic and inorganic chemicals and converts them into simpler forms that become easily decomposed in the atmosphere.

Ozone is 12.5 times more soluble in water than oxygen, leading to better mixing in water treatment [6]. Other advantages of ozone over conventional chlorination process are: (i) no need to store and handle toxic chemicals; (ii) by-products with no known adverse effects on health or the environment; (iii) can safely destroy a broader range of organic contaminants; (iv) helps in removal of colour, odour and suspended solid materials; (v) far more efficient in killing bacteria, viruses, spores and cysts; (vi) also oxidizes and precipitates iron, sulphur, and manganese so they can be filtered out of solution. Ozone is very reactive because it has redox potential +2.07 V whereas chlorine has only +1.36V [6].

EXPERIMENTAL SETUP

Ozone is produced by a coaxial dielectric barrier discharge system (Fig. 1). The discharge is generated using a high voltage (0-50 kV) power supply at 50 Hz manufactured by Nepal Engineering Eakarar Co. Pvt. Ltd. The rms input voltage applied to the electrodes can be varied between 0 to 21kV. The voltage applied for

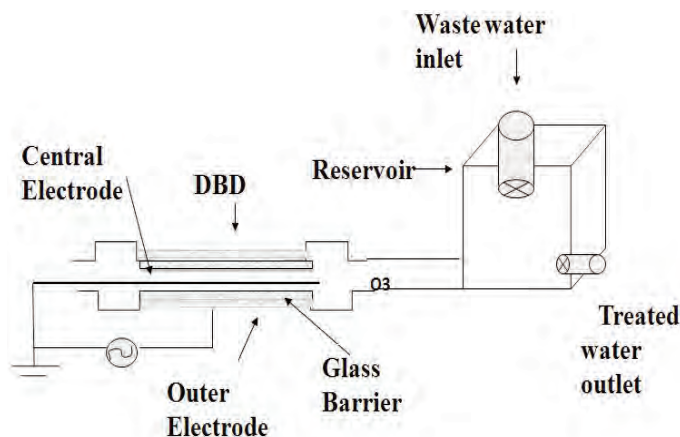


Figure 1. Schematic diagram of ozonation system.

our experiment was 14 kV with a current limiting resistance of 8M Ω .

Co-axial type of electrode made up of aluminum was used in the experiment. The outer electrode was made of wrapping an aluminum foil over a polycarbonate tube which was used as dielectric material in this case. The inner electrode was made of aluminum wire of length of 22 cm and diameter of 0.4 cm. The length of the outer electrode was 20 cm and that of the dielectric material was 24 cm. The outer and inner diameters of the dielectric material were 1 cm and 0.7 cm respectively. The inner electrode was connected to the output of the power supply and the outer electrode was grounded.

When a high voltage was applied across the electrodes, a strong electric field was created and discharge was generated. For the purpose of producing ozone, air was pumped into the electrode gap by an air pressure pump, at the rate of about 300cm³/min. The concentration of the ozone output from the generator was determined by the standard iodometric method [7].

SELECTION OF SOURCES OF WASTE WATER

Samples of waste water from various sources located in the Bhaktapur Industrial sector of Bhaktapur, Nepal were collected.

Waste water from household/domestic sources

Waste water from residential, commercial, institutional and similar facilities are referred to as domestic waste water. Domestic sewage consists of organic as well as inorganic substances which may include protein, carbohydrate, fats as well as grits, salts and metals in varying proportions. A significant amount of heavy metals like copper, manganese, cobalt, lead, etc may also be present in significant proportions. In our experiment the discharge from various households (excluding discharge from sewerage system) was considered.

Dairy industry

The dairy industry is generally considered to be the largest source of food processing waste water in many countries. In general, wastes from the dairy processing industry contain high concentrations of organic material such as proteins, carbohydrates, and lipids, high concentrations of suspended solids, high biological oxygen demand (BOD) and chemical oxygen demand (COD), high nitrogen concentrations, high suspended oil and/or grease contents, and large variations in pH, which necessitates 'specialty' treatment so as to prevent or minimize environmental problems [8].

Paint industry

Acrylics and styrene-butadiene polymers are mainly used in water-based paints

for interior and exterior use. Other materials that paints may contain include organic and inorganic pigments which have varying degrees of toxicity. Cadmium, lead, chrome and nickel-containing pigments may still be added to some paints. Zinc chromate which is added to metal primers has now been found to be strongly carcinogenic and will no longer be produced. Plastic polymers and solvents with very slow rates of biodegradability, and solvents that contain aromatic hydrocarbons may also be present. These wastes are strongly eco-toxic and should not be allowed to enter any water systems [9].

EXPERIMENTAL PROCEDURES

Different physical, chemical and microbiological parameters (Table 1) were investigated for both treated and untreated samples of waste water. The analytical procedures were performed using standard methods [10].

RESULTS AND DISCUSSION

Ozonated water samples were titrated with sodium thiosulphate to find out the concentration of dissolved ozone. The concentration of dissolved ozone increased with the increase in treatment time (Fig. 2). Since cost of treatment is also one of the important factors, a suitable treatment time for effective treatment has to be chosen. It was found that 20 minutes treatment was sufficient to produce observable effects for all the tests carried out in this work. The qualities of the waste water samples were then analyzed both before and after ozone treatments using ANOVA test (at 0.05 level of significance).

Removal of colour

When ozone was bubbled into samples of waste water from domestic, dairy and paint industries, only a slight change in colour of the water samples was observed visually. Surface waters are generally coloured by natural organic materials such

Table 1. Parameters selected and method of analysis.

Parameters	Unit	Method/Instrument used
Color		Visual
Total Solids	mg/L	Gravimetric method
Conductivity	$\mu\text{S}/\text{cm}$	Conductivity meter (Hanna probe, HI 98107)
pH	scale	pH meter (Hanna probe, HI 98303)
Dissolved oxygen	mg/L	Winkler's method
Chemical oxygen demand	mg/L	Reflux method
Manganese	mg/L	UV-Visible Spectrophotometer
Chromium	mg/L	UV-Visible Spectrophotometer
Fecal coliform	CFU/100 mL	Membrane filtration method

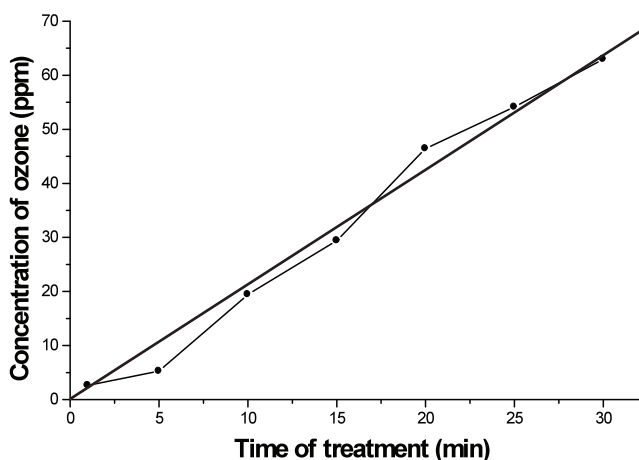


Figure 2. Concentration of ozone dissolved in waste water after different treatment times. — Linear fit

as humic, fulvic and tannic acids. These compounds are produced from the decay of vegetative materials and have conjugated carbon-carbon double bonds. Ozone is effective in breaking organic double bonds. As more of these double bonds are eliminated, the colour disappears.

Colour in dairy waste water is usually whitish because of high content of milk and organic compounds. In the case of water from paint industry, colour is usually of different types depending upon the pigment used. The main chemical used is 'chrome' which is a combination of chromium ion. Manganese is also commonly used as pigment.

Ozone causes structural change in organic compounds especially humic material causing rapid decrease in colour [11]. The yellow-brown humus can be oxidized, producing a clear product [12]. Ozone oxidizes both the organic compounds as well as heavy metals. It is very effective in breaking the hydrocarbons, which create colour and is widely used in different applications where colour has to be removed or made less noticeable.

Total solids (TS)

TS load is mainly due to organic or inorganic constituents that include salts of various metals as well as sand, grits etc. TS in the three types of samples before and after the treatment are shown in Figure 3.

Domestic waste water shows high TS because it contains a variety of waste from organic to inorganic of different sizes. In an average domestic waste water, total solids are about half organic and half inorganic, and about two-thirds in solution (dissolved) and one-third in suspension.

In the case of dairy waste water, the value is lower than domestic source but

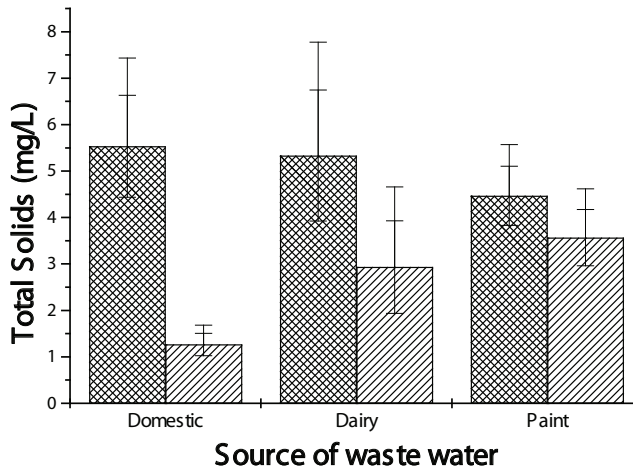


Figure 3. TS before and after treatment. : Untreated : Treated

greater than paint waste water because it mainly contains high organic compounds mostly milk and less chemicals except those used as preservatives.

Lastly, waste water from paint industry mainly contains chemicals and pigment which are very small in size and are found in dissolved state.

The maximum tolerance limit of industrial effluents into inland surface water according to CBS2008 for TSS is 50 mg/L. All three sources of waste water under study have TSS value lower than the tolerance limit. For TDS, there is no maximum tolerance limit given.

Oxidation of dissolved organic materials by Ozone results in polar and charged molecules that can react with polyvalent aluminum or calcium to form precipitates. Since the precipitates are heavier they tend to settle down faster. Thus, after treatment the value of TS decreases.

Analysis of pH

Figure 4 shows the pH of different samples before and after the treatment. According to CBS2008, the maximum tolerance limit of industrial effluents into inland surface water for pH is 5.5 to 9. The waste water from all the sources studied has pH well below the prescribed values.

The pH of waste water from dairy was less than that of the samples of domestic and paint sources because in dairy, most of the compounds used are organic which include amino acids, carboxylic acid which are slightly acidic in nature and hence the pH is lower. Although in all cases the difference after treatment is not statistically significant, a point to be noted is that all the values are moving toward neutral point, i.e. pH 7 which means neither acidic nor basic.

Literally pH refers to the concentration of hydrogen ions within any solution.

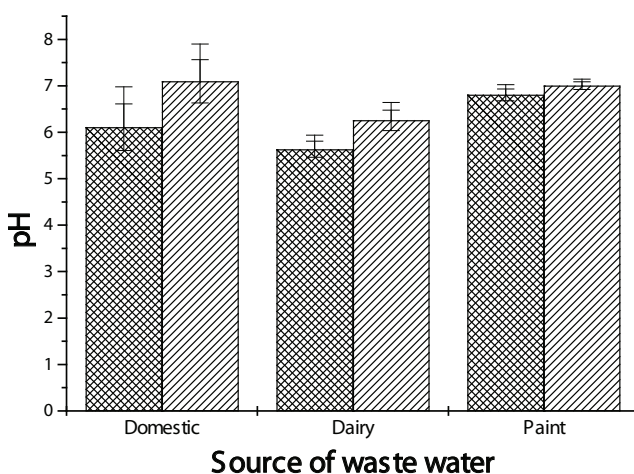


Figure 4. pH before and after treatment. : Untreated
: Treated

Low pH values are connected with high concentrations of hydrogen ions and vice versa. Generally, water with a pH above 7 is much less likely to dissolve heavy metals than water with a pH below 7, and precipitates are formed at higher pH levels since ozone oxidizes the free ions in the solutions to form different salts and the pH value was increased after treatment. Also, there is a negative correlation between dissolved oxygen and hydrogen ion concentration. Since ozone decomposes in water to give oxygen molecules, the pH tends to increase.

Analysis of conductivity ($\mu\text{s}/\text{cm}$)

Electrical conductivity is used as an indication of the amount of total dissolved salts, or the total amount of dissolved ions in water. Conductivity of the samples before and after the treatment is shown in figure 5. As the current is the rate of flow of electric charges, the presence of higher concentration of dissolved ions in the sample leads to higher conductivity. The values of conductivity for all the samples of waste water after treatment do not show large variations.

Ozone in water oxidizes the heavy metals and organic compounds to a form that can be filtered so the total salt concentration is not heavily reduced and hence the conductivity of the solution does not change significantly. Earlier work also reported no significant change in conductivity after ozonation [13].

Analysis of dissolved oxygen (DO)(mg/L)

DO in the case of waste water from paint industry is much greater than dairy source because in dairy and domestic wastes, much of the constituents in them are organic compounds which are degradable by micro-organisms and consume oxygen during degradation.

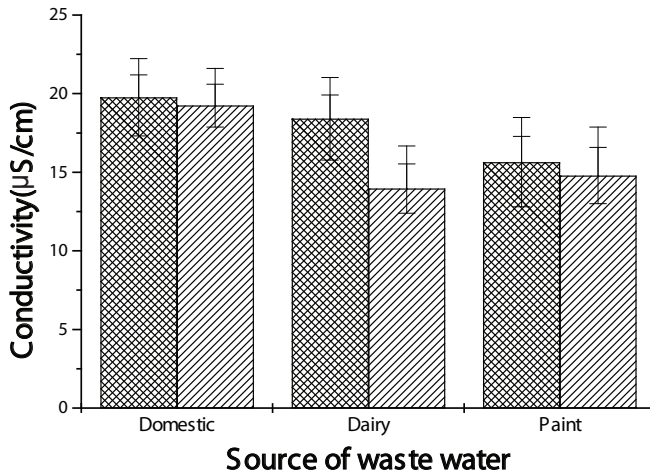


Figure 5. Conductivity before and after treatment. : Untreated : Treated

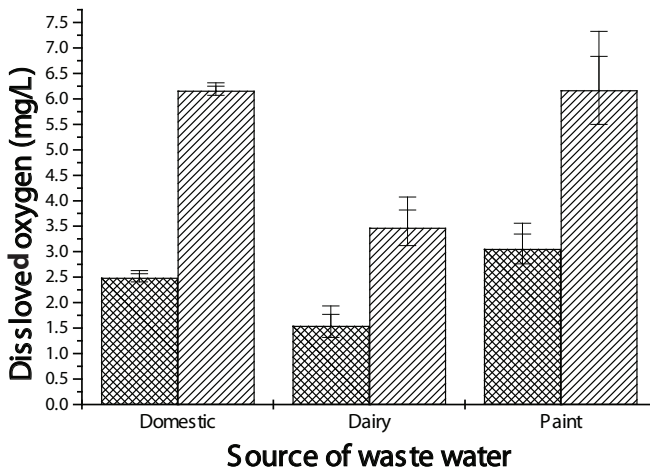


Figure 6. Concentration of DO before and after treatment. : Untreated : Treated

According to USEPA, 1972 the minimum DO levels required for protection of aquatic life is 5.8 to 6.8 [2]. After treatment, the values are found to reach or even become higher than the given limits (Fig. 6). Normally, oxygen is not a very soluble gas and the dissolved oxygen concentrations in waste waters are very low. When micro-organisms and an available food supply are present, dissolved oxygen will be consumed.

Ozone is more soluble than oxygen in water and since it is unstable, it decomposes to oxygen in minutes in aqueous media. Use of oxygen feed gas results in treated effluent dissolved oxygen levels as high as 40 ppm [12]. Neutral

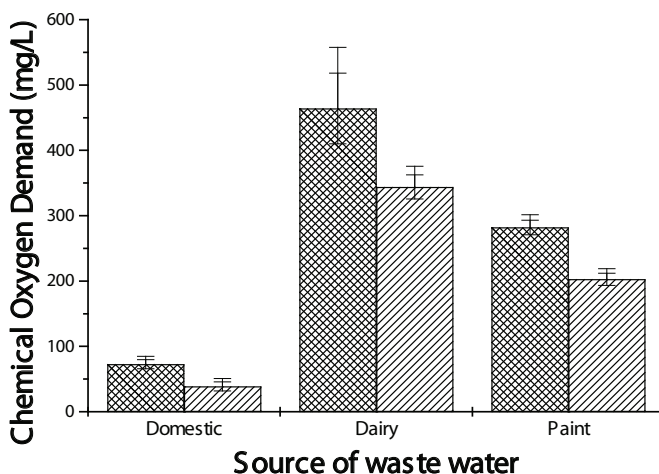


Figure 7. COD before and after treatment. : Untreated
: Treated

salts and hydroxylations accelerate this decomposition, which in pure aqueous solution occurs as: $O_3 + H_2O \rightarrow HO_3^+ + OH^-$; $HO_3^+ + OH^- \rightarrow 2HO_2$; $O_3 + HO_2 \rightarrow HO + 2O_2$ and $HO + HO_2 \rightarrow H_2O + O_2$.

Since ozone is formed by addition of oxygen atom to oxygen molecule, when it reacts chemically it releases or decomposes back to oxygen and causes the dissolved oxygen content to increase rapidly. It had been reported that this was one of the principal reasons of choosing ozone as disinfectant in Indiana [11].

Analysis of chemical oxygen demand (COD)(mg/L)

The maximum tolerance limit for COD of industrial effluents discharged into inland surface water, according to CBS, 2008 is 250 mg/L. In the case of the samples of waste water from domestic and paint industry, COD was higher than the given limit and treatment by ozone brought the levels below the limit. However, the COD value for dairy industry waste is very high. Although COD decreased after treatment, the value was still well above 250 mg/L (Fig. 7).

This suggests that for waste water from dairy industry the treatment time is not sufficient and has to be increased. DO in the case of waste water from paint industry was much greater than samples from dairy industry but waste water from paint industry showed high COD. This is because, although COD refers to oxygen required to break down organic compound by potassium dichromate, ozone being a strong oxidizing agent may also oxidize chemicals present in the paint. Ozone readily attacks carbon-carbon double bonds, certain carbon-nitrogen double bonds, and nucleophiles such as amines and selenides. Other bonds, such as carbon-hydrogen, react favourably with ozone but only in the absence of competition from the above [12]. Oxidation of organic compound by ozone and

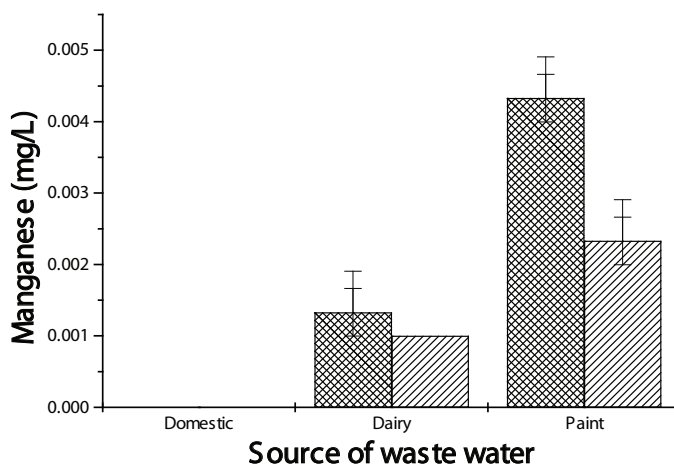


Figure 8. Concentration of Manganese before and after treatment. : Untreated : Treated

generation of oxygen decreases the demand for oxygen and reduces the COD level.

Analysis of heavy metals (mg/L)

Manganese. Manganese was not found in domestic waste water. Manganese in paint is used as a pigment and hence its concentration is higher than in samples from dairy waste. Normally, manganese is not added in dairy products hence its presence in the waste water is probably due to contamination. But in both cases the concentration is very low (Fig. 8).

Manganese in water is usually present in dissolved form. After ozonation, the ozone oxidizes the metal ion into higher oxidation state, i.e. +4 state and gets precipitated. Oxidation of manganese occurs as follows: $Mn^{+2} + O_3 + 2H_2O \rightarrow Mn^{+4} + O_2 + 2OH^-$.

Chromium. In the samples from paint industry the concentration of chromium is higher because it is the colour forming agent used in paint. The maximum tolerance limit of industrial effluents into inland surface water according to CBS, 2008 for Cr is 2mg/L, and in all sources of waste water the concentration of chromium is fairly low (Fig. 9).

Ozone oxidizes the transition metals to form $Cr(OH)_3$, which is in colloidal form which is then easily separated by filtration. Other metals such as arsenic (in the presence of iron), cadmium, chromium, cobalt, copper, lead, manganese, nickel, and zinc can be treated in a similar way. Ozone does not remove iron or manganese from water, but it can facilitate their removal. Once these metals are oxidized, they can be easily filtered.

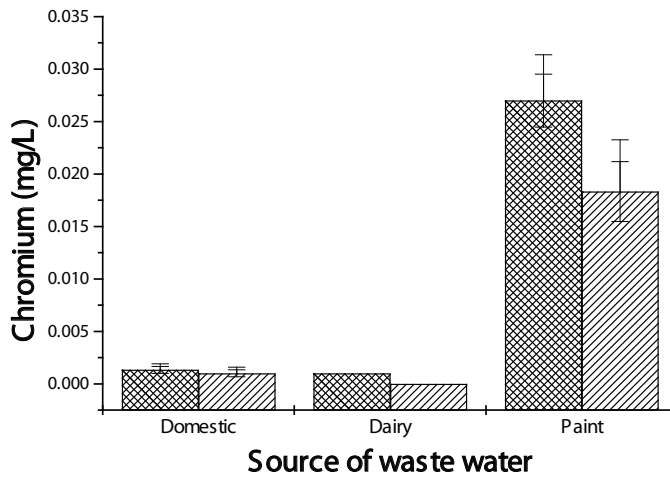


Figure 9. Concentration of Chromium before and after treatment. : Untreated : Treated

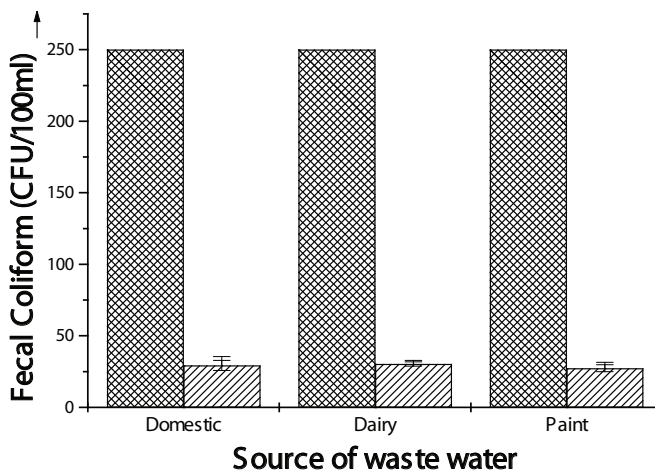


Figure 10. Fecal coliform count before and after treatment. : Untreated : Treated

Analysis of fecal coliform (CFU/100 mL)

The mean value of concentration of Coliform Formation Unit (CFU) per 100 mL of fecal coliform for the three replicates of samples of waste water from domestic, dairy and paint industry (Fig. 10) were Too Many to Count (TMC), i.e. more than 250 which is the maximum number of pores in the membrane filter. The heavy contamination of fecal coliform in the waste water may be due to contamination during storage.

The ANOVA test shows that ozone is a very good disinfectant. Ozone causes damage to cell membrane, nucleic acid and some enzymes. Similar result has also

been reported in our earlier experiment on treatment of drinking of water [14].

It has also been reported that ozone concentration as low as 0.01 ppm is toxic to *Escherichia coli* and *Streptococcus faecalis* at pH 7.0 and 25 °C in pure systems and it is more effective than chlorination. In general, ozone dosage of 5 to 10 ppm is adequate to achieve disinfection to a plate count of 200/100 mL of fecal coliform, which is a typical waste water requirement [12].

Disinfection by ozone occurs through the rupture of the cell wall because bacteria are single cellular and their cell wall consists of lipid layer. Ozone attacks the double bond of the lipid bi-layer causing lysis of cell wall [15]. This is more efficient than chlorine which depends upon diffusion into the cell protoplasm and inactivation of the enzymes.

CONCLUSION

After 20 minutes of treatment time for all sources of waste water, ozone did not change the physical property of water significantly. However, the results indicated the increase in DO concentration and pH to some extent. Ozone also lightens the colour of waste water, decrease COD and TS. It was also observed that, ozone efficiently precipitated metals and caused substantial reduction of fecal coliform, a key element for various water related health problems in a country like Nepal. For practical application of ozonation for waste water treatment, which is expected to be carried out in large scale, the treatment time should be increased to longer than 20 minutes.

Acknowledgements – This research was supported by the International Foundation for Science (IFS), Stockholm, Sweden, and the Organization for the Prohibition of Chemical Weapons, The Hague, The Netherlands, through grant No. W/4373-2.

REFERENCES

1. Ramasamy R.K., Rahman N.A. and Wong C.S. (2001) Effect of temperature on the ozonation of textile waste effluent. *Coloration Technology* **117**: 95-97.
 2. Goel P.K. (2006) *Water pollution causes, effects and control*. 2nd Ed. New Age International (P) Limited, Publishers, New Delhi.
 3. Eliasson B., Hirth M. and Kogelschatz U. (1987) Ozone synthesis from oxygen in dielectric barrier discharges. *Journal Physics D: Applied Physics* **20**: 1421-1437.
 4. Kuraica, M.M., Obradovic, B.M., Manojlovic, D., Ostojic, D.R. and Puric, J. (2004) Ozonized water generator based on coaxial dielectric-barrier-discharge in air. *Vacuum* **73**: 705-708.
 5. Malik M.A., Ghaffar A. and Malik S.A. (2001) Water purification by electrical processing. *Plasma Sources Science Technology* **10**: 82-91.
 6. Khadre, M.A., Yousef, A.E. and Kim, J. (2001) Microbiological aspects applications in food: a review. *Journal of Food Science* **6**: 1242-1252.
-

7. Morris K. (1977) *Methods of air sampling and analysis*. 2nd Ed. Alpha Intersociety Committee, Washington D.C.
 8. Britz T.J. and Schalkwyk C. (2006) *Treatment of dairy processing wastewaters*. University of Stellenbosch, Matieland, South Africa and Cleveland State University, Cleveland, Ohio, U.S.A.
 9. Small R. (1993) *House paint – a gloss over*. The RIC Good WOOD Guide, Bogong.
 10. Franson N., Clesceri L., Greenberg A. and Eaton A. (eds.) (1998) *Standard methods for the examination of water and wastewater*. 20th Edition, American Public Health Association, Washington, D.D., USA.
 11. Paraskeva P. and Graham N.J. (2002) Ozonation of municipal waste water effluents. *Water Environment Research* **74**: 569-581.
 12. Keenan J.D. and Hegemann D.A. (1978) Chlorination and ozonation in water and wastewater treatment. *Chemosphere* **1**: 9-28.
 13. Khadgi A., Subedi D.P. and Tyata R.B. (2010) Analysis of drinking water treated by ozone produced in a dielectric barrier discharge. *The National Youth Confernece on Environment Proceeding* **1**: 12-21.
 14. Subedi D.P., Tyata R.B., Khadgi A. and Wong C.S. (2009) Treatment of water by dielectric barrier discharge. *Journal of Science and Technology in the Tropics* **5**: 117-123.
 15. Bryant E.A., Fulton G.P. and Budd G.C. (1992) Disinfection alternatives for safe drinking water. *C.B.S (2008) Environment Statistic of Nepal*. National Planning Commission, Government of Nepal.
-

Low speed bearing monitoring using acoustic emission technique

Tonphong Kaewkongka^{1,*} and Jirapong Lim²

¹ Department of Physics, Faculty of Science, Chulalongkorn University, Patumwan, Bangkok 10330, Thailand

² Department of Production Engineering, Faculty of Engineering, King Mongkut University of Technology, North Bangkok, Bangsue, Bangkok 10800, Thailand

(*Email: tonphong.k@chula.ac.th)

Received 30-10-2012; accepted 07-11-2012

Abstract This paper provides a method of acoustic emission (AE) technique to monitor low speed bearings. A piezoelectric transducer was used to capture dynamic envelope which was extracted from the spatial-domain signal and processed to its bearing frequencies spectrum. The bearing frequencies are used as characteristic features to identify bearing operating conditions. The experiments on low speed bearings were investigated in-situ on dryer bearings. The proposed method can give early warning of defective bearing in timely fashion using both AE envelope and its spectrum.

Keywords acoustic emission – low speed – bearing

INTRODUCTION

Bearings are omnipresent machine elements as it can be found on almost all machines. Unpredicted failure of bearings has consequences and sometimes even health and safety consequences. Therefore, a timely and reliable condition monitoring system is highly beneficial for it will reduce the cost of these consequences and increase the overall equipment effectiveness.

For rotating equipment maintenance, two methods have been used, which are the statistical bearing life estimation and the bearing condition monitoring and diagnostics [1, 2]. The first method relies on a model of the bearing services probability in terms of the dynamic load rating and the equivalent load to give an estimation of the fatigue life of a bearing [3-5]. However, because operating conditions can vary significantly from one machine to another, the prediction based on the assumption of normal duty on a bearing can be inaccurate. The second method is more precise than the first if the signals monitored have useful features that can reliably indicate an early warning of the occurrence of the potential failure [6-8]. Signals that have been studied for bearing condition monitoring include time and frequency domain of acoustic emission signal.

In this paper, a frequency-domain technique, namely the Fast Fourier Transform (FFT) was assessed in terms of its ability to indicate early abnormal

condition from low speed bearings. These signals were collected from bearing operating condition in-situ.

The objective of this research is to demonstrate that a condition-based monitoring using acoustic emission (AE) can provide not only timely detection of low speed bearing but also the fault identification so that maintenance or replacement can be performed prior to the loss of safety function. Therefore the use of acoustic emission method has been proposed for low speed machineries monitoring instead of the conventional method.

THE PROPOSED APPROACH

Figure 1 shows a block diagram of the proposed bearing condition monitoring procedure. The acquired AE signals were first filtered and amplified to remove noise and then processed in order to obtain AE envelope signal. Then, the Fast Fourier Transform was used to produce its frequency domain pattern. The frequency domain has a horizontal axis representing frequency and a vertical axis representing the intensity of the frequency component. The bearing frequencies were used to indicate the presence of bearing failure condition.

The pre-processed parameter of the dynamic envelope of the AE signal can be obtained from AE Ultraspan (Holroyd Instruments, UK) (Fig. 2). The AE Ultraspan is the wireless sensor which provides many opportunities for diagnosing the nature of faults. The time dependence of the AE signal can reveal the occurrence and timing of subtle actions within machineries.

The AE dynamic envelope is suitable for both burst type and continuous AE signals. Effect of signal averaging is to improve statistical significance but distorts shape of activity giving time decays and reduced peak value. It is also represented in logarithmic scale of AE signals since it allows a greater signal range to be simultaneously observed with its unit in dB and is a ratio with respect to a reference voltage [9].

$$AE \text{ Log Magnitude in dB} = 20 \log_{10} (V_{sig} / V_{ref})$$

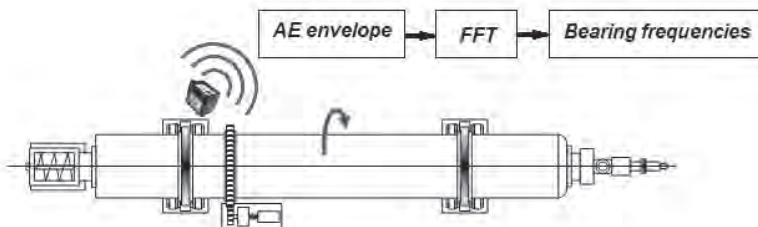


Figure 1. The low speed bearing monitoring using acoustic emission scheme.

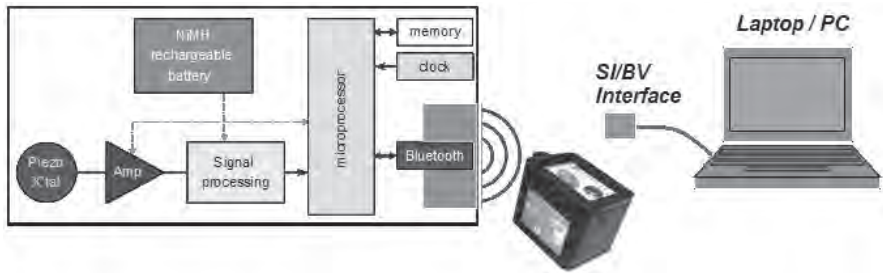


Figure 2. AE Ultraspan wireless sensor (Kittiwake Holroyd Instruments, UK).

To identify the roto-dynamic faults of low speed machineries, the Fast Fourier Transform is used in this study. The Fast Fourier Transform (FFT) does exactly that [10]. The Fourier transform of a signal $x(t)$ is defined as:

$$F[x(t)] = X(f) = \frac{1}{2\pi} \int_{-\infty}^{+\infty} x(t)e^{-j2\pi f t} dt$$

For Equation to be valid, the signal $x(t)$ being transformed must be stationary, which means that its amplitude distribution does not depend on absolute time. In other words, the moments of the distribution – for example, mean, variance, and so on – are stationary.

EXPERIMENTAL APPLICATION OF THE PROPOSED METHOD

The experimental data were taken from the low speed bearings which supported the rotating of the drum dryer (Fig. 3). The rotating speed of the bearing was running at 15 rpm. The bearing was NTN 23164BK spherical double row roller bearing.

Acoustic emission signal at the bearing was measured using AE Ultraspan sensor manufactured by Kittiwake Holroyd Instruments, UK (on the bearing housing). The AE sensor had resonance frequency at 100 kHz. The acquired AE signals, having been band-pass filtered at 20 kHz to 500 MHz for noise-removal and amplified to 60 dB, were sampled into a data acquisition card.

Measurements were obtained from eight different bearings. Each data collection was acquired for at least 4000 ms in order to assure at least a complete rotation of the bearing. For each bearing, five signals were collected as for data processing.

EXPERIMENTAL RESULTS AND DISCUSSION

Figure 4 shows the signal measured on bearing housing from different operating conditions – normal and defective bearings.

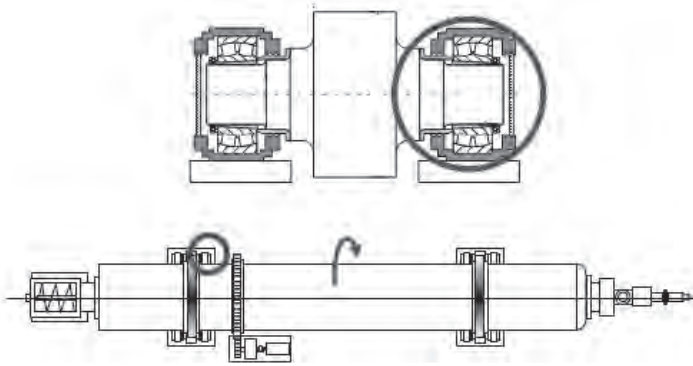


Figure 3. Low speed machinery set up and its bearings

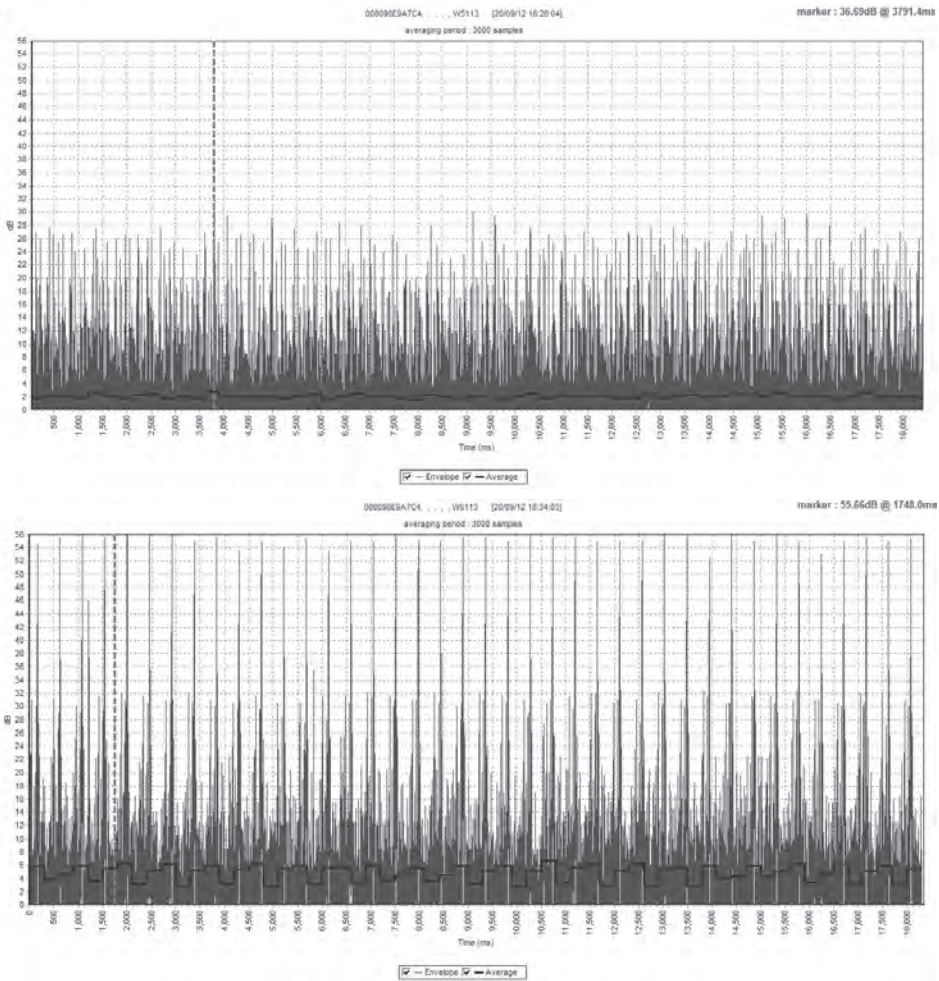


Figure 4. Results of AE dynamic envelope from (a) normal bearing, and (b) defective bearing

In the experiment, the AE dynamic envelope collected from a normal condition yielded peak of logarithm intensity about 36 dB whilst the intensity obtained from the one with suspect condition was about 56 dB. With machine fault condition resulting in higher energy release rates they produced higher continuous signal levels (this is resulted from the overlapping of many small burst signals). The AE envelopes which were extracted from sensors from normal and defective bearings are shown in Figure 4.

In order to discriminate different bearing operating condition, one has to perform bearing defect frequencies calculation. From the calculation, it was found that the defect frequencies from outer race, inner race and rolling elements were of 2.13, 2.94 and 2.01 Hz respectively. In normal bearing condition, the spectrum

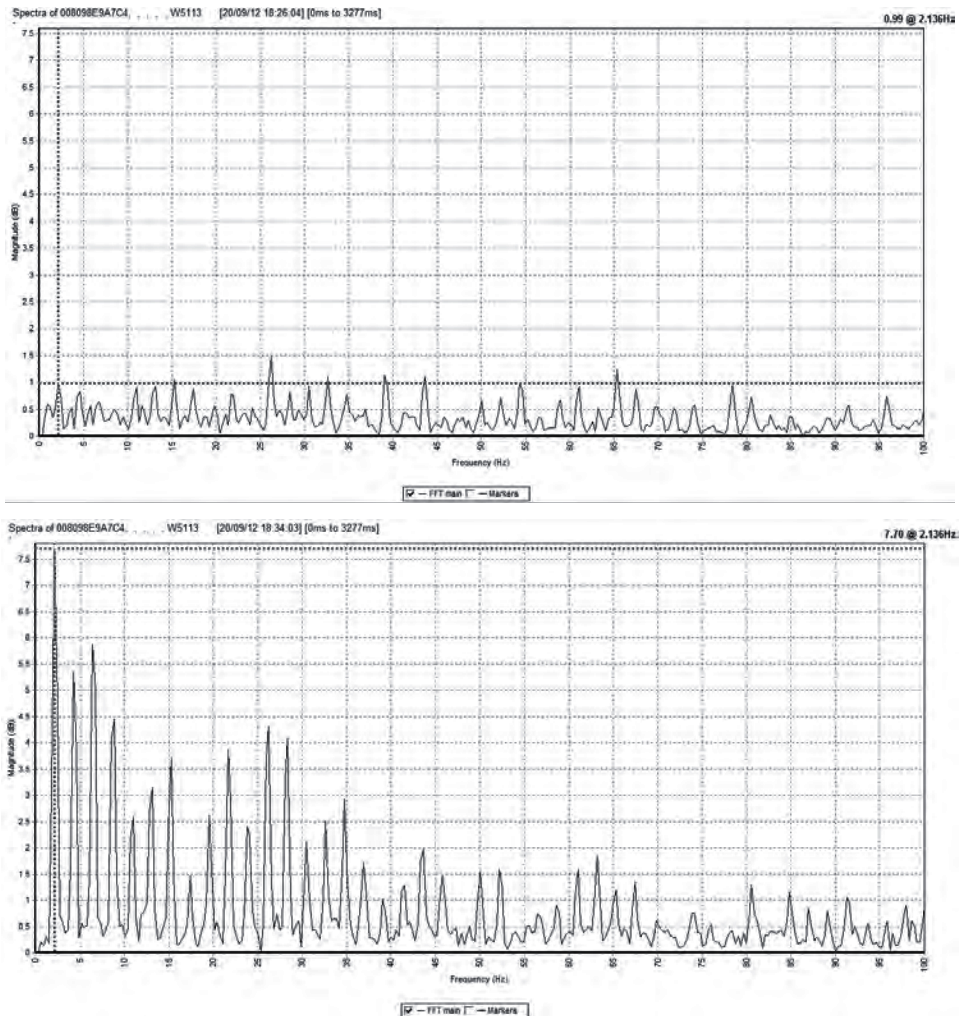


Figure 5. Results of spectrum from normal bearing (top), and defective bearing (bottom).

is shown in Figure 5 (top). In contrast to normal condition when motions were sinusoidal, nonlinear behaviour of a bearing in the presence of higher order of its outer race defect frequencies (2.13 Hz and its 2x, 3x) is shown in Figure 5 (bottom).

To verify the results, during the shut down period, the suspect bearing was stripped off to evaluate its operating condition. It was found that fine line crack occurred at the inner race (Fig. 6). In addition, the outer race was found flaking on the load zone at the bottom side (Fig. 7).

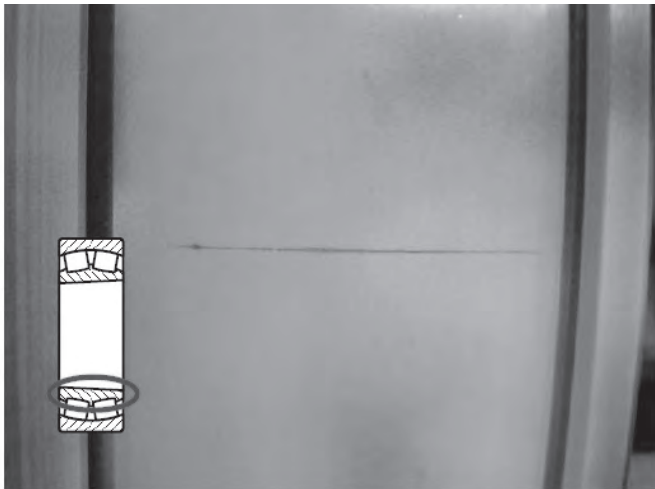


Figure 6. Hair line crack at the inner race.

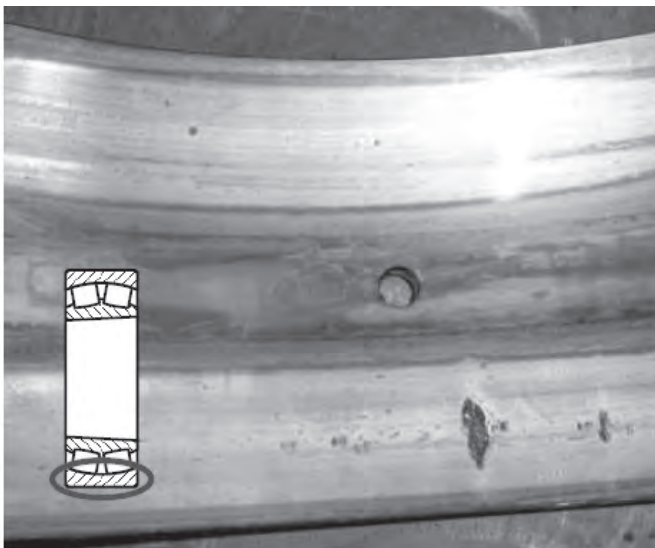


Figure 7. Flaking was found at the load zone of outer race.

The experiments indicated that both AE dynamic envelope and its FFT spectrum of acoustic emission signals from low speed bearings – normal and defective bearing – produced distinct pattern of signals that could be discriminated by using its spectrum. The experimental data showed that the use of the proposed method can reduce unplanned machine downtime with correctly and timely results.

REFERENCES

1. Shiroishi J., Li Y., Liang S., Kurfess T. and Danyluk S. (1997) Bearing condition diagnostics via vibration and acoustic emission measurement. *Mechanical systems and signal processing* **11**: 693-705.
 2. Li Y., Billington S., Zhang C., Kurfess T., Danyluk S. and Liang S. (1999) Adaptive prognostics for rolling element bearing condition. *Mechanical systems and signal processing* **13**: 103-113.
 3. Pachaud C., Salvetat R. and Fray C. (1997) Crest factor and kurtosis contributions to identify defects inducing periodical impulsive forces. *Mechanical Systems and Signal Processing* **11**: 903-916.
 4. Qu L., Liu X., Peyronne G. and Chen Y. (1989) The Hologram: A new method for rotor surveillance and diagnosis. *Mechanical Systems and Signal Processing* **3**: 255-267.
 5. Safizadeh M.S., Lakis A.A. and Thomas M. (2000) Using short-time fourier transform in machinery fault diagnosis. *International Journal of COMADEM* **3**: 5-16.
 6. Paya B.A. and Esat I.I. (1997) Artificial neural network based fault diagnostics of rotating machinery using wavelet transforms as a preprocessor. *Mechanical Systems and Signal Processing* **11**: 751-765.
 7. Wang W.J. and McFadden P.D. (1993) Early detection of gear failure by vibration analysis – I. Calculation of the time-frequency distribution. *Mechanical Systems and Signal Processing* **7**: 193-203.
 8. Holroyd T.J. (2002) Acoustic emission sensors for OEM applications. *Engineering Science and Education Journal* **11**: 29-35.
 9. Kaewkongka T. and Lim J. (2011) Roto-dynamic faults investigation using acoustic emission technique. *Journal of Science and Technology in the Tropics* **7**: 109-114.
 10. Eshleman R.L. (2005) *Basic machinery vibrations*. VIPress Incorporated, Clarendon Hills, IL.
-